Development of an Atlantis Model for Hawai‘i to Support Ecosystem-based Management

Mariska Weijerman

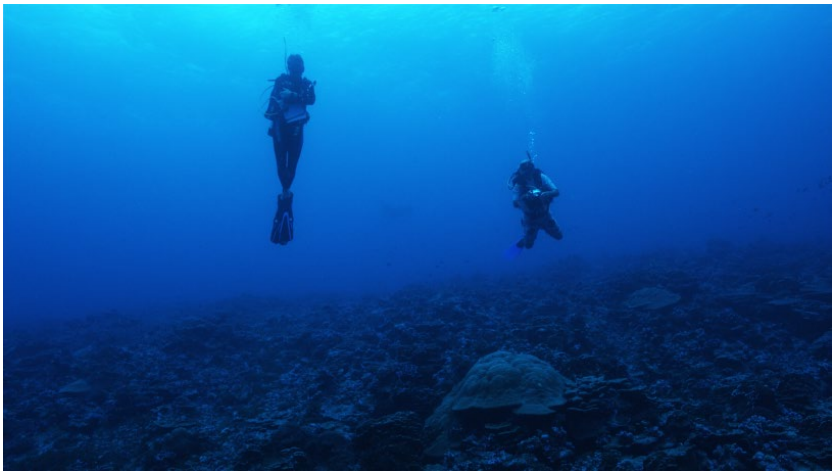

With contributions from: Kirsten Leong, Zack Oyafuso, Tomoko Acoba, Thomas Oliver, Benjamin Richards, Johanna Wren, Hannah Barkley, Kaitlyn Lowder, Stacie Robinson, Réka Domokos, Donald Kobayashi, Joey Lecky, and Jennifer Raynor

U.S. DEPARTMENT OF COMMERCE
National Oceanic and Atmospheric Administration
National Marine Fisheries Service
Pacific Islands Fisheries Science Center

NOAA Technical Memorandum NMFS-PIFSC-113
https://doi.org/10.25923/cwqb-1z04

December 2020

Development of an Atlantis Model for Hawai‘i to Support Ecosystem-based Management

Mariska Weijerman

With contributions from Kirsten Leong, Zack Oyafuso, Tomoko Acoba, Thomas Oliver, Benjamin Richards, Johanna Wren, Hannah Barkley, Kaitlyn Lowder, Stacie Robinson, Réka Domokos, Donald Kobayashi, Joey Lecky, and Jennifer Raynor

Pacific Islands Fisheries Science Center
National Marine Fisheries Service
1845 Wasp Boulevard
Honolulu, HI 96818

NOAA Technical Memorandum NMFS-PIFSC-113

December 2020

U.S. Department of Commerce
Wilbur L. Ross, Jr., Secretary

National Oceanic and Atmospheric Administration
Neil A. Jacobs, Ph.D., Acting NOAA Administrator

National Marine Fisheries Service
Chris Oliver, Assistant Administrator for Fisheries

Recommended citation

Weijerman, M. 2020. Development of an Atlantis model for Hawai‘i to support ecosystem-based management. U.S. Dept. of Commerce. NOAA Technical Memorandum NOAA-TM-NMFS-PIFSC-113, 140 p. doi:10.25923/cwqb-1z04/TM-PIFSC-113.

Copies of this report are available from

Pacific Islands Fisheries Science Center
National Marine Fisheries Service
National Oceanic and Atmospheric Administration
1845 Wasp Boulevard, Building #176
Honolulu, Hawai‘i 96818

Or online at

https://repository.library.noaa.gov/

Table of Contents

List of Tables

List of Figures

Executive Summary

We developed an Atlantis model for the insular ecosystems around the inhabited Hawaiian Islands (HI Atlantis). Key steps in this model development were to (1) summarize socio-economic and ecological objectives from multiple stakeholders in combination with robust performance indicators; (2) select candidate management strategies; (3) initialize the model for which thousands of parameters were needed; (4) model calibration and validation with a hindcast simulation of fishery and environmental stressors; (5) model uncertainty; (6) model application; and (7) summarize the results and discuss next steps. Although the ultimate goal of the model is to evaluate effectiveness of alternative management strategies, in this report we focus on the steps involved to develop the HI Atlantis model.

Most data sets for model initialization were obtained from 2010 to 2015. Largest uncertainties around parameter values were diet composition of especially non-commercial deep water species, spatial distribution of the mesopelagic scatter layer (i.e., myctophids), spatial distribution and habitat affinity of juvenile fish of most groups, spatial distribution of plankton community, and sensitivity of fishes and marine mammals to temperature increase and pH decrease. The model would also greatly improve from increased spatial resolution of the oceanographic fluxes; currently, the model uses the HYCOM data with a grid size of 0.25 degrees (~4 km) and loops over the available, non-particular years 2010–2013.

We successfully validated and calibrated the model. It can reproduce historic catches and biomass, and the modeled ecosystem conforms general ecological rules such as a trophic pyramid with few apex predators and a large base of primary producers and detritus consumers, and a linear relationship between log-biomass and size/trophic level. Sensitivity analyses showed that changes in biomass of some groups have a large impact on the biomass of other groups. These groups had a top-down (sharks) or a bottom-up control (large phyto- and zooplankton). This means that in future model applications, uncertainty around biomass and/or rate parameters of these groups should be taken into account to address this parameter uncertainty.

We applied the model to look at changes in socio-ecological indicators driven by projected climate change effects. Values of selected social indicators were similar between a simulation with climate change impacts and the base case (no climate change impacts), but the coral reef ecosystem structure will change with an increase in planktivores driven by an increase in phyto- and zooplankton and a decrease in corals driven by pH and temperature-induced mortality. The ecosystem productivity and resilience, as quantified by the selected indicators, showed a severely degraded system under the climate change scenario.

Introduction

Marine ecosystem modeling supports management that seeks to balance sustainable development and resource use with the conservation of biodiversity and functioning marine ecosystems. The overall goal of an end-to-end ecosystem model is the development of a simulation model in which all key biogeophysical and social-ecological dynamics are linked in order to address scientific and management questions and to evaluate the effectiveness of candidate management strategies so as to maintain or improve the supply of ecosystem goods and services we rely on from the ecosystems of interest. In this manner, ecosystem models can serve as decision-support tools, highlighting potential trade-offs among the different objectives of marine resource users. One such end-to-end model is the Atlantis model.[1] The success of Atlantis lies in its capacity to strike a balance between realism and tractability. Ecosystems are created in Atlantis three-dimensionally, using linked polygons that represent major geographical features of somewhat homogenous biogeophysical characteristics. Information is added on local oceanography, chemistry, geology and biology—such as currents, nutrients, plankton, invertebrates and fish—and key ecological processes are simulated. Atlantis is currently one of the most comprehensive and up-to-date ecosystem models (Plagányi et al. 2007), and it has successfully been applied to ecosystems spanning from the polar region to the tropics and from Australia to Europe (Weijerman et al. 2016). The Atlantis framework is very suitable for management strategy evaluation as it incorporates sub-modules for each major step in the management cycle: the marine environment, the behavior of industry, fishery monitoring and assessment processes, and management actions and implementation (Fulton et al. 2007). Similar to the approach taken to conduct a management strategy evaluation (Kaplan et al. In review) is the approach to develop an ecosystem model. One has to clearly define a set of management objectives and performance criteria related to achieving these objectives. Alternative management scenarios of interest to evaluate need to be identified and means to calculate the performance of each strategy under uncertainty. Lastly, one needs to quantify the (social-ecological) tradeoffs and communicate these to decision makers. Building on existing research (Weijerman et al. 2020), in this report we outline these steps in relation to HI Atlantis model development (Steps 1–5), we apply the model to explore climate change (Step 6), and we summarize results and discuss next steps (Step 7).

[1] https://research.csiro.au/atlantis/

Step 1. Identified Management Objectives and Performance Indicators

Contributors: Kirsten Leong and Zack Oyafuso

In the United States, the National Marine Fisheries Services has formulated a "Roadmap to Ecosystem-Based Fisheries Management" (EBFM; NOAA Fisheries, 2016) to explicitly account for social-ecological trade-offs due to environmental and management changes. An important aspect of EBFM is the synergy between management and science. Managers should communicate to the scientists the specific data and information needs they have and describe the form in which these products are most useful. In general, fisheries management has been focused on biological objectives while economic and especially social objectives are stated in very broad, non-specific terms (Benson and Stephenson 2018). However, for EBFM to be effective, a holistic approach is required that clearly links comprehensive (social and natural) scientific research and management objectives (Harvey et al. 2017). Implementation of EBFM has been slow in part because these objective settings are not always fully specified (Arkema et al. 2006; Link and Browman 2017).

To address this gap, Weijerman et al. (2020) identified socio-economic objectives and indicators reflecting currently available data. Future work will identify crucial data gaps and recommendations for including important concepts that are not already measured and may improve future iterations of the HI Atlantis model. At a stakeholder workshop (Weijerman, Leong et al. 2019) we also identified additional objectives which were not suitable to include in the Ecopath with Ecosim modeling framework (Christensen and Walters 2004) used in Weijerman et al. (2020) but can be incorporated into the Atlantis framework. Ultimately, eight objectives specified by multiple agencies, and therefore deemed important for most stakeholders, were included with associated indicators. In some instances, existing data did not address the objective as fully stated in the documents, e.g., for the objective "equitable access" – we do not have data for equitable but do have data to address access. We noted these data gaps within each objective.

Socio-economic objectives

1. ***Access to fishing grounds***.

    - Number of closed areas: management scenarios for both coral reef and bottomfish fisheries include spatial closures which restrict spatial access to fisheries
    - Number of fishing days: total allowable catch management is relevant to the bottomfish fishery. Number of fishing days measures the length of the fishing year, subjected to a total allowable catch that when met closes the fishery for the rest of the fishing year.
    - Per-capita fishing opportunities/access to resources

    ➢ Data gap: none of these metrics address equitable access. Key locations for sustainable subsistence/livelihood and artisanal fishing have not been systematically identified with stakeholder input.

2. ***Maintain intangible benefits***.

- Diving/snorkeling experience related to conditions of the marine environment
- Frequency of recreational fishing (number of trips per year)
- Viewing option of charismatic megafauna

➢ Data gap: Data on intangible benefits (e.g., aesthetic, sense of place) is extremely limited, although we do have some data on forms of recreation (diving, recreational fishing, wildlife viewing).

3. ***Food provision***.

- Variability in fish catches (an indicator for stability of food provisioning)
- Catch allocated for home consumption
- Catch allocated for sharing in the community
- Biomass of culturally important species (e.g., bottomfish [snappers and a grouper], goatfishes [kumu], forage fish [opelu, akule], parrotfishes [uhu], unicornfishes [kala])

➢ Data gap: These indicators do not measure social cohesion and resilience; however, it recognizes the importance of fisheries as a means for providing social cohesion in family and community units through the sharing of the catch.
➢ Data gap: Identification of culturally important marine species through systematic and formal means, such as expert solicitation and literature review, is not available. Species of economic importance (sale $3 or higher) were used as an initial proxy for a subset of culturally important species. In addition, the identified indicators do not address nutritional security of vulnerable populations.

4. ***Coastal protection***.

- Coral cover fronting human coastal communities

➢ Data gap: Hard coral cover is presumed to bolster an area's coastal resilience and therefore we use it as a proxy for a socio-economic indicator for coastal resilience. However, we do not have a relationship between coral cover and indicators related to the sensitivity of an area to negative coastal effects, such as, number of homes in flood zones, damage from king tides, coastal erosion rates.

5. ***Sustain marine revenue***.

- Revenue from fishing
- Trophic level of the fish catch
- Fishing expenditures
- Livelihood profile: number of jobs are related to the marine sector
- Number of commercial fishing licenses
- Number of registered Deep-7 bottomfish boats

- Number of species groups sustainably harvested

Biological Objectives

6. ***Maintain productive ecosystems***.

    - Biodiversity
    - Trophic level of the community
    - Total fish biomass
    - Biomass of sharks and other predators

7. ***Maintain resilient ecosystems***.

    - Ratio of coral + crustose coralline algae (CCA) /turf and fleshy algae
    - Ratio of demersal/planktivorous fish
    - Herbivorous fish biomass
    - Biomass of large (> 50 cm) parrotfishes

Description of select indicators:

- Fish biomass: total biomass of all fish groups, or of particular functional groups of interest (e.g., parrotfishes, piscivores) aggregated by Atlantis box level or an appropriate spatial scale
- Trophic level of the fish community: A high trophic level implies a lightly fished ecosystem or a system that fishes all trophic levels and not just top predators resulting in a fish community representing all ecological functions
- Diving/snorkeling experience scores are based on attributes of the marine environment considered important to divers/snorkelers or affecting their likelihood of diving/snorkeling in the future from a Hawai‘i dive-expenditure survey (Weijerman et al. 2020)
- Total catch: total catch of all fish groups, or of particular functional groups of interest (e.g., parrotfishes, piscivores) aggregated at the Atlantis box level or other appropriate spatial scales
- Catch allocation: catch that is allocated for sale, home consumption, or sharing in the community
- Number of closed areas: number of closed areas as specified by the management scenario
- Number of fishing days: for scenarios with total catch limits, the number of days where the total catch limit is not met
- Ratio of coral and CCA/turf and fleshy algae: ratio of the total cover of CCA and coral divided by the total cover of turf and fleshy macroalgae
- Number of species groups sustainably harvested: with sustainably harvest we assume that the biomass of the species group > 40% of the initial biomass (Weijerman et al. 2018)

Step 2. Climate and Management Scenarios

Reefs in Hawai‘i are predicted to be directly threatened by climate change stressors over the next few decades. Hawai’i’s high-latitude reefs are likely to suffer soonest from ocean acidification (OA) stress, compared to other tropical reefs, and will experience annual bleaching from approximately 2035 onwards (van Hooidonk et al. 2016). Based on an EBFM workshop ((Weijerman, Leong et al. 2019) numerous local management actions were identified, targeting governance, ecological state components, equitable access issues and social state components to mitigate the global impacts. In a parallel study, we developed an Ecopath with Ecosim model to explore the efficacy of alternative fisheries management scenarios to maintain or improve identified societal goals (Weijerman et al. 2020). Here, we explored the effects of projected climate change and compared model output with and without climate change impacts simulated (see Step 6).

Figure 1. Severe thermal-induced “bleaching” of Cauliflower corals (*Pocillopora meandrin*a) along the Kona coast of Hawai’i. Photo courtesy of Bill Walsh DAR Kona.

Step 3. Model Initialization

To obtain an understanding of the ecosystem complexities we briefly describe the key biophysical features and the human uses of marine resources with respect to our study area (section 3A) and then detail the model development (section 3B). For a simplified overview of the model development, see the Story Map.[2] For general model structure and algorithms please review (Fulton et al. 2004; Fulton et al. 2011; Audzijonyte et al. 2019). For coral specific relationships (e.g., coral growth, coral-algal interactions, coral-sediment relationship, and structural complexity-predator avoidance relationships) please see Weijerman et al. (2015). Underlying the usefulness of model forecasts is the availability of pertinent data and expert opinion on the implementation of key ecosystem dynamics into more simplistic algorithms and identifying parameters for each of the biological groups and ecological dynamics, hydrodynamics and socio-economic dynamics. To obtain these data, partnerships were formed between management agencies and various science disciplines (University of Hawai‘i at Mānoa, Hawai‘i Institute of Marine Biology, Pacific Island Fisheries Science Center, Hawai‘i Division of Aquatic Resources, Pacific Islands Regional Office, and Western Pacific Regional Fisheries Management Council).

3A. Study area: Insular ecosystems of the southeastern Hawaiian Islands

Our area of interest is the insular ecosystems surrounding the eight inhabited Hawaiian Islands located in the Pacific Ocean (Figure 2).

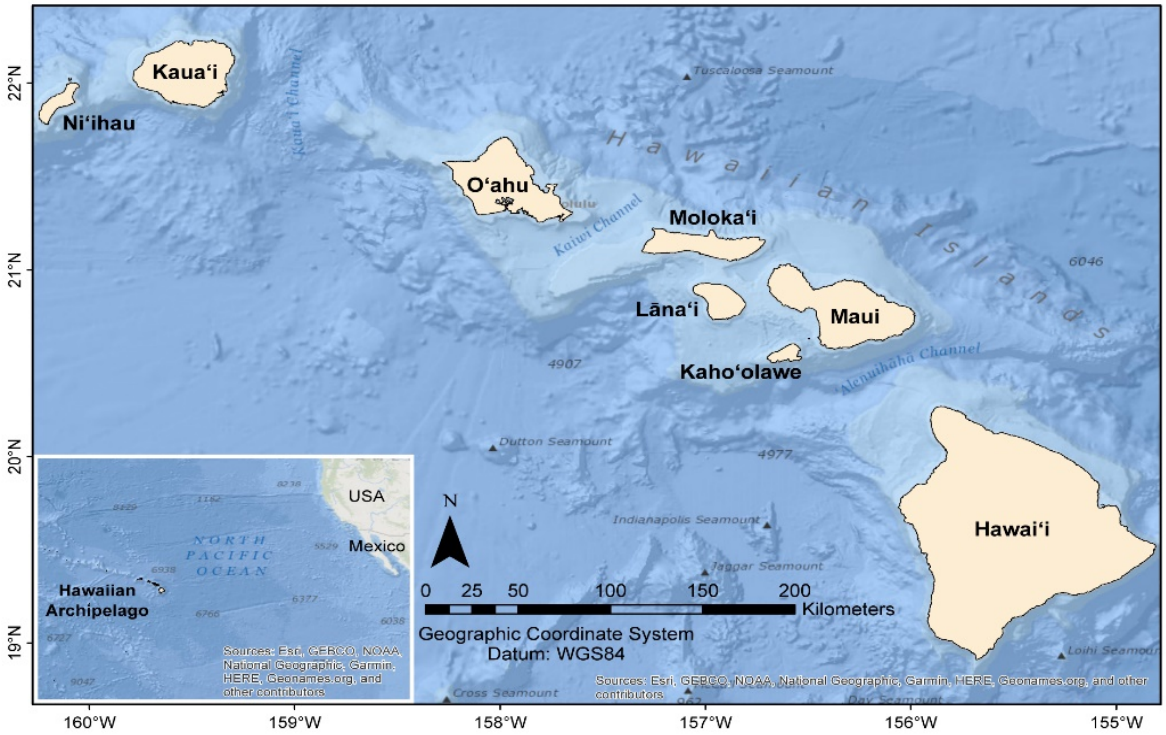

Figure 2. The eight Hawaiian islands of our study area with the inset figure showing the location of the Hawaiian Archipelago in the Pacific Ocean.

[2] https://storymaps.arcgis.com/stories/c1898d0cb90745feb008e9c9daff8f39

Physical Environment

The Hawaiian Islands are located in the oligotrophic (nutrient poor) subtropical gyre of the North Pacific. The ocean is characterized by water temperatures of around 25°C at the surface (0–30 m) with temperatures of around 22°C at 50 m after which it gradually declines to 8°C at 400 m.[3] Salinity and oxygen varied minimally in these 0–400 m water depths and are around 35 ppt and 200 µmolO_2/kg, respectively.[4] Due to the clarity of the water, light penetrates to 200–400 m depth. Decadal changes are driven by the North Pacific Gyre Oscillation that respond to regional and basin-scale variations in wind-driven upwelling and horizontal advection (Di Lorenzo et al. 2008).

Open ocean water is the primary source water for coral reef systems. Once on the shallow reef, this source water can be dramatically altered by physical, chemical, and biological processes. The conditions of adjacent open ocean surface waters strongly impact coral reef ecosystem metabolism and health. For example, offshore biological productivity impacts delivery of inorganic and organic nutrients that serve as critical energy sources for biological processes within coral reef ecosystems. Upwelling of deep, cool waters via internal waves or topographic upwelling can provide additional nutrients as well as intermittent refuge to thermal stress in shallow coral reefs. Offshore circulation patterns influence larval dispersal and recruitment, which can enhance biodiversity and increase ecosystem resilience to anthropogenic stressors.

The physical properties of the ocean water also influence the abundance of corals. Corals have a very narrow range of optimal conditions. For example, when the temperature rises for prolonged periods (4–8 weeks) above the mean summer maximum, the corals will expel their symbiotic algae that live in their tissue giving them a bleached look (Jokiel and Coles 1990). The polyps can still filter feed but prolonged absence of their symbiotic algae will often lead to coral mortality. Global acidification of open ocean waters results in the transport of progressively more acidified source water to coral reefs which leads to declining rates of calcification, increasing dissolution, and a shift in calcium carbonate reef budgets toward net dissolution (Langdon and Atkinson 2005). The current effects of climate change have a profound impact on the growth and mortality of corals and other calcifying organisms (Kroeker et al. 2013; Busch and McElhany 2016).

Biological Environment

The shallow (0–30 m) coral reefs ecosystems fringing the Hawaiian Islands are home to about 70 species of scleractinia or hard corals (Veron and Stafford-Smith 2002) but only a handful dominate the benthos. These prominent structural corals include *Porites lobata*, *Porites compressa*, *Pocillopora meandrina* and *Montipora* spp. These coral colonies provide food and habitat for many invertebrate and fish species making it a very productive ecosystem despite the surrounding oligotrophic open ocean waters. Fish diversity and abundance is very high in coral reef ecosystems compared to other coastal ecosystems partly because of the protection provided by the structural complexity of reefs for juvenile and small fishes (Graham et al. 2006; Rogers et

[3] http://hahana.soest.Hawai'i.edu/hot/hot-dogs/
[4] http://hahana.soest.Hawai'i.edu/hot/hot-dogs/

al. 2014). Corals compete for benthic space with, for example, algae, soft corals, tunicates, zooanthids and sponges.

The steep slopes and clear waters around the islands lead to distinct biological transitions between the highly productive, photic shelf areas and the more depauperate light-limited lower slopes (Struhsaker 1973; Kelley et al. 2006; Weijerman, Grüss, et al. 2019). The upper slope limits are at about 130–150 m and the lower depth limits extend beyond our model boundaries of 400 m to 1000–4000 m. Ecosystems associated with mesophotic depths, which are characterized as located between 30 and 150 m (Kahng et al. 2014), still have scleractinian, zooxanthellate coral species present, with patchily distributed reef environments dominated by *Leptoseris* and *Montipora* spp. with increasing depth (Pyle et al. 2016). Calcareous algae are the dominant algal group between 30 and 150 m, particularly with extensive *Halimeda* spp. beds in the Maui Nui area (the islands of Moloka'i, Maui, Lana'i and Kaho'olawe). Large areas of the calcareous crustose rhodoliths also have been observed to depth of 170 m (Rooney et al. 2010). However, little remains known about the broader spatial distribution of these algal beds.

At deeper, subphotic, depths which we characterize as located between 150 and 400 m, productivity is largely based on the organic "snow" from sloppy feeding and sinking planktonic particles (Siegel and Deuser 1997; Baldwin et al. 2018). Subphotic habitats are typically uniform, low-relief, hard bottom with patches of CCA at 160–180 m (Rooney et al. 2010), and at deeper depths the primary benthic taxa are azooxanthellate corals, soft corals, sea anemones, benthic ctenophores, feather stars and gorgonians (Kelley et al. 2006). The low habitat diversity has resulted in less affinity with habitat type for deep-water fishes compared to the shallow reef zone (Parrish 2006). Benthopelagic fish (i.e., fishes associated with benthic substrates) rely on currents to transport zooplankton into their foraging areas and hence greater concentrations of fish are found along features on the sea bottom where currents form (e.g., seamounts and cliffs). Changes in fish community structures are thought to be more influenced by top-down (predators, fishing) than bottom-up (productivity) controls (Parrish 2009; Weijerman et al. 2017). Clear faunal breaks in fish communities have been found in these deeper (150–400 m) waters with the largest break at 230 m and other breaks at 190 m and 310 m (Weijerman, Grüss, et al. 2019).

The chlorophyll maximum is around 150 m (Cullen 1982) which leads to night-time vertically migrating zooplankton, squid and fishes from depths of around 400–800 m to the shallow (30–200 m) depths, collectively known as the mesopelagic scatter layer (Benoit-Bird et al. 2001). Fish species include zooplanktivorous myctophids and gonostomatids, and carnivorous *Bethosema* spp, *Polymixia* spp., and *Synagrops* spp. (Struhsaker 1973). Marine mammals and large piscivorous fish species target these migrating species during their night-time feeding dives (Benoit-Bird and Au 2003). These vertical feeding migrations likely provide a means for the exchange of energy between the different depth zones (Steinberg et al. 2008; Drazen and Sutton 2017; Gloeckler et al. 2018).

Human Dimensions

Coastal communities engage with, and rely on, marine ecosystems; therefore, they face a complex set of interlocking challenges. Changes in marine ecosystems driven by global-scale shifts in ocean warming and acidification, as well as local human-induced disturbances, may be eroding the ability of these ecosystems to provide the goods and services on which humans rely. Less clear are the protocols to address and adapt to these declines. To respond intelligently to

these changes we must understand the complex interactions among the coastal environment, marine organisms, and human communities.

Coral reefs are economically productive, with estimates of the direct total economic value of Hawai'i's reefs topping $360 million per year, or $9.7 billion over the next 50 years (Cesar and Van Beukering 2004). They also provide other critical ecosystem services, such as coastal protection (Storlazzi et al. 2019), food security (Grafeld et al. 2017), cultural benefits (Ingram et al. 2018), and strengthening social relations (Kittinger et al. 2015). Through a coupling of the biophysical components with the human use sector and tracking relevant indicators, it is possible to quantify the impacts of changes in the ecological state components on human well-being (social state components) and changes in the social state on the ecological well-being (Tam et al. 2019). In Hawai'i the most important human well-being domains related to coral reef ecosystem viability are the following (Breslow et al. 2016; Leong et al. 2019): Culture and Spirituality; Social Relations; Health; Economic/Material well-being; and Safety and Security. Indicator development and data collection for each of these human domains and the ecosystem services related to those domains are in progress. However, for some indicators existing data sets are present to operationalize the relationships between human and ecological well-being and to develop a robust understanding of how ocean and management changes affect the reliance on and engagement of human communities on the coral reef ecosystems (Weijerman et al. 2020).

3B. Atlantis Ecosystem Model Development

The structure of Atlantis consists of various submodels that can be as detailed as the user desires (Figure 3).

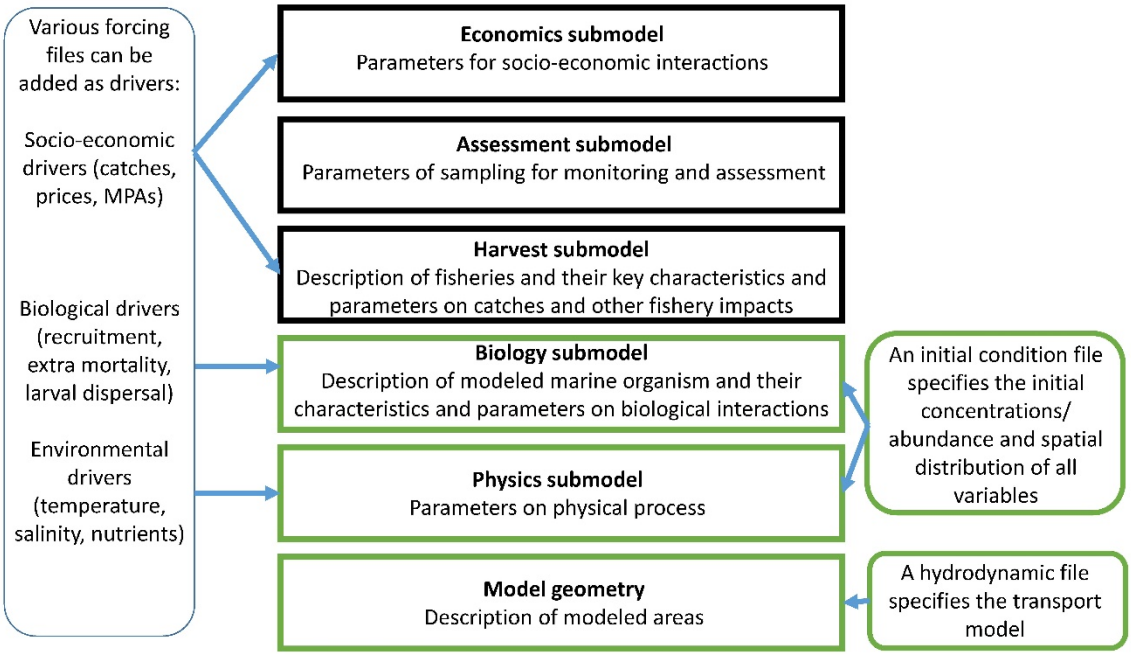

Figure 3. Schematic representation of the Atlantis model structure and input files. Submodels and files colored in green are obligatory, others are optional.

We will discuss each of these building blocks in relation to the development of the Hawai‘i model and explain where parameter values came from for our study area.

Model geometry

Contributors: Tomoko Acoba, Thomas Oliver, Benjamin Richards

HI Atlantis covers approximately 8905 km^2 from 0 to 400 m deep (Figure 4). The design of the spatial structure involved placing boundaries around areas with similar biogeographic and oceanographic conditions as well as aligning boundaries with those of fishery reporting zones. The geography was categorized by hard/soft substrate information and bathymetry. Selected depth contours at 30 m, 150 m, and 400 m were derived from the synthesis of the bathymetry available from the University of Hawai‘i (UH), Hawai‘i Mapping Research Group (HMRG). Biological components (benthic cover composition and fish communities) were obtained from the PIFSC Reef Assessment Monitoring Program survey data[5] for the 0–30 m shallow areas. These resulted in 28 spatial areas (boxes) with (somewhat) homogenous fish and benthic composition for the shallow (<30 m) spatial areas.

For the deeper (30–400 m depth) areas, we used a hierarchical clustering technique to identify spatial blocks with similar oceanographic characteristics. Variables used for clustering were satellite-derived 2003–2015 monthly means of chlorophyll-*a* (MODIS-Aqua), photosynthetically active radiation (PAR), a proxy for turbidity (K490), and sea surface temperature (SST). We clustered these variables based on Euclidian distance and joining linkages based on outliers (complete-linkage). By changing the number of required clusters we identified distinct areas around each of the islands that were robust (same clusters) under these changes which resulted in twenty-seven 30–150 m boxes and nineteen 150–400 m boxes (Weijerman 2017).

For all spatial areas, habitat characterization was based on hard/soft substrate information derived from two sources: (1) benthic habitat maps generated from satellite images analysis for the 0–20 m depth range ((Battista et al. 2007) and (2) backscatter data collected during multi-beam surveys for the 30–400 m depth range (UH, HMRG). The major structures of the benthic habitat maps derived from the satellite images were re-categorized into hard and soft substrate classes. Backscatter data reflected the hardness of the substrate as values between 0 (soft, e.g., sand) and 255 (hard, e.g., basalt) for each 400 x 400 m pixel. We classified pixels with values ≥ 110 as hard. In ArcGIS we used the tool ‘zonal statistics’ to aggregate the pixels for each of the spatial Atlantis areas and calculated the percentage hard and soft.

Islands are connected by four boxes (81–84 in Fig. 4) to allow for movement between islands. Around the entire model domain we created six ‘boundary boxes,’ which allow for the advection of plankton (including larvae) and nutrients, but which have no dynamic processes. Each spatial area was further divided into vertical water column layers and one sediment layer. For the inshore boxes (0–30 m) we assume complete mixing and they only have one layer (0–30 m = ‘shallow’), the 0–150 m boxes have two layers (‘shallow’ and ‘mesophotic’), and the 0–400 m and deeper boxes have three layers (‘shallow’, ‘mesophotic’, and ‘subphotic’). Boundaries of boxes close to the delineation of the Hawai`i Division of Aquatic Resources (DAR) fishery

[5] https://www.pifsc.noaa.gov/cred/pacific_ramp.php

reporting zones, were adjusted to align with the fishery grids to facilitate the allocation of catch time series in the Atlantis harvest submodel. Once the Atlantis boxes were finished, small adjustments were made to ensure that the modeled area matched as closely as possible (<2% difference) to the true area (Appendix A). The total 0–400 m area included 13% shallow habitat (1129 km^2), 44% mesophotic habitat (3890 km^2) and 44% subphotic habitat (3886 km^2).

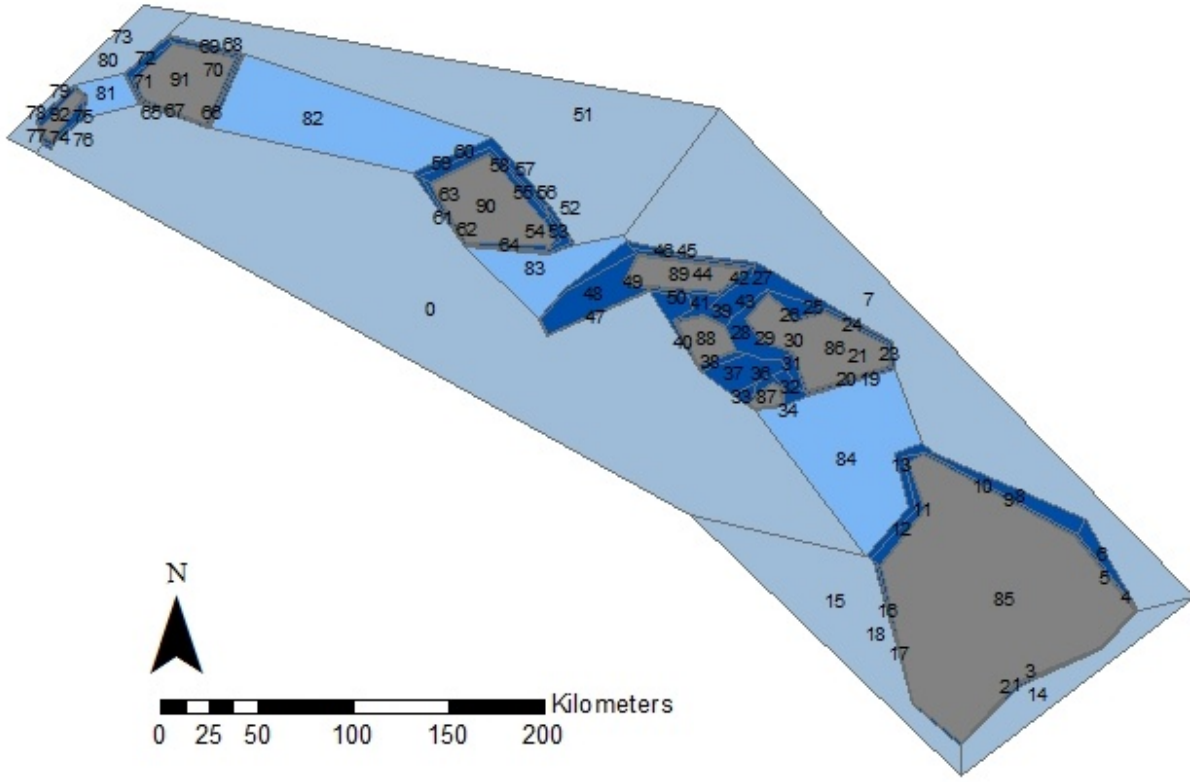

Figure 4. Geometry of the southeastern Hawaiian Islands Atlantis model.

The outer boxes (0, 7, 14, 15, 51, and 80) are non-dynamic "boundary," and boxes 85–92 are island boxes with no dynamics; others are dynamic boxes with closest to shore, 0–30 m depth and 1 vertical layer, adjacent to those are 0–150 m with 2 vertical layers; and farther offshore are 0–400 m boxes with 3 vertical layers. Four boxes between the islands (81–84) allow for interisland movements.

Physics submodel

Most of the physical parameters in Atlantis were not changed. For example, the functional response curve for bioirrigation and bioturbation activity were left as parameterized for the original southeast Australia model. We adjusted some parameters based on sensitivity analysis (see under Step 5 "Recycling of Nutrients").

Hydrodynamic forcing

Contributor: Johanna Wren

Physical exchanges (advection and diffusion) between Atlantis boxes were calculated from the regional HYbrid Coordinate Ocean Model (HYCOM) for the Hawaiian Islands Region with KPP mixed layer provided by Dr. Yanli Jia at the International Pacific Research Center, University of Hawai‘i at Mānoa.[6] The regional HYCOM model has a spatial domain spanning 166–150°W and 16–26°N and consists of daily snapshots with $^{1}/_{25}$-degree (~4 km) horizontal resolution and 32 depth layers. We used the non-particular years 2010–2013 (2009 was the first year, but only has data for half a year, 2014 had an extreme recruitment pulse, 2015 and 2016 had abnormally warm waters) as our baseline and looped over these years for the duration of a baseline simulation. The potential temperature, salinity and vertical velocity variables were re-gridded to an evenly spaced grid using bilinear interpolation, then disaggregated to increase the spatial resolution by a factor of 3 for better coverage inside the coastal Atlantis polygons. We averaged the temperature and salinity for each Atlantis box and water column layer. Vertical flux was calculated for each box and layer by averaging the vertical velocity and multiplying it by the area of the box and the depth of the layer. Horizontal fluxes over the sides of each of the Atlantis boxes were calculated by defining an area around each side of each polygon and calculating the mean horizontal current speed and direction inside each area for each depth layer. Additionally, we calculated the relative angle between the side of each polygon and the flow direction and multiplied the mean current speed by the cosine of the relative angle to account for non-perpendicular flow. The resulting current speed was multiplied by the surface area of the polygon’s side to obtain a flux across the side in m^3s^{-1}.

Initial conditions for physical, biological and chemical oceanographic data came from in-situ observations and literature (Table 2). For the shallow boxes, we used primarily observational data from NOAA PIFSC Reef Assessment Monitoring Program surveys.[7] For the offshore spatial areas (depth >30 m), light attenuation, temperature, salinity, oxygen, nutrients, and chlorophyll-*a* data were downloaded from the Hawai‘i Ocean Time-Series database[8] using the bottle-extracted data. For nitrogen in the upper (0–200 m) water column, we used the results of the “High Precision, High Sensitivity Method” since the concentrations are so low in the waters around Hawai‘i that other methods do not properly measure them.

Environmental drivers

Ocean acidification

Contributor: Hannah Barkley

Surface tropical seawaters are generally supersaturated with respect to the carbonate minerals (e.g., calcite, aragonite, and high-magnesium calcites) from which marine organisms construct their shells and frameworks. At deeper water depths, seawater becomes undersaturated and these minerals begin to dissolve, imparting an important control (amongst other factors) on the distribution of coral reefs. The effects of ocean acidification on calcification rate appears not to

[6] Available for download at: http://apdrc.soest.Hawai’i.edu/datadoc/hycom_Hawai’i_0.04_kpp.php.
[7] https://www.pifsc.noaa.gov/cred/pacific_ramp.php
[8] http://hahana.soest.Hawai’i.edu/hot/hot_jgofs.html

be directly related to changes in pH, per se, but instead to corresponding changes in the degree to which seawater is supersaturated with respect to the carbonate minerals (e.g., aragonite) (Langdon and Atkinson 2005). A change in carbonate ion concentration results in a proportional change in Ω_{arg} such that as ocean acidification continues, the surface ocean Ω_{arg}-values will decline. As the saturation state declines, it is harder for marine calcifiers to precipitate the calcium carbonate they need to build their skeletons. By the year 2065, rates could decline 60 ± 20% relative to preindustrial levels.

Projected changes in the aragonite saturation were included as force files. The variables sea surface temperature (SST), surface salinity, surface pressure of CO_2 and pH were obtained from fully coupled models in the Coupled Model Intercomparison Project 5 (CMIP5)[9]. All model outputs were re-gridded to the same 1×1° regular grid using bilinear interpolation. If multiple runs were available for a model, these runs were averaged first. Based on these data, a multi model ensemble was created. Missing values over land were filled in using a Poisson grid filter in the zonal direction. Values where sea ice was present in the GFDL-ESM2M_rcp85 model were masked out. Monthly values were averaged to obtain yearly or decadal averages. Aragonite saturation state was calculated from SST, surface pressure of CO_2, pH, and salinity.

Ocean warming

Contributor: Johanna Wren

Projected changes in ocean temperature (SST) also came from CMIP5 using just the AR 8.5 scenario. All 22 model outputs were used to calculate the average SST over the inhabited Hawaiian Islands (161°W–154.5°W and 18.5°N–22.5°N) spatial area. We first subtracted the historic average (1970–2000) from the future projection to obtain the projected change for each model and then took the average across all 22 models. To keep the spatial variation as determined by the hydrodynamic model, we added (or subtracted) the projected change to the last year of the hydrodynamic model (2013). We also included the historical peaks in temperature in 2014–2015 and 2018 that led to severe coral bleaching in Hawai‘i (Sale et al. 2019).

Sensitivity of marine organisms to environmental changes

Contributor: Kaitlyn Lowder

An increasing number of laboratory and field studies provide insight into the sensitivity of a broad range of marine organisms by replicating future increases in ocean temperature and changes to carbonate chemistry (decreases in pH and aragonite saturation). We applied a meta-analytic framework to estimate sensitivity of organisms from tropical Pacific or Indo-Pacific marine waters, encompassing bacteria, algae, invertebrates, and fishes (Appendix B). From an initial screening of 1,543 full papers, we identified 334 papers with controlled experiments that exposed organisms to either changes in pH or temperature. For each experiment, we extracted metadata on a broad range of variables, including species, life stage, treatment level, and experimental duration, as well as response data that ranged from survival and growth to predation susceptibility and nutritional quality. Response values and sample sizes from

[9] http://pcmdi9.llnl.gov/ esgf-web-fe/

individual experiments were converted to effect size (Hedges' g or odds ratio, depending on the data type). For temperature, intercept values from intercept-only models were converted to an approximation of Q10, a coefficient that reflects the measure of the rate of change in a response as temperature increases by 10 °C. Responses to pH were fit as intercept-only, linear, or quadratic relationships of effect size with pH decreases up to 1 unit. All effect sizes were standardized to the most sensitive organism and these resulting 'survival' scalars were incorporated into Atlantis as a scalar on growth-related parameters (Appendix B).

Land-based sources of pollution

Contributor: Joey Lecky

Coastal areas are impacted by river and groundwater flows carrying pollutants, nutrients, and sediments to nearshore waters. Sediment and nutrient data of these daily loads came from the Ocean Tipping Point (OTP) project[10] and were aggregated for each coastal Atlantis box in a forcing file. These data represent current (2010–2015) sediment and nutrient inputs into coastal waters. To get seasonal patterns we downloaded monthly climatological rainfall data (1981–2010) from 75 coastal stations in the inhabited Hawaiian Islands[11] and took the mean rainfall for each Atlantis box. We assumed that there was a linear relationship between rainfall and the sediment loads and estimated the monthly sediment input. Sediments were modeled as the nitrogen in labile detritus (20%) and refractory detritus (80%) by converting carbon to nitrogen. We further assumed that the OTP sediment load contained 1% nutrients from fertilizer consisting of $N–NO_3$. Since OTP nutrient inputs were from Onsite Sewage Disposal Sites (OSDS, e.g., cesspools) only, we assumed that those inputs were constant over time and consisted of $N\text{-}NH_4$.

Biology submodel

Multispecies functional groups

Inclusion of species in the model was dependent on a minimal time span of 10 months spent in the model domain, especially with regard to its energy cycle (feeding, excretion, and reproduction). For example, humpback whales spend a part of their time in the nearshore Hawaiian waters; however, they hardly feed here and, therefore, are assumed not to be a great contributor to the energetic pathways of the insular ecosystem and are excluded from the model. In contrast, some spinner and bottlenose dolphin pods that are resident in Hawai'i defecate in shallow bays and feed in deeper waters on vertically migrating myctophid fishes, squids, and shrimps. Therefore, they and their diet components are included in the model. Generally, species were aggregated into functional groups based on similar life history, diet, and habitat, with finer taxonomic resolution for species of special concern (conservation, fishery). We defined 59 functional groups (Table 1) including marine mammals (3 groups), reptiles (2), reef fish (9), meso- and subphotic fish (5), commercially important deep-water fish (3), invertivorous rays (1), coastal pelagics (4), micronekton (2), zooplankton (4), macrobenthic invertebrates (5), meiobenthos (2), filter feeding sessile invertebrates (3), structural benthos (6), primary producers (5), bacteria (2) and detritus (3). Species composition of vertebrate functional groups is provided in Appendix C.

---

[10] http://www.pacioos.Hawai'i.edu/projects/oceantippingpoints/#datasources
[11] http:// www.ncdc.noaa.gov/cdo-web/datatools/normals

Table 1. Functional groups included in the southeastern Hawaiian Islands Atlantis model.

Category	Code	No	Functional group name (with examples of main families/species)
Marine mammals	MS	1	Monk seals
	SPD	2	Spinner dolphins
	BND	3	Bottlenose dolphins
Sea turtles	GT	4	Green sea turtle
	HT	5	Hawksbill turtles
Reef fish	RCO	6	Corallivores (butterflyfish)
	RBR	7	Herbivore browsers (chub, unicornfish)
	RGR	8	Herbivore grazers (surgeonfish)
	RPA	9	Parrotfishes
	RBC	10	Benthic carnivores (snapper, goatfish, squirrelfish)
	RLP	11	Large planktivores (unicornfish, soldierfish)
	RSP	12	Small planktivores (sergeant, chromis, cardinalfish)
	ROF	13	Other reef fish
	RBP	14	Benthic piscivores (grouper, moray eel, scorpionfish)
Meso and sub benthic piscivores	MBP	15	Benthopelagic piscivores (eel, scorpionfish, trumpetfish)
Mesophotic fish	MBC	16	Benthic carnivores (wrasse, goatfish, flounder, perch)
	MPL	17	Planktivores (anthias, flame wrasse, triggerfish)
Subphotic fish	SBC	18	Benthic carnivores (flounder, beard fish, orange rakefish)
	SPL	19	Planktivores (spikefish, boarfish, armorhead)
Bottomfish	BFW	20	Bottomfish in water column: Opakapaka, Onaga, Kaleakale, Lehi
	BFB	21	Bottomfish close to substrate: Ehu, Hapu'upu'u, Gindai
	UKU	22	Uku
Invertivorous rays	IVR	23	Invertivorous rays (sting ray)
Coastal pelagics	PIS	24	Roving piscivores (jack, barracuda)
	SHR	25	Sharks (reef and pelagic shark)
	SHP	26	Mackerel scad, bigeye scad
	RAY	27	Manta ray
Mesopelagic scatter layer	MSL	28	Planktivorous micronekton (myctophid, gonostomatid)
	CEP	29	Squid
Mobile inverts	LOB	30	Large crabs, lobster, heterocarpus
	BC	31	Benthic carnivores (sea star, mollusk, crustacean)
	BD	32	Benthic detritivores (amphipod, isopod, sea cucumber, crab, brittle star)
	BG	33	Benthic Grazers (urchin, snail, sea hare)
	OCT	34	Octopus,
	BM	35	Small inverts (small shrimp, crab, mollusk, foraminifera)
Meiobenthos	INF	36	Infauna (burrowing inverts e.g., polychaete, nematod)
Filter feeders	BFF	37	Shallow filter feeders (sponge, tunicate, octocoral, zoanthid, sand dollar, bryozoan)
	BIV	38	Bivalve, clam, oyster, pen shell
	DFF	39	Deep filter feeders (deep water coral, anemone, benthic ctenophore, feather star, gorgonian)

Category	Code	No	Functional group name (with examples of main families/species)
Structural benthic species	PRM	40	*Porites* massive
	PRB	41	*Porites* branching
	MON	42	*Montipora*
	POC	43	*Pocillopora*
	LEP	44	*Leptoseris*
	CCA	45	CCA
Primary producers	MAF	46	Macroalgae fleshy
	MAC	47	Macroalgae calcareous
	TRF	48	Turf algae
	PL	49	Large phytoplankton (diatom, Trichodesmium, dinoflagellate, diazotroph)
	PS	50	Small phytoplankton (cyanos (prochlorococcus, synechococcus), picoeukaryote, coccolithophorid)
Micronekton	ZS	51	Small zooplankton (ciliate, protozoa, nanoflagellate)
	ZM	52	Meso zooplankton (copepod, pteropod, polychaete)
	ZL	53	Large zooplankton (chaetognath, Stomadidae, larvae, decapod shrimp, amphipod, ostracod, euphausiid)
	ZG	54	Gelatinous zooplankton (jellies, salp, siphonophore, pyrosome, ctenophore, hydrozoan, pelagic tunicate)
Nutrient cyclers	PB	55	Pelagic bacteria
	BB	56	Benthic bacteria
Detritus	DL	57	Labile detritus
	DR	58	Refractory detritus
	DC	59	Carrion detritus

Initial conditions: Biomass and spatial distribution

The currency of Atlantis is nitrogen so we converted all biomass values to nitrogen based on the Redfield ratio of C:N being 5.7 and a dry-weight-to-wet-weight ratio of 20%. These ratios are hard-wired into the code so could not be changed. The vertebrates can have up to 10 age classes, with a minimum 1 year represented in each class. Age-classes of vertebrate groups were further divided into structural (skeleton) and reserve (soft tissues) weights based on the reserve to structural weight ratio of 2.65. Invertebrates are divided into juveniles and adults. Atlantis does not include larval stages; recruits in Atlantis are represented by the youngest individuals settling from their pelagic larval stage into their (benthic) juvenile habitat.

For the <30 m boxes, biomass and horizontal distribution of chlorophyll-*a* (phytoplankton), benthic sessile organism (corals, algae) and reef fish came from PIFSC Reef Assessment Monitoring Program surveys.[12] Site-level data were pooled up to Atlantis boxes for each functional group (Table 2). Mobile crypto invertebrate data came from the Autonomous Reef Monitoring Units (ARMS) program (Appendix D). Recovered species were grouped in the functional group based on their main diet components and we estimated their biomass. Biomass for the octopus and lobster functional groups for the shallow boxes (for deep boxes see below) were derived from commercial fishery data where we assumed a sustainable fishery effort of 0.2

[12] https://www.pifsc.noaa.gov/cred/pacific_ramp.php

per year and a ratio of commercial to recreational (un-reported) catch of 1:5 and that ⅔ of the reported catch came from the 0–30 m area.

For the meso- and subphotic depth layers, phytoplankton data came from the Hawai‘i Ocean Time-Series database.[13] Zooplankton and squid biomass and vertical distribution data were obtained from literature (Steinberg et al. 2008; Choy et al. 2016). The obtained biomass values per unit of volume of each box and layer was summed and divided by the total biomass to get a relative value for each box which was used as the horizontal distribution. Benthic sessile invertebrate data were obtained from PIFSC surveys, HURL data (Appendix E) and Veazey et al. (Veazey et al. 2016). The deep filter feeder (DFF), octopus (OCT), lobster and large crab (LOB), and bivalves (BIV) functional group data were obtained directly from HURL data (Appendix E) in which abundance was estimated for sessile and mobile invertebrates. For the DFF group we assumed that 1 organism occupies 0.1 m^2 to convert abundance to cover. These abundance estimates were multiplied with average weight for the functional species group, i.e., 375 g for DFF (Wilkinson and Cheshire 1990), 750 g for OCT (Van Heukelem 1976), 500 g for LOB (assumed), and 10 g for BIV (assumed). The bivalve biomass was further multiplied by 100 and the OCT and LOB biomasses by 10 to account for unnoticed species. Spatial allocation of the meso- and subphotic DFF, OCT and BIV groups was based on the percentage of hard substrate derived for the seaflor of the model domain (Dove et al. 2019). As the LOB functional group combines lobsters, which favor hard substrate, and large crabs, which favor soft sediments, this functional group was assumed to be homogeneous across the modeled area. Biomass of benthic detritivores and benthic carnivores was based on the same calculations as the cryptofauna (Appendix D) as these organisms can be quite small and hard to detect in the submarine surveys. For these calculations, where we did not have *in situ* complexity estimates, we used the percentage hard substrate as a complexity indication with >80% hard being equivalent as complexity 4, between 60% and 80% as complexity level 3, between 40% and 60% as complexity 2 and below 40% complexity 1.

Fish abundance came from meso- and subphotic surveys conducted by PIFSC (Asher et al. 2017, PIFSC unpublished data), Struhsaker (Struhsaker 1973) and the University of Hawai‘i at Mānoa (UH) Drazen lab (Moore et al. 2016) and Hawai‘i Underwater Research Lab (HURL) and was converted to biomass (Appendix E).

Spatial distribution for the meso- and subphotic species was based on species-specific affinities with seafloor characteristics and depth (Dove et al. 2019). Each functional group had slightly different variables that explained the deviance between observed and predicted encounter or biomass data (Weijerman, Grüss, et al. 2019).

Vertical diurnal distribution for plankton came from Steinberg et al., (2008) and for all other groups from fishBase, literature and expert opinion.

[13] http://hahana.soest.Hawai'i.edu/hot/hot_jgofs.html

Biomass estimates and spatial distribution of "Shallow prey fish" and the "Mesopelagic Scatter layer"

Contributors: Réka Domokos and Donald Kobayashi

The fish functional groups "shallow prey fish" and "mesopelagic scatter layer" play a crucial role in the trophodynamics and shallow prey fish are also an important component in fish landings. However, observations from available surveys only had occasional sightings of these groups and therefore it was not possible to make predictions based on habitat associations (Weijerman, Grüss, et al. 2019). We conducted a thorough review of available published and gray literature to estimate their biomass and spatial distribution (Appendix F).

Biomass and spatial distribution for protected species

Contributor: Stacie Robinson

Data on marine mammals and sea turtles were provided by the PIFSC Protected Species Program[14] and literature (Piacenza et al. 2016). Sea turtles were assumed to be equally distributed among the boxes to 150 m (shallow and mesophotic areas) and spend most of their time in the shallower habitats (Dr. T. Todd Jones pers. comm.). Dolphins spend the day in shallow to mesophotic depth ranges whereas at night they forage in mostly deeper waters (Dr. Erin Oleson pers. comm.). We allocated their distribution accordingly, assuming they spend 25%:30%:45% of their time (24 hours) in respectively shallow, meso- and subphotic habitats. For monk seals, tagging data provided reliable estimates of distribution among the Atlantis boxes and depth dive profiles for vertical distribution (Appendix G).

Table 2. Initial biomass values in metric tons (t) for all functional groups.

Group	Biomass (t)	Source	Assumption
Small phytoplankton	324,438	PIFSC surveys unpublished data, HOTDOGS[a] website	Coastal areas represented by PIFSC RAMP[b] surveys; offshore areas represented by station Aloha
Large phytoplankton	*124,216*[c] (629,400)	PIFSC surveys unpublished data, HOTDOGS website	Coastal areas represented by PIFSC RAMP surveys; offshore areas represented by station Aloha
Microzooplankton	173,201	HOTDOGS website	Coastal areas represented by PIFSC RAMP surveys; offshore areas represented by station Aloha
Meso zooplankton	*390,857* (276,706)	Choy et al. 2016, Steinberg et al. 2008	Coastal areas represented by PIFSC RAMP surveys; offshore

[14] www.pifsc.noaa.gov/psd/

Group	Biomass (t)	Source	Assumption
			areas represented by station Aloha
Large zooplankton	*1,140,208I* (232,442)	Choy et al. 2016, Steinberg et al. 2008	Same as (Choy et al. 2016) decapod and other crustaceans groups
Gelatinous zooplankton	140,173	Choy et al. 2016, Steinberg et al. 2008	Same as (Choy et al. 2016) filter-feeding and carnivorous gelatinous groups
Corals	395,330	https://www.pifsc.noaa.gov/cred/pacific_ramp.php	Biomass = 126 g/m^2 (Ruiz Sebastián and McClanahan 2013)
Leptoseris	36,443	(Veazey et al. 2016), PIFSC unpublished mesophotic surveys	Assume same biomass as shallow water corals: 126 g/m^2
Turf algae	328,578	https://www.pifsc.noaa.gov/cred/pacific_ramp.php	Assumed to be 1% at mesophotic depths. Biomass = 250 g/m^2 (Smith et al. 2001) conversion factors from (Atkinson and Grigg 1984)
Calcareous macroalgae (MA), CCA	238,992 132,269	https://www.pifsc.noaa.gov/cred/pacific_ramp.php, PIFSC mesophotic surveys	Substrate suitability is same as for *Leptoseris* at mesophotic depths with 1.25**Leptoseris* cover based on PIFSC surveys and 0.5 for CCA. Biomass = 140 g/m^2 (Smith et al. 2001) conversion factors from (Atkinson and Grigg 1984)
Fleshy MA	240,239	https://www.pifsc.noaa.gov/cred/pacific_ramp.php, PIFSC mesophotic surveys	Substrate suitability is same as for *Leptoseris* at mesophotic depths with 1**Leptoseris* cover based on PIFSC surveys. Biomass = 447 g/m^2 (Smith et al. 2001) conversion factors from (Atkinson and Grigg 1984)
Shallow filter feeders	1,071	https://www.pifsc.noaa.gov/cred/pacific_ramp.php	Biomass =375 g/m^2 (Wilkinson and Cheshire 1990)
Deep filter feeders	68,689	HURL	Biomass =375 g/m^2 * density * % hard substrate. Cover is biomass/375
Bivalves	8,356	https://www.pifsc.noaa.gov/cred/pacific_ramp.php, HURL	ARMS results multiplied by 1.5 to account for undercounting in shallow water; for meso and subphotic zones HURL densities * 100 to account for

Group	Biomass (t)	Source	Assumption
			undercounting and a biomass of 10 g per bivalve
Squid	169,200	(Choy et al. 2016)	Same as Choy et al. (2016) epi- and mesophotic mollusks groups
Octopus	4,836	Based on commercial fishery data	Fishery is sustainable at F=0.2. Recreational fishery is 5* commercial fishery yield. Biomass = total Yield * F
Infauna (polychaetes)	3,181,629	https://www.pifsc.noaa.gov/cred/pacific_ramp.php	ARMS results multiplied by 10 to account for uncounted spp. for shallow; for meso and subphotic zones assume same density as in Horne et al. 2010
Meiofauna	383,274	https://www.pifsc.noaa.gov/cred/pacific_ramp.php	ARMS results for shallow water; for meso and subphotic zones assume same density as in (Horne et al. 2010)
Benthic carnivores	58,958	https://www.pifsc.noaa.gov/cred/pacific_ramp.php	ARMS results for shallow water; for meso and subphotic zones assume same density as in (Horne, 2010)
Benthic detritivores	158,391	https://www.pifsc.noaa.gov/cred/pacific_ramp.php	ARMS results multiplied by 1.5 to account for larger detritivores (e.g., sea cucumbers)
Benthic grazers	177,560	https://www.pifsc.noaa.gov/cred/pacific_ramp.php	ARMS results multiplied by 1.5 to account for larger grazers (e.g., urchins)
Large crabs and and lobster	19,717	PIFSC Stock Assessment	Fishery is sustainable at F=0.2. Recreational fishery is 3 * commercial fishery yield. Biomass = total Yield * F
Reef corallivores	341	https://www.pifsc.noaa.gov/cred/pacific_ramp.php SPC surveys	
Reef herbivore browsers	1,939	https://www.pifsc.noaa.gov/cred/pacific_ramp.php SPC surveys	

Group	Biomass (t)	Source	Assumption
Reef herbivore grazers	7,376	https://www.pifsc.noaa.gov/cred/pacific_ramp.php SPC surveys	
Reef Parrotfish	2,071	https://www.pifsc.noaa.gov/cred/pacific_ramp.php SPC surveys	
Reef benthic piscivores	1,572	https://www.pifsc.noaa.gov/cred/pacific_ramp.php SPC surveys	
Reef benthic carnivores	4,147	https://www.pifsc.noaa.gov/cred/pacific_ramp.php SPC surveys	
Reef large planktivores	1,100	https://www.pifsc.noaa.gov/cred/pacific_ramp.php SPC surveys	
Reef small planktivores	833	https://www.pifsc.noaa.gov/cred/pacific_ramp.php SPC surveys	
Reef other fish	3,434	https://www.pifsc.noaa.gov/cred/pacific_ramp.php SPC surveys	
Meso benthic carnivores	5,043	HURL, University of Hawai‘i Drazen Lab, Struhsaker 1973, PIFSC ESD BRUV surveys	See Appendix E
Meso planktivores	3,382	HURL, University of Hawai‘i Drazen Lab, Struhsaker 1973, PIFSC ESD BRUV surveys	See Appendix E
Meso and sub benthic piscivores	2,159	HURL, University of Hawai‘i Drazen Lab, Struhsaker 1973, PIFSC ESD BRUV surveys	See Appendix E
Sub benthic carnivores	948	HURL, University of Hawai‘i Drazen Lab, Struhsaker 1973, PIFSC	See Appendix E
Sub planktivores	1,297	HURL, University of Hawai‘i Drazen Lab, Struhsaker 1973, PIFSC	See Appendix E
Shallow prey fish	481	Calculations by Don Kobayashi Appendix F	see Appendix F for assumptions made
Mesopelagic scatter layer	*466,340* (46,634)	Calculations by Reka Domokos Appendix F	We divided the original value by 10 assuming they are spatially clustered - see section

Group	Biomass (t)	Source	Assumption
			"Validating/Sanity check of biomass calculations"
Bottomfish in water column	3,770	PIFSC Stock Assessment	Total biomass =1.3 × exploitable biomass from Stock Assessment
Bottomfish near substrate	826	PIFSC Stock Assessment	Total biomass =1.3 × exploitable biomass from Stock Assessment
Uku	758	PIFSC Stock Assessment	(Nadon et al. 2020)
Roving piscivores	4,129	https://www.pifsc.noaa.gov/cred/pacific_ramp.php towed-diver surveys, meso and subphotic surveys	
Sharks	1,523	https://www.pifsc.noaa.gov/cred/pacific_ramp.php towed-diver surveys, meso and subphotic surveys	
Invertivorous rays	3,473	(Weijerman, Grüss, et al. 2019)	
Manta ray	585	https://www.pifsc.noaa.gov/cred/pacific_ramp.php towed-diver surveys, meso and subphotic surveys	
Monk seals	39	PIFSC Monk Seal Program	See Appendix G for details
Spinner dolphins	101	PIFSC Cetacean Program; www.fisheries.noaa.gov/pr/species/mammals/dolphins/spinner-dolphin.html	
Bottlenose dolphins	214	PIFSC Cetacean Program; www.nmfs.noaa.gov/pr/species/mammals/dolphins/bottlenose-dolphin.html	
Green sea turtle	1545	PIFSC Marine Turtle Program; (Chaloupka and Balazs 2007)	
Hawksbill turtles	153	PIFSC Marine Turtle Program	Assumption that Hawksbill population is about 10% of Green turtle population

Group	Biomass (t)	Source	Assumption

[a]HOTDOGS = Hawai‘i Ocean Time-series Data Organization and Graphical System; details at http://hahana.soest.Hawai'i.edu/hot/hot-dogs/interface.html.

[b]RAMP = Reef Assessment and Monitoring Program, SPC = stationary point count surveys; details at https://www.pifsc.noaa.gov/cred/survey_methods.php.

[c]Values in italics were changed during tuning, new values are in parentheses.

Validating/Sanity-check of biomass calculations

To validate the assumptions made in the estimations of the biomass values, diet and rate parameters of quite a few functional groups, we developed an Ecopath with Ecosim (EwE) model. Validation consisted of meeting two criteria: (1) mass balancing the EwE model; and (2) under a status quo simulation with EwE (i.e., no forcings such as fishing or climate change), all biomass values stay stable (Weijerman et al. 2020). We had to adjust the biomass of some groups by <10%. These changes were also incorporated in the final values of Atlantis. The only group we had to drastically change the initial biomass for (from the estimated 120 g/m^2 to 4 g/m^2) was the mesopelagic scatter layer (Appendix F). This is the group that resides at greater depth during the day and migrates up at night. As spatial data is unavailable, the estimate was based on the assumption that this group was equally distributed around the islands. However, if they occur in clusters it could be that the surveys were conducted in high-concentration areas, hence, assuming a skewed distribution could be appropriate. But since we do not have the data to make these spatial allocations we kept the distribution homogeneous and divided the estimated biomass by 10. We also had to change the biomass of some of the plankton groups. Even though the EwE model was mass balanced with the initial values from the literature, the actual amount of zooplankton far exceeded the amount of phytoplankton leading to a depletion of food for zooplankton. We decreased zooplankton (ZM and ZL) and increased large phytoplankton (PL) making sure the model still mass balanced in EwE and conformed tropho-dynamics rules (Link 2010). In EwE, diet also needed to be adjusted but since Atlantis uses the diet matrix as an availability matrix and other factors determine the actual consumption (e.g., occupying the same space at the right time and fitting in a predator's mouth) we left the original values and checked the realized diet in Atlantis to make sure it corresponded with what is known from the literature.

Life History Parameters

Dynamic rate parameters were obtained from surveys, literature or expert opinion (Table 3, Table 4). For each functional group we used weighted means of species-specific life history data for all parameters where possible. During tuning, some of these values had to be adjusted.

For turtles, monk seals, spinner, and bottlenose dolphins we included a non-predation mortality to represent mortalities from entanglement in marine debris or other human-related causes not specifically represented by the model. On average 1 spinner and 0.5 bottlenose dolphins die in the Hawaiian Islands each year from anthropogenic causes. Bottlenose dolphins and monk seals also interact with bottomfish and shore-based hook-and-line fisheries, respectively, and can steal bait/catches from the hooks.

Table 3. Initial and after tuning (italics) rate parameters for invertebrate functional groups

Group	Growth rate (MUM) (per day)	Consumption rate (per day)	Mortality ml - mQ	Source
Small phytoplankton	0.013 (*0.13*)	NA	0 0	(Weijerman et al. 2013; Choy et al. 2016)
Large phytoplankton	0.014 (*0.14*)	NA	0 0	(Weijerman et al. 2013; Choy et al. 2016)
Microzooplank-ton	0.139	0.040 (*0.010*)	*1E-07* 0	(Choy et al. 2016)
Mesozooplank-ton	0.079	0.0099 (*0.0150*)	0 0	(Choy et al. 2016)
Large zooplankton	0.052	0.0164 (*0.054*)	0 0	(Choy et al. 2016) other crustaceans
Gelatinous zooplankton	0.062	0.0077	0 0	(Choy et al. 2016) filter-feeding and carnivorous gelatinous
Squid	0.0265	0.0033 (*0.0015*)	0 0	(Choy et al. 2016)
Massive Porites	0.00016 (*0.0032*)	0.0011	0 0	(Richmond and Hunter 1990; Weijerman et al. 2013)
Branching Porites	0.00027 (*0.0054*)	0.0011	0 0	(Richmond and Hunter 1990; Weijerman et al. 2013)
Montipora	0.00044 (*0.0088*)	0.0011	0 0	(Cox and Ward 2002; Kolinski and Cox 2003; Weijerman et al. 2013)
Pocillopora	0.00030 (*0.0060*)	0.0011	0 0	(Kolinski and Cox 2003; Weijerman et al. 2013)
Leptoseris	0.000050 (*0.00027*)	0.0011	0 0	Assumption
CCA	0.0054	NA	0 0	(Weijerman et al. 2013)
Calcareous macroalgae	0.0059	NA	0 0	(Weijerman et al. 2013)
Fleshy macroalgae	0.0060	NA	0 0	(Weijerman et al. 2013)
Turf algae	0.081	NA	0 0	(Weijerman et al. 2013)
Shallow benthic filter feeders	0.029 (*0.050*)	0.0037	0 0	See Appendix D
Deep benthic filter feeder	0.0106	0.0013	0 0	See Appendix D
Bivalves	0.0170	0.0021	0 0	See Appendix D
Benthic infauna	0.0263	0.0033	0 0	See Appendix D
Meiofauna	0.0277	0.0035	0 0	See Appendix D
Benthic detritivores	0.0424 (*0.020*)	0.0053	0 *1E-07*	See Appendix D
Benthic carnivores	0.0298 (*0.010*)	0.0037	0 *1E-06*	See Appendix D

Group	Growth rate (MUM) (per day)	Consumption rate (per day)	Mortality ml - mQ	Source
Benthic grazers	0.0225 (*0.040*)	0.0028	0 0	See Appendix D
Lobster	0.0391	0.0049 (*0.0025*)	0 0	See Appendix D
Octopus	0.0210	0.0026	0 0	See Appendix D

Table 4. Key life history parameters for vertebrate functional groups.

Group	k	Infinite length (cm)	Max. age (year)	Age at maturity (year)	Larval duration (days)	Natural Mortality (M)	Source
Reef corallivores	1.50	17.35	10.0	0.60	40	LN(0.01)/-max_age = 0.97	(MacDonald 1981; Tricas 1985; Berumen 2005)
Reef herbivore browsers	0.23	53.8	27.7	3.31	70	LN(0.01)/-max_age = 0.38	(Wilson and McCormick 1999; Nadon et al. 2015)
Reef herbivore grazers	0.8	32.6	27.1	2.12	60	LN(0.01)/-max_age = 0.20	(Thresher et al. 1989; Wilson and McCormick 1999; Choat and Robertson 2002; Longenecker and Langston 2008; Nadon et al. 2015)
Reef Parrotfish	0.73	46.2	15.1	1.70	35	0.30	(Ishihara and Tachihara 2011; Taylor 2012; Nadon et al. 2015)
Reef benthic piscivores	0.10	79.3	24.0	3.86	60	LN(0.01)/-max_age = 0.23	(Nadon et al. 2015)
Reef benthic carnivores	0.41	43.2	10.2	2.82	23	LN(0.01)/-max_age = 0.58	(Wilson and McCormick 1999; Nadon et al. 2015)
Reef large planktivores	0.29	42.3	31.6	5.86	55	LN(0.01)/-max_age = 0.15	(Wilson and McCormick 1999; Longenecker and Langston 2008; Nadon et al. 2015)
Reef small planktivores	0.52	11.8	4.9	0.82	29	LN(0.01)/-max_age = 0.93	(Kohn and Helfrich 1957; Thresher et al. 1989; Fowler 1990; Hawn et al. 2005)
Reef other fish	0.48	32.3	8.1	1.86	121	LN(0.01)/-max_age = 0.65	www.fishbase.org; B. Taylor pers. comm.

Group	k	Infinite length (cm)	Max. age (year)	Age at maturity (year)	Larval duration (days)	Natural Mortality (M)	Source
Meso benthic carnivores	0.30	36.9	6.5	1.9	40	LN(0.01)/-max_age = 0.70	www.fishbase.org and assumptions based on ecological rules
Meso planktivores	0.20	34.5	9.1	2.54	91	0.91	www.fishbase.org and assumptions based on ecological rules
Meso and sub benthic piscivores	0.1	174.5	LN(0.01)/-M = 0.24	4.1	50	0.19	www.fishbase.org and assumptions based on ecological rules
Sub benthic carnivores	0.25	28.2	LN(0.01)/-M = 8.2	3.5	50	0.56	www.fishbase.org e and assumptions based on ecological rules
Sub planktivores	0.30	26.2	5	2.7	50	LN(0.01)/-max_age = 0.92	www.fishbase.org and assumptions based on ecological rules
Shallow prey fish	1.21	31.9	3.48	1.33	120	LN(0.01)/-max_age =1.48	(Kawamoto 1973; Clarke and Privitera 1995; Weng and Sibert 2004; Welch et al. 2013)
Mesopelagic scatter layer	0.80	7.5	5	0.4	50	LN(0.01)/-max_age = 0.92	www.fishbase.org and assumptions based on ecological rules
Bottomfish in water column	0.23	68.4	43.5	4.09	75	LN(0.01)/-max_age = 0.11	(DeMartini et al. 1994; Moffitt and Parrish 1996; Andrews et al. 2012; Luers et al. 2018) A. Andrews, pers comm
Bottomfish near substrate	0.27	57.6	47.2	5.07	75	LN(0.01)/-max_age = 0.11	(DeMartini et al. 1994; Moffitt and Parrish 1996; Andrews et al. 2012; Luers et al. 2018) A. Andrews, pers comm
Uku	0.14	81.0	32	4.3	120	0.10	(Nadon et al. 2020)

Group	k	Infinite length (cm)	Max. age (year)	Age at maturity (year)	Larval duration (days)	Natural Mortality (M)	Source
Roving piscivores	0.22	142.7	LN (0.01)/-M=12.4	3.21	120	0.37	(Sudekum et al. 1991; Nadon et al. 2015)
Sharks	0.08	368.2	32.4	4.3	360	LN(0.01)/-max_age = 0.14	(Struhsaker 1973; Cortés 2000)
Invertivorous Ray	0.03	257.9	28	8.3	360	0.07	(Schluessel 2008; Schluessel et al. 2010; Dale and Holland 2012); www.fishbase.org
Manta Ray	0.1	796.0	LN(0.01)/-M = 34.8	4	360	0.13	www.fishbase.org and assumptions based on ecological rules
Monk Seals	0.39	230	30	5	315	LN(0.01)/-max_age = 0.15	(Winship et al. 2001)
Spinner Dolphins	0.59	220	20	7	335	LN(0.01)/-max_age = 0.15	(Carretta et al. 2019); expert opinion
Bottlenose Dolphins	0.59	385	50	11	365	LN(0.01)/-max_age = 0.09	(Carretta et al. 2019); expert opinion
Green Sea Turtle	0.09	106	70	25	365	LN(0.01)/-max_age = 0.07	(Piacenza et al. 2016), T.T. Jones pers. comm.
Hawksbill Turtles	0.09	100	40	20	365	LN(0.01)/-max_age = 0.12	(Van Houtan et al. 2016), T.T. Jones pers. comm.

Predator-prey interactions

Diet data for reef fish came from literature (Humphreys and Kramer 1984; Sudekum et al. 1991; Bruggemann et al. 1994; Meyer et al. 2001; Chen 2002; Choat et al. 2002; Glynn 2004; Kulbicki et al. 2005; Papastamatiou et al. 2015; Kelly et al. 2016; Nalley 2020), and fishBase. For pelagic functional groups (zooplankton, micronekton) diet data was derived from literature (Bernal et al. 2015; Choy et al. 2016; Choy et al. 2017; Gloeckler et al. 2018). Little is known about the diet of subphotic species but they are assumed to be more generalist although niche partitioning occurs (Hopkins and Gartner 1992); since food is scarce most species have adapted to be able to eat a wide source of prey items depending on their location in the water column (benthic, benthopelagic) and forage behavior (hunter, ambush predator) (Gartner Jr et al. 1997; Drazen and Sutton 2017). Bottomfish diet is better documented (Haight et al. 1993; DeMartini et al. 1996; Seki and Callahan 1988; B. Schumacher unpubl data; C. Kelley unpubl data; J. Drazen unpubl data). Dolphin diet came from (Trites and Pauly 1998; Benoit-Bird 2004; Bearzi 2005) and diet data for monk seals came from isotope and fecal analyses (Appendix G). In general, hawksbill turtles eat predominantly sponges whereas green turtles eat algae. However, since sponges are limited in Hawai'i, the diet of hawksbill is almost identical to that of green turtles (T.T. Jones, NOAA-PIFSC pers. comm). Invertebrate diet came from an unpublished PIFSC database for the small invertebrates and from literature for the macroinvertebrates (Moriarty 1982; Choy 1986; Stimson et al. 2007; Bell 2008) and suspension feeders (Bak et al. 1999; Houlbrèque et al. 2004; Rossi et al. 2004).

The Atlantis model uses an availability matrix where the fraction of prey available to predators is defined. Actual consumption depends on temporal (day/night) and spatial overlap. Further restrictions to consumption are based on the gape size of the predator if it eats age-structured prey and on whether a prey can hide in the substrate and hence become less available. Predatory fishes show significant correlations in both their maximum and median prey size with body size and also with gape size (Dunic and Baum 2017). Gape size is a fraction of how large the prey can be compared to the body size of the predator.

For all functional groups except filter feeders we assumed a Holling Type II functional response. For filter feeders we assume a Holling Type I functional response (Houlbreque *et al*., 2004).

Other ecological dynamics

Movement — Since seasonal variation in temperature is small around the inhabited Hawaiian islands, we assumed there was no seasonal movement for any group as was shown for lobsters (O'Malley and Walsh 2013). Some species migrate for a short period to spawning grounds but we did not explicitly include these spawning migrations.

Mortality — Mortality in Atlantis is mostly determined through the predator-prey interaction. However, to capture other mortalities, mortality can be applied as linear (e.g., disease, old age) or quadratic (density-dependent) and is used to tune the model to avoid extinctions and obtain reasonable estimates of modeled abundance in comparison to observed values. Atlantis also has the option to include mortality related to starvation, oxygen limitation, or ocean acidification. For the HI Atlantis model, we used 0.0001 d^{-1} for starvation mortality and have not used the oxygen limitation mortality. For simulations including ocean acidification we included a response curve from a meta-analysis (see the "Environmental drivers" section and Appendix B).

Spawning period — Reef fishes spawn monthly around the full moon with peak spawning in the summer months. To simplify this, we only included the summer months. Spawning patterns for bottomfish, uku, and jacks were compiled by C. Kelley from various literature sources (unpubl. report; Table 5). Dolphins, monk seals, sharks, rays, and turtles were assumed to have offspring in the summer months.

Table 5. Summary of bottomfish reproductive seasons (compiled by C. Kelley of University of Hawai‘i, Hawai‘i Undersea Research Laboratory).

Species	J	F	M	A	M	J	J	A	S	O	N	D
E. quernus												
Caranx ignobilis												
C. lugubris		?	?	?	?	?	?	?	?			
P. cheilio								?	?			
Seriola dumerili												
A. rutilans	?	?							?	?	?	?
Aprion. virescens												
E. carbunculus												
E. coruscans												
Lutjanus kasmira												
P. auricilla												
P. filamentosus												
P. sieboldii												
P. zonatus				?	?	?	?		?			

Recruitment — There are several options for recruitment in Atlantis. We defined a Beverton-Holt relationship for fish species. For the recruitment of mammals, sharks, rays, and sea turtles, each adult is assumed to have a fixed number of pups/calves. Recruitment and recruitment success of most stocks are uncertain and difficult to estimate, therefore these are tuned in the model to achieve realistic abundance levels for the different stocks, and to a lesser degree are based on literature values.

Structural complexity — Rugosity was visually estimated by PIFSC-CRED survey divers whereby approximately each 25 cm height increase resulted in a point higher in the rugosity

score with values bounded between 1 (flat) and 5 (highly complex). Atlantis distinguished geomorphological structures that can provide complexity (such as the boulders around Ni'ihau) and structural complexity from bioengineers (corals and crustose coralline algae). Since the rugosity scores were an aggregated value, we accounted for coral cover and subtracted the following amounts from the rugosity values; coral cover < 10% resulted in a subtraction of 0.5; coral cover between 10 and 15% a subtraction of 1, coral cover between 15% and 20% a subtraction of 1.5 and if coral cover was >20% we subtracted 2. In the model, rugosity increases with coral growth and decreases with coral erosion or coral predation. We included erosion by boring urchins (BG) and benthic carnivores (BC) and coral predation by parrotfishes (RPA). Corallivorous butterflyfishes just eat the coral polyps and were assumed not to contribute to bioerosion. We also included a relationship between complexity (or rugosity) and prey availability whereby prey becomes less available to predators when complexity increases (Bozec et al. 2015).

Harvest submodel

Atlantis allows for different ways to include fishing. For example, you can force fishing by a functional group specific fishing mortality, total catches per functional group, total catches per functional group per fishery fleet and/or gear type or by (dynamic) effort. In HI Atlantis, we included reef fish fishery as catches by functional group by spatial area by gear type (spear, net, line, other). The bottomfish fishery was divided into a commercial and recreational fleet and both were included as catches by functional group by spatial area by year.

Historic commercial landings

Contributor: Zack Oyafuso and Jennifer Raynor

Hawai'i DAR commercial data reported from 1995 to 2017 was requested from the West Pacific Fisheries Information Network[15] by species, area, gear type and year. We received 128,761 data records including pelagic species and unknown species. About 1,200 records, making up 20.9 t in weight had no associated species and were deleted from further analysis. For 406 observations (7.5 t of weight), only the common (Hawaiian) name was given and we included an assumed species name. For example, "wana" is the Hawaiian word for urchin so we included the collector's urchin as species-specific record as these were mostly encountered in the catch data. The remaining records all included a scientific species name, which we assigned to functional groups. All pelagic species (mostly tuna) and records where both numbers and weight were zero also were excluded leaving us with 94,659 usable records. We corrected two apparent data entry errors, one each for *Caranx lugubris* and *Coris flavovittata*. In each case, we divided the reported value by 10. Two-hundred-eighteen species had numbers caught but no associated weight. For the 28 fish species we used the mean length from fish surveys or the common length from fishBase and calculated the mean weight. For the invertebrates we assumed their weight was 5 g for small mollusks and crabs and 10 g for larger invertebrates. We then multiplied the mean weight by the numbers caught. All species were allocated to the appropriate functional group and we computed the annual catch per year per fishery reporting zone per functional group.

[15] https://www.pifsc.noaa.gov › wpacfin

In ArcGIS, we allocated each fishery reporting zone to the corresponding Atlantis box. The coastal reporting zones are a fixed distance from shore so in some cases it represented the 0–150 m and in others 0–400 m (or deeper) depth zone. Depending on the species we allocated the catches to the reef fish, mesophotic or subphotic groups. As catches are reported per trip it is possible that, for example, reef fish species are reported from a reporting zone offshore if that was the main area of fishing, so we inspected each record and allocated them to the appropriate Atlantis box based on the depth strata of that species. For functional groups that span the entire 0–400 m depth (e.g., sharks, invertebrates) or just the top 150 m (uku, piscivores), we allocated 50% of the catches as reef fish catches, 30% as mesophotic piscivore catches and 20% as subphotic piscivore catches and 60% reef fish and 40% mesophotic fish, respectively. For invertebrates we used the relative catch composition per gear type. For example, 95% of urchins (functional group benthic grazers) were handpicked so we assumed they were all handpicked from shore in the shallow areas. Squid (functional group CEP) was caught for 25% by inshore handline which can extend to 150 m, 38% by "iki-shibi" which operates in waters >30 m and 20% by bottom/deep-sea handline and we assumed that was also in waters 150–400 m and 12% by whipping. So we allocated the catches as 50% in 30–150 m and 50% in 150–400 m of the Atlantis areas closest to the reporting zones. Finally, we allocated the invertebrates caught by shoreline/gear types and all reef fish species to the reef fishery and all others (bottomfish, sub- and mesophotic fish and invertebrates caught by deep set gear types) to the bottomfish fishery.

Historic recreational landings

Contributor: Zack Oyafuso

Since commercial landings are poor reflections of the actual total catches for reef fish (Weijerman et al. 2013; McCoy et al. 2018), we used landings data from the Ocean Tipping Point (Wedding et al. 2017) for the recreational coral reef fish landings. Total recreational landings for the t^{th} year, s^{th} coral reef functional group, b^{th} Atlantis Box and g^{th} gear type (C_{tsbg}) were calculated using data sets from the Marine Recreational Information Program (Williams and Ma 2013; McCoy et al. 2018). Reliable time series data on total recreational landings are only available on an archipelagic scale from 2004 to 2015 ($C_{ts..}$). Compositional catch data were available across islands (index i) and gears for each functional group ($p(i, g|s)$) and are assumed to be constant across years. Recreational reef catch for the t^{th} year, s^{th} coral reef functional group, i^{th} island and g^{th} gear type (C_{tsig}) was calculated as: $C_{tsig} = C_{ts..}\, p(i, g|s)$. Lastly, compositional data across Atlantis boxes within islands for each gear (assumed constant across years) were used to disaggregate island-level catch to Atlantis box-level catch, calculated as: $C_{tsbg} = C_{tsig}\, p(b|i, g)$. For the years between 1995–2003 and 2016–2017, not covered by the recreational dataset, values were imputed by bootstrapping values from 2004 to 2015. For bottomfish recreational landings we used a 1:1 ratio (commercial to recreational landings) as an approximation of the unreported recreational catch used by the PIFSC stock assessment group (Langseth et al. 2018). For other subphotic and mesophotic fishes and all invertebrates we assumed a 1:1 commercial to recreational catch ratio.

Step 4. Model Calibration and Validation

To calibrate the model we followed best practices identified in Pethybridge *et al*. (2019) and simulated: (1) no fishing and (2) fishing with incremental increases. To validate the model we forced it with historical fishing and ocean changes (i.e., a hindcast simulation) and assessed model skill (Stow et al. 2009; Olsen et al. 2016). We also compared the modeled trophic structure with other tropical reef systems.

Calibration: No Fishing

We first tuned the model in a control simulation (no fishing or other external stressors) to make sure no group became extinct or had biomass values of >5 times initial biomass after a 100-year simulation (Figure 5, Appendix I). We also checked that numbers-at-age and weight-at-age stayed between 0.5 and 1.5 times the initial conditions and were as expected (i.e., decrease in numbers from juveniles to older age classes; Figures 6 and 7, Appendix I). Lastly, we checked the realized diet from the model output with the known diet from the literature.

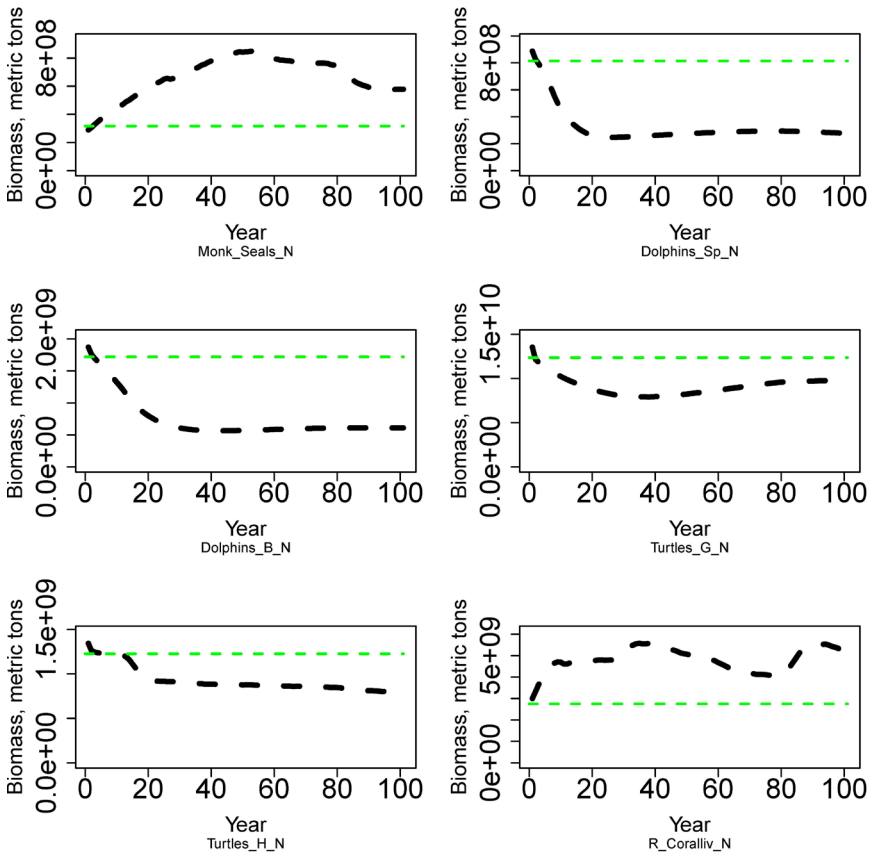

Figure 5. Biomass trajectories for 6 functional groups of a 100-year simulation with no external disturbances. The dashed green line is the calculated biomass at carrying capacity (i.e., B0) or initial biomass for reference.

Biomass trajectories of other functional groups are in Appendix I. N=Nitrogen, SP=spinner, B=bottlenose, G=green, H=hawksbill. R=Reef.

Dolphins decreased but stabilized as did the turtle groups to a lesser extend (Figure 5). It could be that our initial biomass was too high for these groups. Groups that were exploited by the fishery recovered and reached a new equilibrium as can be expected when released from fishing pressure (Appendix I).

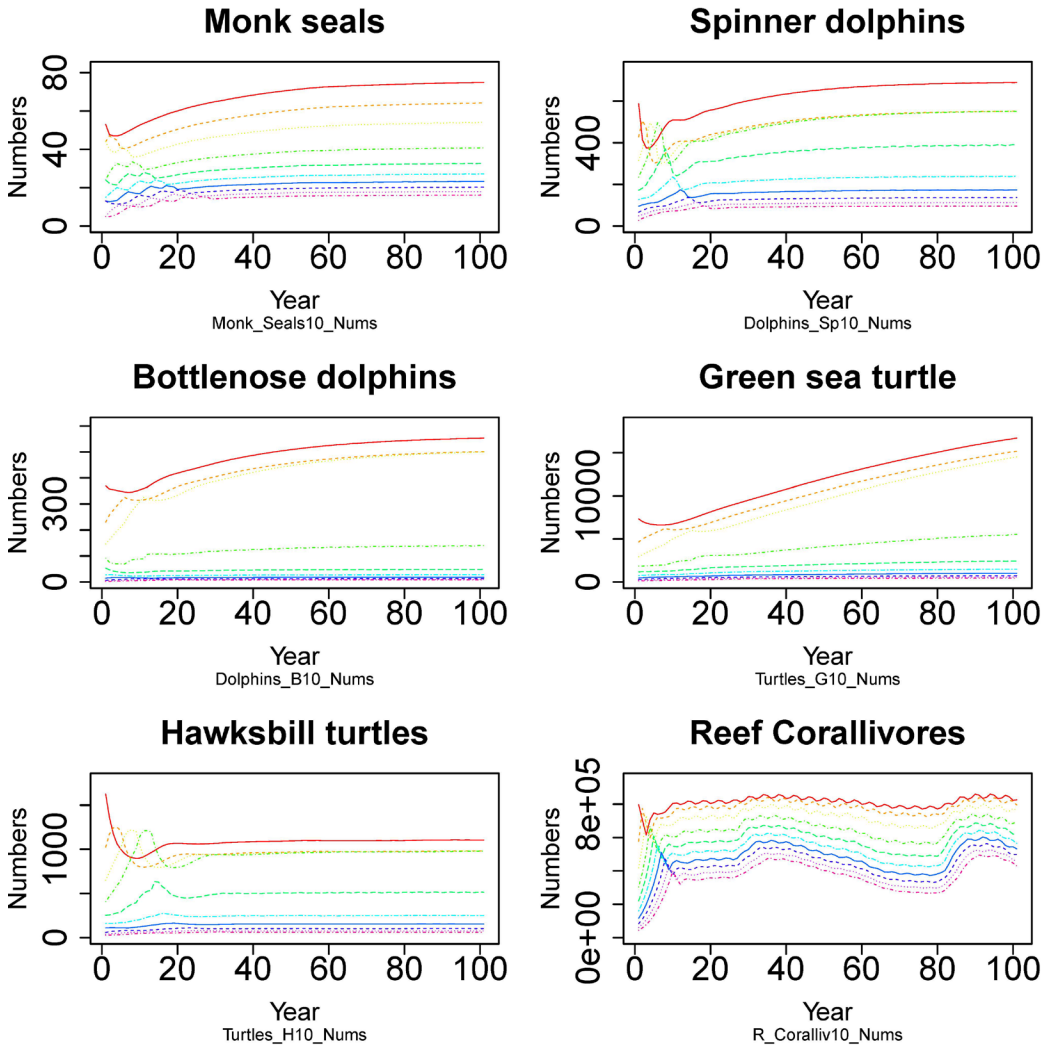

Figure 6. Numbers-at-age for 6 vertebrate functional groups of a 100-year simulation with no external disturbances.

Rainbow colors represent the age classes with red being the youngest and violet the oldest age class. Numbers-at-age of other vertebrate functional groups are in Appendix I.

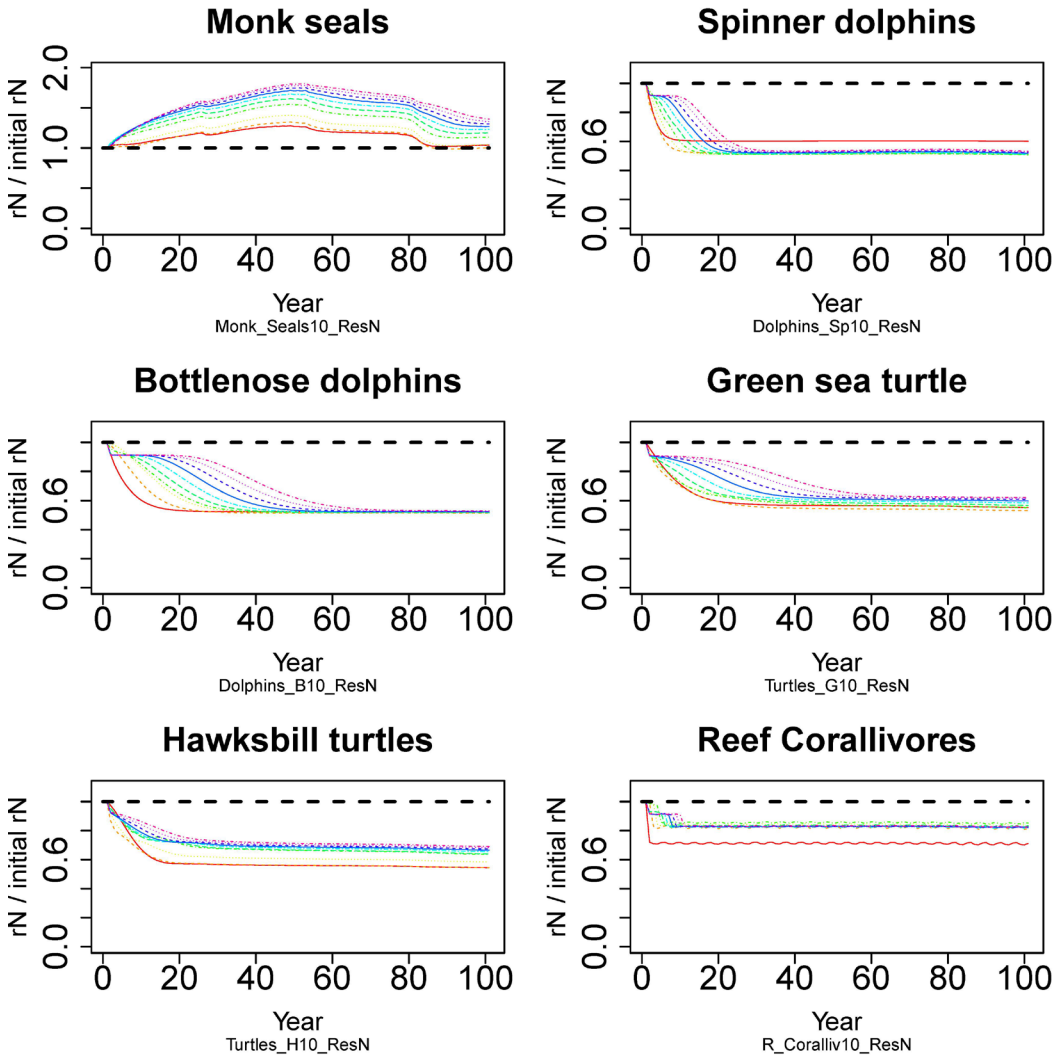

Figure 7. End to initial ratio of weight-at-age for 6 vertebrate functional groups of a 100-year simulation with no external disturbances.

Rainbow colors represent the age classes with red being the youngest and violet the oldest age class. Weight-at-age of other vertebrate functional groups are in Appendix I.

Calibration: Incremental increase in fishing mortality

To check productivity of the groups, we forced the model with incremental increases in fishing mortality (*mFC*) and checked the catches with equilibrium curves (Figure 8). We ran the model for 30 years to reach stability and saved the results of the last 5 years of the catches. We increased annual fishing mortality rate to 0.05, 0.1, 0.2, 0.4, and lastly 0.5. Using the mean of the last 5 years of catches of each simulation, we plotted the catch equilibrium values to make sure that with increases in fishing mortality (on x-axis), the catches increase (y-axis) until they reach a maximum sustainable yield (top of the curve) after which catches decrease as the remaining standing spawning stock declines below a critical size.

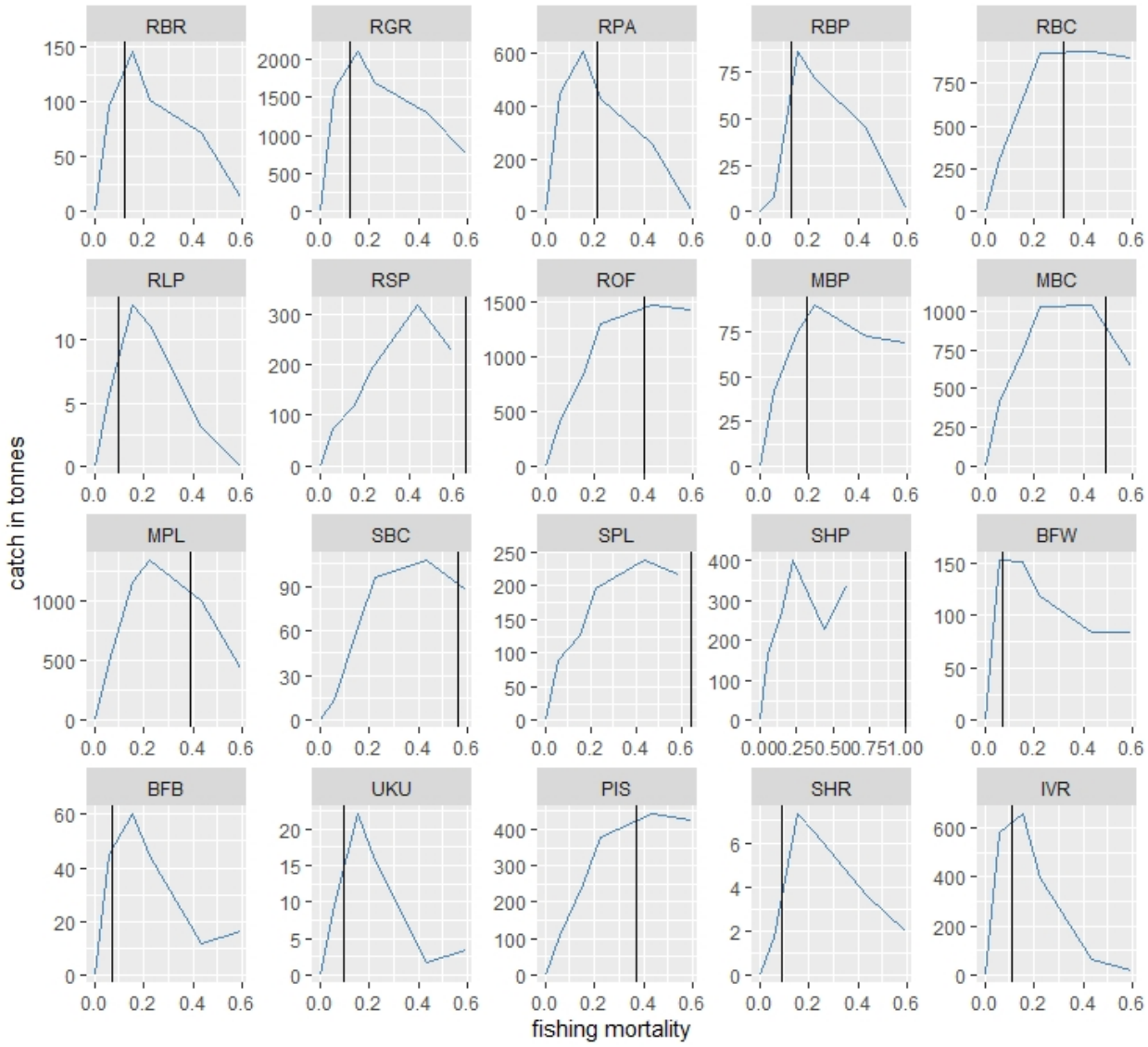

Figure 8. Catch equilibrium plots of targeted functional groups. Catch (blue line) is plotted against fishing mortality rates (F=0, 0.05, 0.10, 0.20, 0.40, 0.60). Black vertical line is the natural mortality added for comparison.

X-axis is fishing mortality rate per year, y-axis is catch in tonnes. Catches are the mean of the last 5 years of a 30-year simulation.

Validation: Historical fishing

Most of our data sources, represent 2010–2015 conditions. To account for the harvest of targeted species, we started the model in 1985 and let the model run for 10 years without any harvest to let exploited groups recover assuming that their biomass represents 1995 conditions. We forced the model with historical catch time series from 1995 to 2017 (including recreational as well as commercial catches) and compared the observed total catches with the modeled total catches. Modeled catches corresponded well with observed catch time series but biomass of some groups kept increasing so we added 'unreported catches' for those groups (Weijerman et al. 2015),

which resulted in higher modeled catches compared to the catch time series for some groups such as grazers (RGR), parrotfishes (RPA) and benthic carnivores (RBC, ROF) (Figure 9).

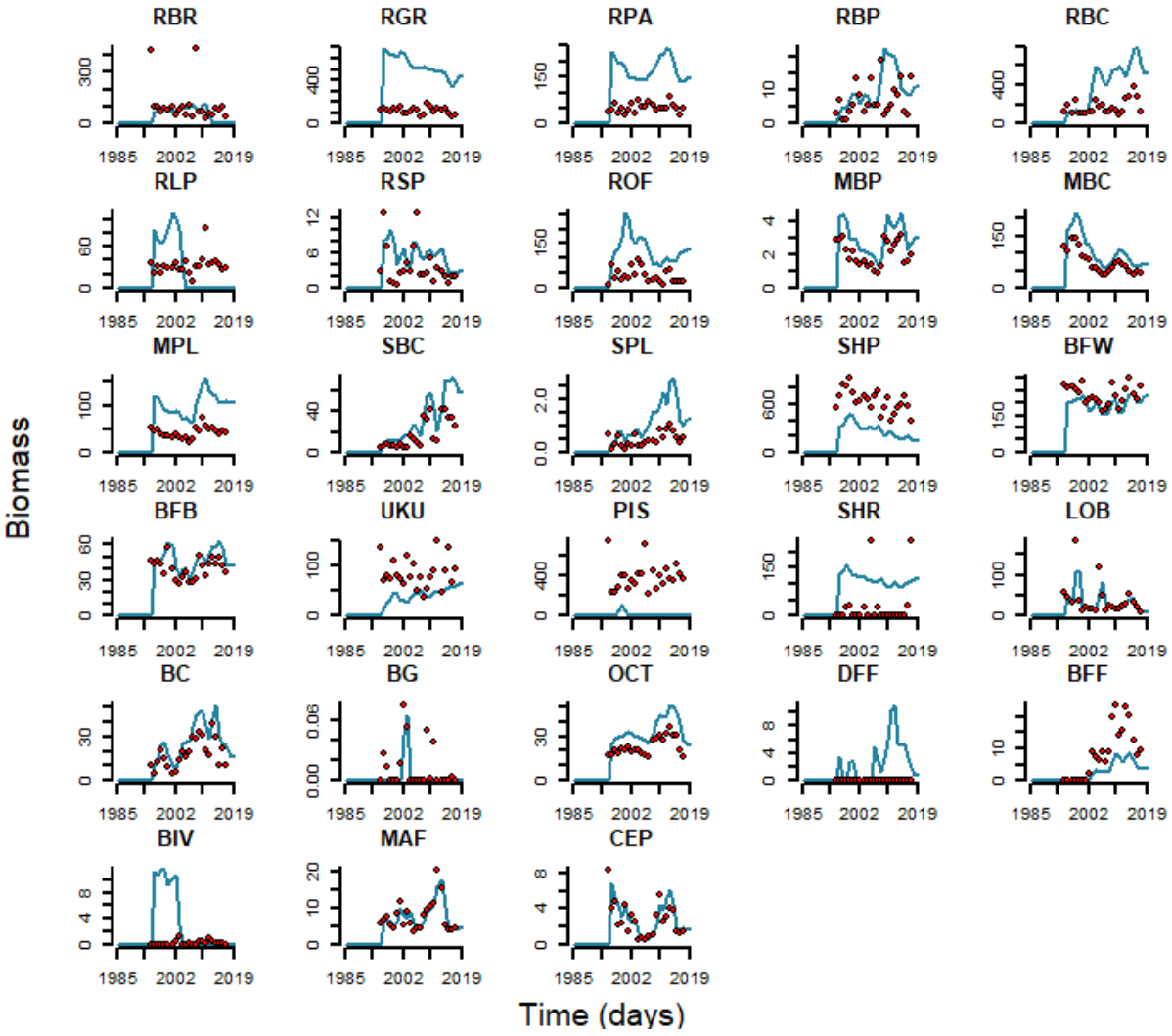

Figure 9. Comparison of observed (red dots) and modeled (blue line) historical time series of catches per functional group.

Codes represent functional groups explained in Table 1. Y-axis shows the biomass of the catch in tons.

We then explored the model's ability to mimic catches per gear type using a fixed fishing mortality rate (*mFC*). We used the first 5 years of catch and biomass to estimate the daily fishing mortality *mFC* according to 1-exp (-*F*/365) whereby *F* the instantaneous fishing mortality calculated as: -LN (1-*mu*) and *mu* is the discrete exploitation rate: Catch/Biomass. Then tuned the *mFC* values until modeled catches were similar to observed catches (Figure 10). We validated model skill by using six complementary model skill assessment methods (Appendix J; Stow et al. 2009; Olsen et al. 2016). Overall model skill assessments were reasonable for the groups we did not change the catches for (non-target groups and invertebrates) and naturally not

as good for the groups we increased the catches for, such as grazers (RGR), parrotfishes (RPA), and goatfishes/snappers/squirrelfishes (RBC).

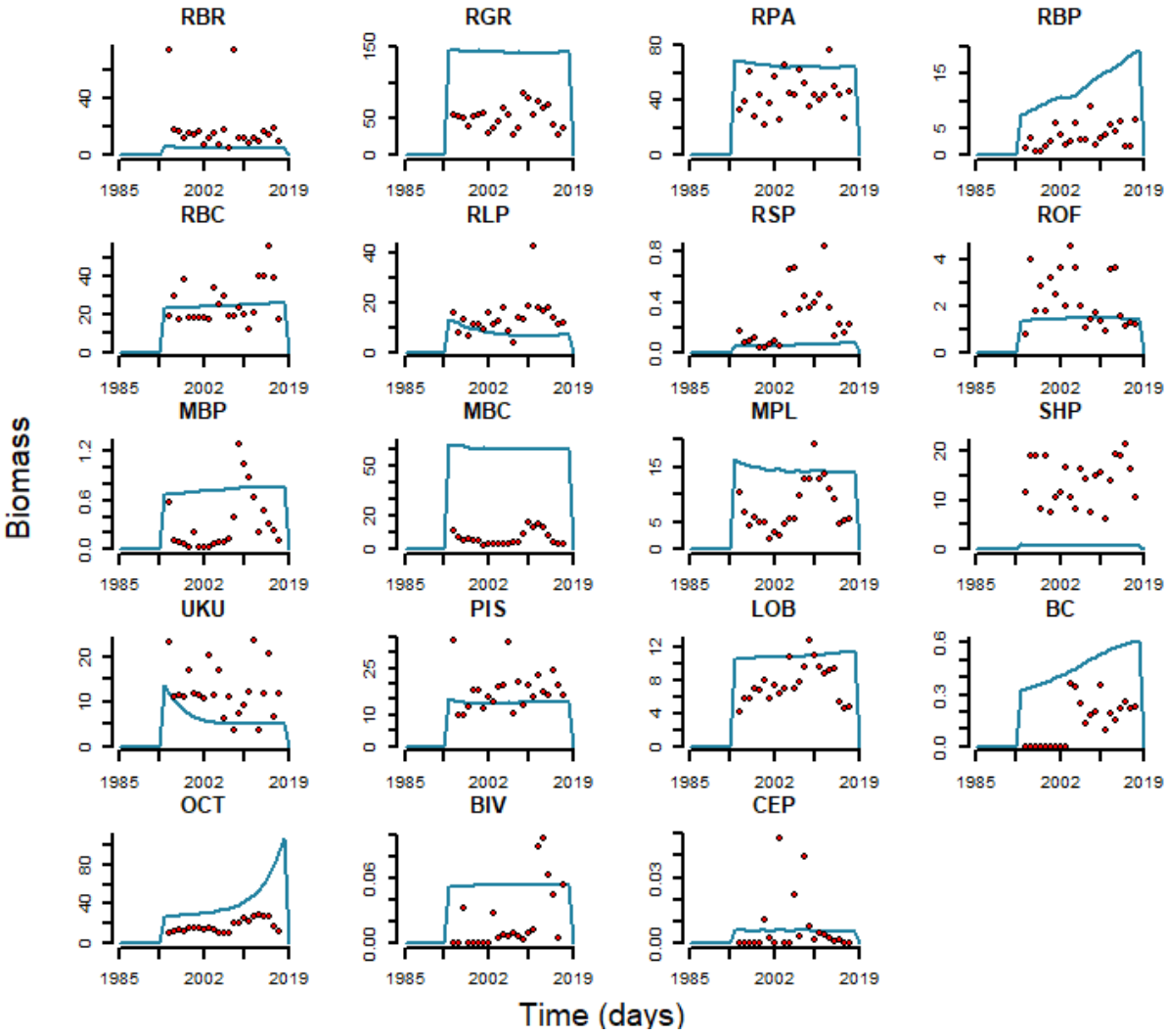

Figure 10. Comparison of observed (red dots) historical time series of spearfish catches per functional groups and modeled (blue line) catches with a gear-specific fixed fishing mortality.

Comparison plots for other gear types appear in Appendix J.

As we are interested to see if the model can mimic the trends in biomass, we standardized the observational and modeled data to the maximum value per functional group trends (Figure 11). Sharks, uku, and shallow prey fishes are a bit higher in the model compared to observational data but this could be because the observational data is just from shallow (<30 m) reef surveys while the model takes into account the total biomass across all depth ranges where the groups occur. Also, reef surveys do not include soft bottom where (juvenile) prey fish are commonly encountered. All other groups showed a good overlap.

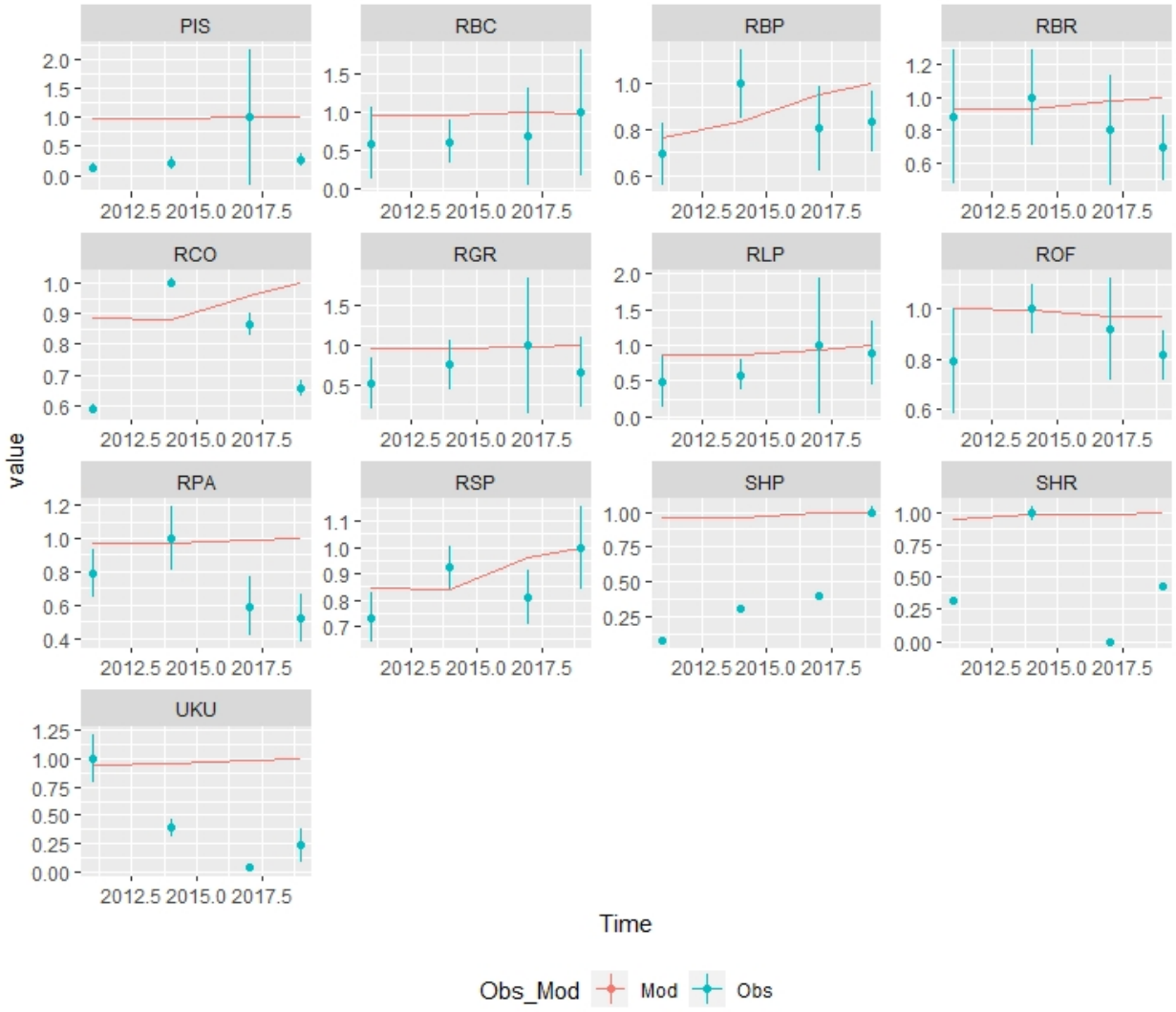

Figure 11. Comparison of modeled (Mod; red line) and observed (Obs; blue dots with 1SE) standardized biomass of fish functional groups.

To validate the modeled green turtle and monk seal biomass, we used visual observation count data of nesting females on French Frigate Shoals for the turtles and monk seal counts around the main Hawaiian Islands. Again, since we are interested in the trend we standardized these counts to the maximum and compared that to the standardized modeled biomass of green turtles and monk seals (Figure 12). For bottomfish we had CPUE-derived relative biomass data of the exploited bottomfish groups. We standardized those values and since ōpakapaka (*Pristipomoides filamentosus*) is the most common species caught, we assumed this trend to be similar to the BFW modeled group (Figure 12). However, because we allowed exploited groups to recover from fishing by not implementing any catches in the first 10 years, the bottomfishes increased in biomass and when fishing started in 1995 decreased (Figure 12). The tail of the modeled biomass shows a stable biomass which corresponds fairly well with the CPUE–derived biomass (blue dots).

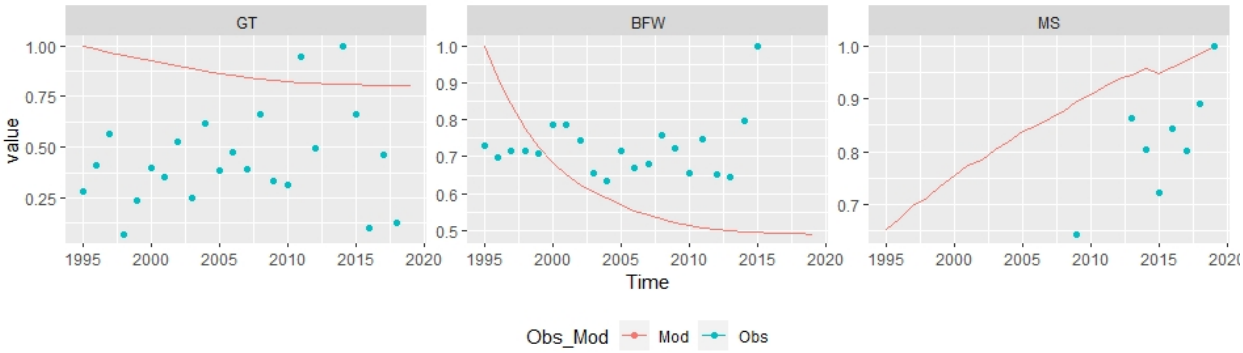

Figure 12. Comparison of modeled (Mod: red line) and observed (Obs: blue dots with 1SE) standardized biomass of green sea turtles (GT), bottomfish (BFW), and monk seals (MS) functional groups.

We also compared the modeled and observed sessile benthic groups (Figure 13).

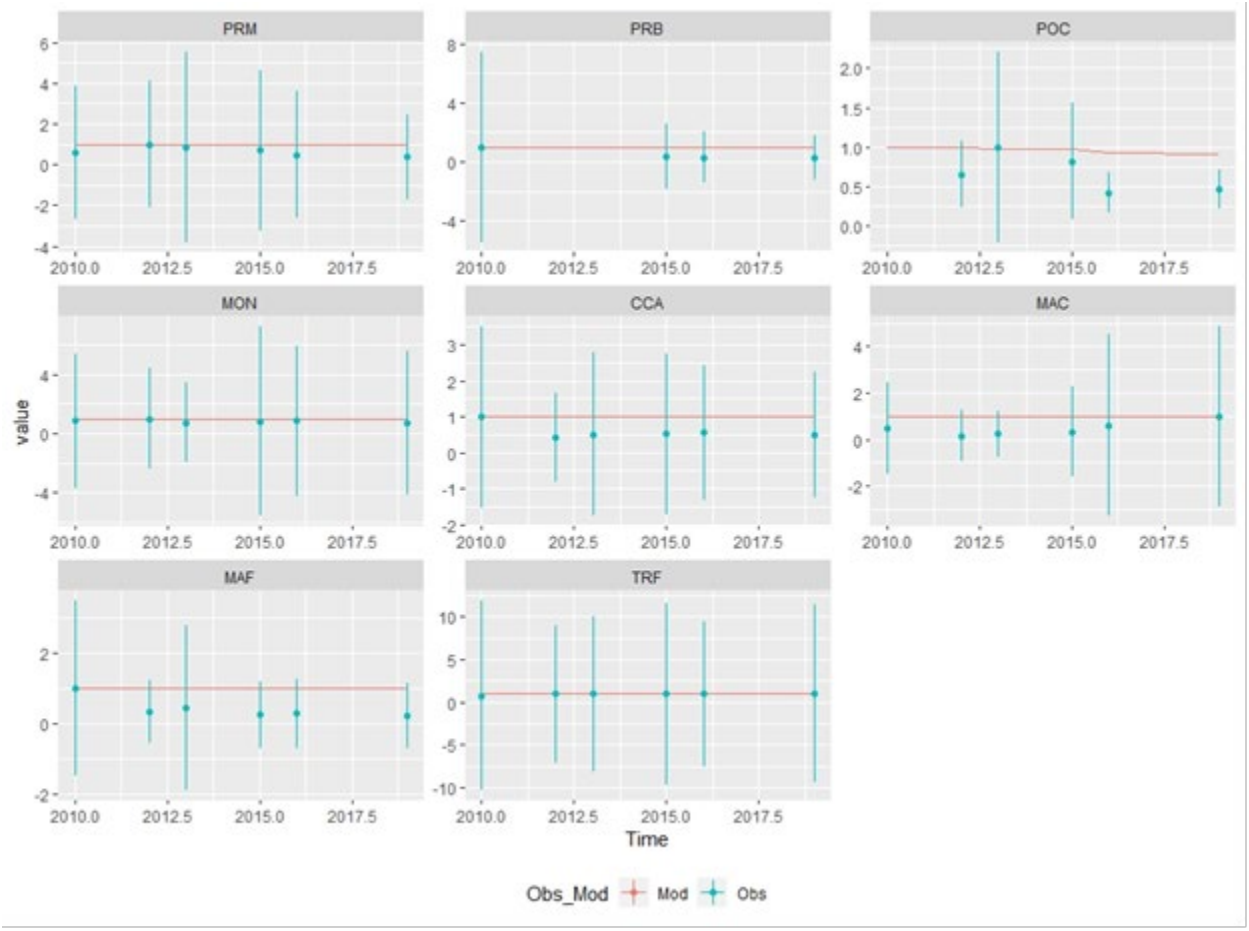

Figure 13. Comparison of modeled (Mod: red line) and observed (Obs: blue dots with 1SD) standardized cover of sessile benthic groups.

Validation: Modeled trophic structure of the community

General ecological rules dictate that the biomass of lower trophic levels is higher than the biomass of higher trophic levels, i.e., the Lindeman trophic pyramid with apex predators at the top and primary producers and detritus eaters at the bottom. The positive correlation between trophic level and size in fish (Jennings et al. 2007) enabled using trophic level as an estimate of size. Previous studies have shown strong linear relationships between log-biomass and trophic level (Kolding et al. 2016). To look if this relationships held true for our modeled system, we aggregated the biomass of our groups in five trophic level (TL) bins: 2–2.49, 2.5–2.99, 3–3.49, 3.5–3.99, and 4 or higher. Conforming to ecological rules we see a clear decrease in biomass with an increase in size (or TL; Figure 14).

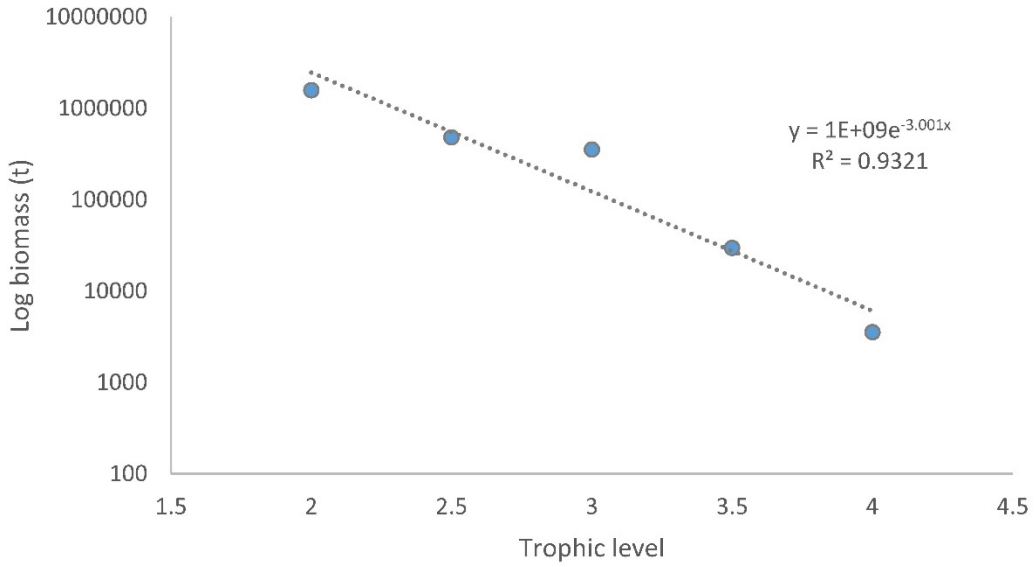

Figure 14. Relationship between the log biomass and size represented by the trophic level of the marine community at initial conditions.

Step 5. Model Uncertainty

Uncertainties in model output can originate from multiple sources, e.g., parameter settings, initial conditions (parameter uncertainty), simplifications of ecological processes (structural uncertainty), and the application of fisheries. Given the complexity and computational costs of running Atlantis, we need to know which groups are most sensitive to parameter uncertainty so that we can address these sensitivities in future scenario simulations by bounding the parameters of those groups between a possible minimum and maximum value and getting an envelope of uncertainty around the model results (Hansen et al. 2019; Bracis et al. 2020).

Sensitivity analyses, aiming to quantify the relationships between model inputs (especially parameters) and the response, are common diagnostic tools used in model development and validation. Sensitivity analyses are used to identify critical and non-critical model parameters. Such analyses help focus efforts around estimation and calibration of the important parameters and provide an assessment of whether the model sensitivity reflects processes that have an impact on the dynamics of the natural ecosystems.

We conducted sensitivity analysis in four model areas: (1) recycling of nutrients; (2) groups with high trophic impact; (3) biomass of meso- and subphotic groups (excluding the bottomfish and uku groups); and (4) parameters of pH and temperature effect size.

Recycling of nutrients

Atlantis has various optional routines that affect the nutrient dynamics. Since our model represents an oligotrophic system, the recycling of nutrients is key to the overall productivity of the system. Processes that influence nutrient turnover and availability in vertical water layers include water column mixing, atmospheric deposition (especially important for waters around the volcanically active Hawai‘i Island), resuspension, and decay (burial of nutrients). To check the model sensitivity to these variables, we developed a NPZD (nutrient, phytoplankton, zooplankton, and detritus) model and compared model output with and without these options included in the model dynamics. We looked at the change in phytoplankton between initial biomass and the end biomass after a 5-year simulation using the parameterized NPZD (nutrients, phytoplankton, zooplankton and detritus) model. The objective was to keep the end–to–start biomass ratio < 3 (Figure 15).

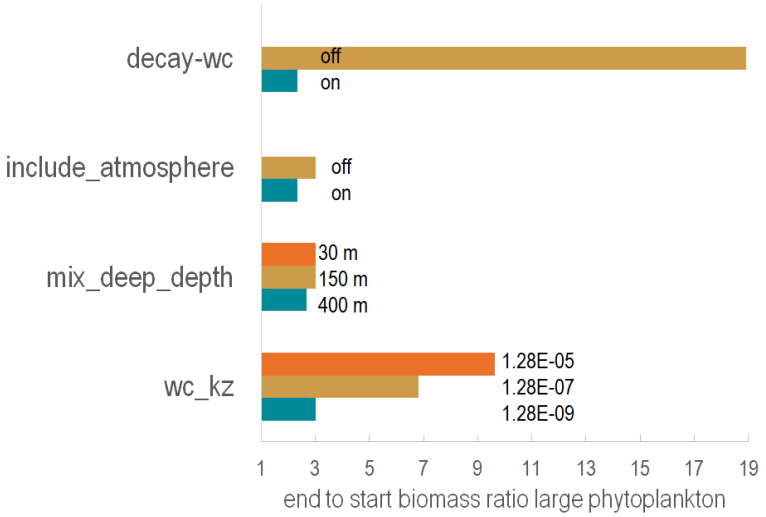

Figure 15. Ratio of end to start biomass of the large phytoplankton group based on a 5-year simulation run adding the decay function (decay-wc), including atmospheric deposits (include_atmosphere), three depths set as the deep mixing depth (mix_deep_depth) and the water column mixing coefficient (wc_kz).

Based on these sensitivity results (Figure 15), we included the decay function and atmospheric deposits (Carrillo et al. 2002), set the deep water mixing depth at 400 m and the water column mixing coefficient at $1.28*10^{-9}$.

Groups with high trophic impacts

The Ecopath software (Christensen and Walters 2004) can assess the relative trophic impact the change in biomass of one group has on another group in an ecosystem by simultaneously assessing the direct predator-prey interaction and the indirect consequences of both positive and negative impacts of trophic interactions (Ulanowicz 1986). Based on these mixed trophic impact factors of the developed EwE model for Hawai‘i (Weijerman et al. 2020), we identified the species with the highest impact factors, i.e., the functional group for which a biomass change has the most influence on other groups. The following criteria were used: (1) the sum of the absolute impact factor across all functional groups was at least 4; and (2) the number of functional groups impacted was at least 6. The resulting groups were the following: Sharks, Large Phytoplankton, Large Zooplankton, Medium Zooplankton and Detritus (Appendix H). This is very important information and in any application of the HI Atlantis model, the user is advised to do multiple simulations to account for this sensitivity. For example, the initial biomass and growth rate can be changed by ± 25% for one group at a time (8 simulations) and for the combined groups with the highest change (2 simulations). The subsequent results will provide an uncertainty envelope which can then be taken into account.

Biomass of meso- and subphotic group

Lastly, because biomass estimates of the meso- and subphotic groups (other than the 2 bottomfish groups and uku) were not available and were estimated based on assumptions (see “Step 3. Model initialization” and Appendix E), we conducted a Monte Carlo assessment

whereby the biomass of the 5 meso- and subphotic functional groups was allowed to change with ±30%. From the mixed trophic impact analysis we know that these groups mostly influence each other but also bottomfish that feed on substrate invertebrates (BFB) and octopus (Appendix H). Results from 20 Monte Carlo simulations, each trying 15 Ecopath input value combinations, show that the absolute biomass of the 5 meso- and subphotic functional groups changed minimally ± 0.05 g/m^2 for subphotic planktivores and at a maximum of ± 0.23 g/m^2 for mesophotic benthic carnivores, likely resulting from predator-prey relations, but that through trophic relations the biomass of BFB and octopus did not really change with a mean SD of 0.0006 and 0.0001, respectively (Figure 16). We therefore conclude that even though the biomass of the meso- and subphotic groups could be 30% more or less, model outcome will be similar.

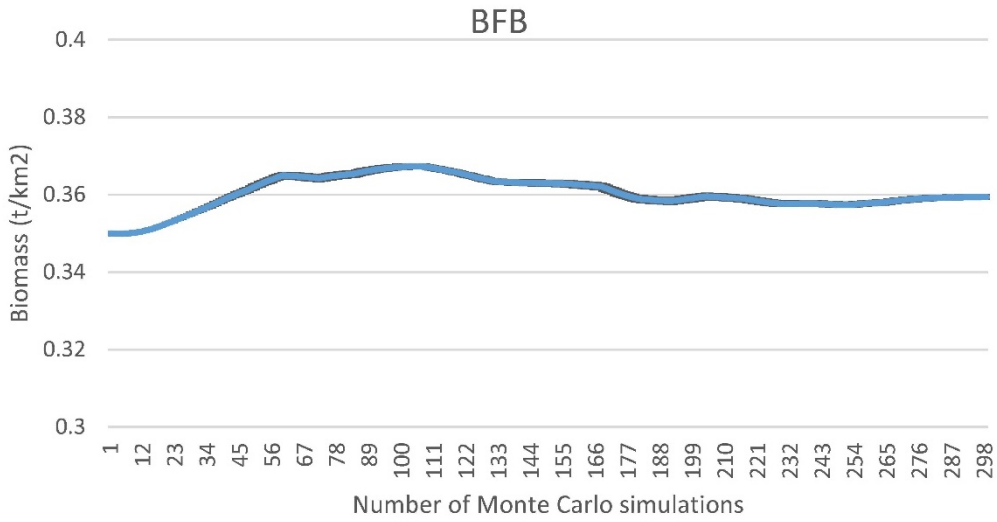

Figure 16. Monte Carlo simulations of changing the initial biomass of 5 meso-and subphotic functional groups (MBP, MBC, MPL, SBC, SPL) with 30% showed very little change in biomass of bottomfish group (BFB). Values show resulting biomass in blue line and 1 SD in black bars.

Parameters of pH and temperature effect size

To assess the sensitivity of the added survival scalar values related to changes in ocean temperature and ocean warming (Appendix B), we ran simulations where (1) we changed the calculation of the scalars, and (2) we increased and decreased both pH and Q10 scalars by 10%. In the first case, we ran simulations where we compared our initial calculation of the survival scalars, which included all studies related to temperature and where we set the maximum survival scalar related to pH to a 30% increase ("unadjusted") with (a) only including studies where the temperature change in experiments was less than 5°C ("under 5") and (b) where also the minimum scalar was set to 30% (i.e. maximum decrease is 30%) for the most sensitive group and all values with a negative relationship with pH were scaled accordingly (Figure 17A). In the second case, we increased and decreased by 10% the adjusted survival scalars (Figure 17B).

Not too surprisingly, the model was most sensitive to bounding the survival scalar related to pH. These groups had survival scalars of 0.1 – 1.3 in the "unadjusted" calculations, whereas in the

adjusted calculations the lowest was 0.7. This change was most noticeable in reef benthic piscivores ("RBP") and sharks ("SHR") and in the small phytoplankton and benthic bacteria groups. Calculating the survival scalar related to temperature based on only studies that included a maximum temperature change of 5°C, resulted in lower biomass of small phytoplankton but when we also bounded the minimum survival scalar related to pH, the phytoplankton biomass was higher than when using the unadjusted scalars. These results correspond with other studies that also show an increase in small phytoplankton and decrease in large phytoplankton when looking at the combined effects of pH and temperature (Seifert et al. 2020).

Changing the survival scalars by 10% shows that for groups where we had a relationship from the meta-analysis (Appendix B), biomass increased or decreased when this relationship was positive or negative, respectively, e.g., the groups RBP and SHR. Trophic ripple effects are noticeable for the other groups, especially on planktivorous fishes driven by changes in the plankton biomass and on most reef fishes (RGR, RPA, RBC, ROF) (Figure 17B).

In general, the most sensitive groups are corals, and the large and small phytoplankton and detritus groups (Figure 17), the later forming the base of the food web and changes in the biomass of those groups can have a noticeable ripple effect to higher trophic levels starting with zooplankton and ending with dolphins and monk seals that prey on planktivorous fishes.

Best practice taking uncertainty into account

From the above mentioned results and the trophic impact sensitivity assessments, it is clear that the system is mostly driven by bottom-up forces which means that the lower trophic levels have an important influence on the ecosystem. Therefore, best available data should be used for the parameters associated with their growth and climate-change-related mortality (i.e., the survival scalars) and should have an envelope of uncertainty in any future applications.

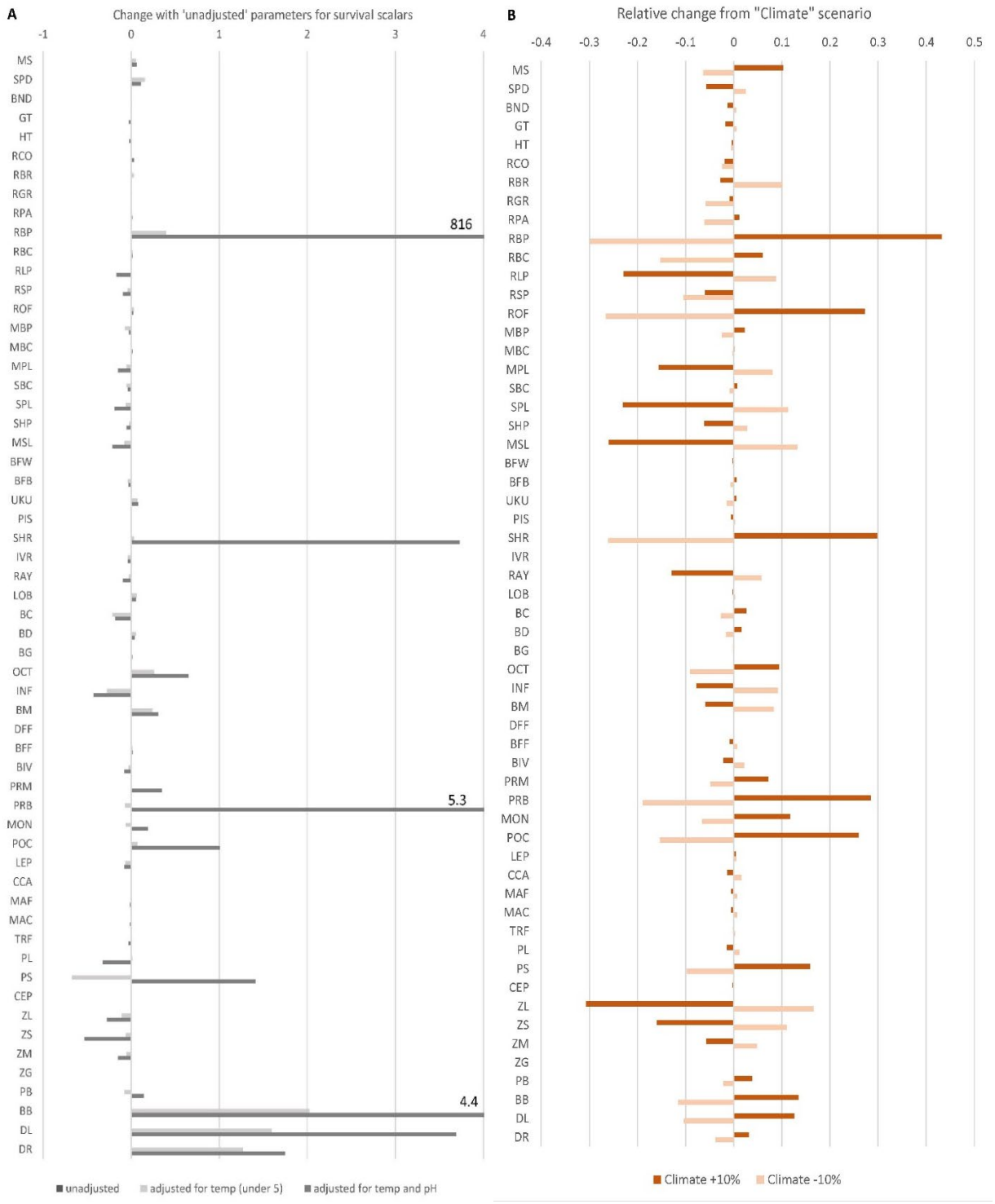

Figure 17. Sensitivity to survival scalars of organisms' response to (A) adjusting calculation of the pH and temperature survival scalars and (B) increasing and decreasing these scalars by 10%. Codes of the functional groups on the vertical axis are explained in Table 1.

Step 6. Model Application: Climate Change Impacts to Fisheries and Ecosystem Productivity

To initialize the model in 2020, we used the output of our validated historical model (see Step 4) and created a new initial condition file. Direct impacts of ocean warming were included as changes in metabolic rate parameters based on a meta-analysis (see "Sensitivity in marine organisms" in section 3B) and thermal-induced coral mortalities. Direct impacts of ocean acidification included a change in the survival scalar of sensitive organisms (see "Sensitivity of marine organisms" in section 3B). Since the groups are sensitive to the values of these scalars, we also included a simulation where we increased those values by 10% and one where we decreased them by 10% to reflect the uncertainty. The simulated projected change in ocean acidity (pH), aragonite saturation and temperature were based on the Coupled Model Intercomparison Project 5 (CMIP 5.0) AR8.5 scenario climate models (see "Environmental Drivers" in section 3B).

To assess the influence of climate change on the ecosystem and fisheries, we compared the mean of the last 5 years of a 50-year simulation (2020–2070) with the effects of climate change to a base case where we did not include climate change impacts. We specifically looked at the following social-ecological[16] indicators for a sustainably fishery and a productive ecosystem (Step 1):

- S: Viewing option of charismatic megafauna (calculated as biomass of monk seals, dolphins and sea turtles)
- S: Biomass of cultural important species catches (groups included are parrotfishes [RPA], reef benthic carnivores [RBC], bottomfish [BFB, BFW], lobster [LOB], and octopus [OCT])
- S: Revenue from catches
- S: Trophic level of the catch
- E: Trophic level of the marine community (primary producers were excluded)
- E: Ratio demersal to planktivores fish groups
- E: Biomass of apex predators (sharks [SHR], jacks [PIS], reef [RBP] and deep-water [MBP] piscivores)
- E: Ratio of calcifiers (corals and CCA) to fleshy algae (MAF, TRF)

Values were all standardized to the mean. Results show that while values for socio-economic indicators were comparable between the base case and the climate scenarios, the ecosystem structure and functioning was dramatically impaired by climate change (Figure 18).

[16] Social = S
Ecological = E

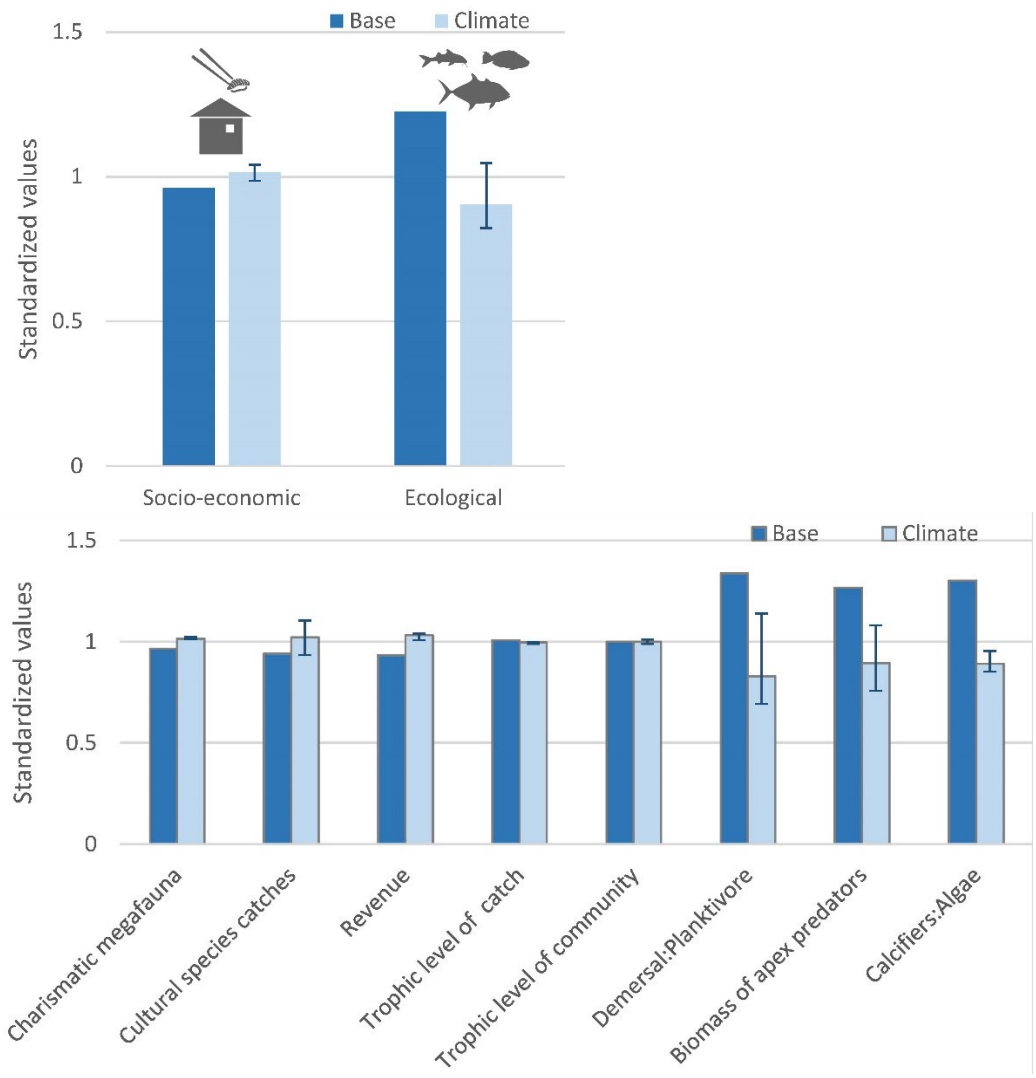

Figure 18. Standardized social-ecological effects of climate change compared to a base case scenario. The top panel shows the mean of the socioeconomic and ecological indicators. In the bottom panel, the left-most four bars represent socio-economic indicators and the right four bars ecological indicators. The error bars are based on parameters reflecting the sensitivity of organisms' survival scalar to changes in pH and temperature and show results of 10% increase and 10% decrease in these parameter estimates.

Step 7. Conclusions and Next Steps

For the development of any model, the first step is a scoping activity to identify the objectives of the stakeholders to select a model framework that can address those needs (Step 1). Objectives identified for the inhabited islands of Hawai‘i included economic (e.g., Maintain marine revenue), social (e.g., Maintain food provisioning), cultural (e.g., Maintain intangible benefits) and biological objectives (e.g., Maintain resilient ecosystems). For each of the eight identified objectives, indicators were also selected to measure performance toward reaching these goals under alternative management and climate scenarios (Step 2).

We developed an Atlantis model for the nearshore ecosystems from 0 to 400 m depth (Step 3). Data synthesis was a major part of this model development since thousands of parameters needed to be parameterized. Data came from PIFSC programs, University of Hawai‘i, and literature reviews. Largest uncertainties around parameter values were diet composition of especially non-commercial deep-water species, spatial distribution of the mesopelagic scatter layer (i.e., myctophids), spatial distribution and habitat affinity of juvenile fish of most groups, spatial distribution of plankton community, and sensitivity of fishes and marine mammals to temperature increase and pH decrease (Table 6).

Table 6. Pedigree of model parameters. Values are confidence intervals of the values used in the model and reported under Step 3. NA = not available.

Category	Biomass	Spatial distribution	Diet	Life history characteristics	Sensitivity to OA and OW
Marine mammals	0.3 dolphins 0.1 monk seals	0.3 dolphins 0.1 monk seals	0.3 dolphins 0.1 monk seals	0.3 dolphins 0.1 monk seals	NA
Sea turtles	0.3	0.3	0.3	0.2	NA
Reef fish	0.2	0.2	0.2	0.3	NA
Meso and sub benthic piscivores	0.5	0.3	0.4	0.6	NA
Mesophotic fish	0.5	0.3	0.4	0.6	NA
Subphotic fish	0.5	0.3	0.4	0.6	NA
Bottomfish	0.2	0.2	0.2	0.1	NA
Invertivorous rays	0.5	0.3	0.4	0.6	NA
Coastal pelagics	0.3	0.3	0.3	0.4	NA
Mesopelagic scatter layer	0.5	NA	0.4	0.6	NA
Mobile inverts	0.5	0.5	0.4	0.5	0.4
Meiobenthos	0.5	0.5	0.4	0.5	0.4
Filter feeders	0.5	0.3	0.5	0.6	0.4

Category	Biomass	Spatial distribution	Diet	Life history characteristics	Sensitivity to OA and OW
Structural benthic species	0.2	0.2	0.2	0.2	0.2
Primary producers	0.3	0.5	×	0.4	0.2
Micronekton	0.3	0.5	0.4	0.4	0.2

A hindcast simulation showed strong model skill when compared with observational data (Step 4). Additionally, the modeled ecosystem conforms general ecological rules, such as, a trophic pyramid with few apex predators and a large base of primary producers and detritus eaters, and a linear relationship between log-biomass and size/trophic level. As models increase in realism they also increase in complexity, making it harder to estimate uncertainties. Therefore, we conducted sensitivity analyses on model components we deemed most important or we had no good data for (Step 5). Based on these results we set parameter values that influence nutrient recycling at the most plausible values (i.e., where plankton did not increase more than 3 times the initial biomass). We concluded that the initial biomass of 5 meso- and subphotic fish groups, has a very small influence on commercially important bottomfish, therefore not knowing the exact biomass is of minor importance. However, uncertainty with regards to the biomass and/or growth rate of sharks and lower trophic levels should be taken into account as a small change in the biomass of these group will have a large impact on other groups. Advice is to bound these parameters between a plausible maximum and minimum rate to show the envelope of uncertainty around the outcomes in future applications. The model is also sensitive to especially the survival scalars of changes in pH, this largely affected phytoplankton with ripple effects to higher trophic levels and to a few fish species. Again, bounding these parameter values between a maximum and minimum will include the uncertainty around the results.

Finally we applied the model to project future climate change impacts to the ecosystem and the goods and services it supplies us focusing on four socio-economic indicators and four ecological indicators (Step 6). Our results indicated that climate change will mostly affect the coral reef ecosystem structure with an increase in planktivores and a decrease in corals. Long-term effects could include a flattening of the reef (Alvarez-Filip et al. 2009) which will likely result in a less productive ecosystem since the habitat for many species will be severely degraded (Darling et al. 2017; González-Rivero et al. 2017).

Acknowledgements

Atlantis models are extremely data hungry, hence the development of this complex model was dependent on many people from various organizations and most disciplines in providing data or expert opinion. The list is too long to include everybody by name but in particular I would like to thank Beth Fulton, Bec Gorton and Javier Porovic from CSIRO for their expert Atlantis software expertise and help throughout the project. I would further like to thank my colleagues at PIFSC who have provided data and/or expert opinions and fruitful discussions. I am particularly grateful for the help from Ivor Williams, Rhonda Suka, Tomoko Acoba, Johanna Wren, Hannah Barkley, Jennifer Raynor, Tom Oliver, Kaitlyn Lowder, Zack Oyafuso, Kirsten Leong, Don Kobayashi, Reka Domokos, Joey Lecky, Brian Langseth, Ben Richards, Brett Taylor, Bruce Mundy, Joseph O'Malley, Ray Boland, Allen Andrews, Dayton Dove, Erin Oleson, T. Todd Jones, Stacie Robinson, Jake Asher, Molly Timmers, Pearl Trick, Summer Martin, Jamie Barlow, Frank Parrish, Justin Hospital, Ryan Nichols, Alohi Nakachi, Lansing Perng, and Elena Cosner. Additionally, I would like to acknowledge my colleagues at other science centers for their support and help, in particular Isaac Kaplan, Raphael Girardin, Ryan Morse and Jason Link. Last but not least, I would like to thank the support in either data provisioning or expert opinion from staff at the University of Hawai‘i at Mānoa, in particular Virginia Moriniake and Chris Kelly at HURL; Jeff Drazen, Brian Powell and Jim Potemra at the Oceanography Department, Kirsten Oleson at NREM; Craig Nelson & Tara Clemente at C-More; and Chelsie Counsell, Eileen Nalley, and Megan Donahue from HIMB.

This project was partially funded by the NOAA Ocean Acidification Program.

Literature Cited

Ainsworth CH, Varkey D, Pitcher TJ. 2007. Ecosystem simulation models for the Bird's Head Seascape, Papua, fitted to field data. In: Pitcher TJ, Ainsworth CH, Bailey M, editors. Ecological and economic analyses of marine ecosystems in the Bird's Head Seascape, Papua, Indonesia: I. Vol. 15. Fisheries Centre Research Reports. p. 6–172.

Alvarez-Filip L, Dulvy NK, Gill JA, Côté IM, Watkinson AR. 2009. Flattening of Caribbean coral reefs: region-wide declines in architectural complexity. Proc R Soc B Biol Sci. 276(1669):3019–3025. doi:10.1098/rspb.2009.0339. http://rspb.royalsocietypublishing.org/content/276/1669/3019.abstract.

Anderson MJ. 2017. Permutational Multivariate Analysis of Variance (PERMANOVA). Wiley StatsRef Stat Ref Online.:1–15. doi:10.1002/9781118445112.stat07841. http://doi.wiley.com/10.1002/9781118445112.stat07841.

Andrews AH, DeMartini EE, Brodziak J, Nichols RS, Humphreys RL. 2012. A long-lived life history for a tropical, deepwater snapper (Pristipomoides filamentosus): bomb radiocarbon and lead–radium dating as extensions of daily increment analyses in otoliths. Can J Fish Aquat Sci. 69(11):1850–1869.

Arkema KK, Abramson SC, Dewsbury BM. 2006. Marine ecosystem-based management: from characterization to implementation. Front Ecol Environ. 4(10):525–532.

Asher J, Williams ID, Harvey ES. 2017. Mesophotic Depth Gradients Impact Reef Fish Assemblage Composition and Functional Group Partitioning in the Main Hawaiian Islands. Front Mar Sci. 4(April):1–18. doi:10.3389/fmars.2017.00098. http://journal.frontiersin.org/article/10.3389/fmars.2017.00098/full.

Atkinson MJ, Grigg RW. 1984. Model of a coral reef ecosystem II. Gross and net benthic primary production at French Frigate Shoals, Hawaii. Coral Reefs. 3:13–22.

Audzijonyte A, Pethybridge H, Porobic J, Gorton R, Kaplan I, Fulton EA. 2019. Atlantis: a spatially explicit end-to-end marine ecosystem model with dynamically integrated physics, ecology and socio-economics modules. Methods Ecol Evol. 10(19):1814–1819. doi:10.1111/2041-210X.13272. https://besjournals.onlinelibrary.wiley.com/doi/full/10.1111/2041-210X.13272.

Ault JS, Smith SG, Richards BL, Yau A, Langseth B, Humphreys RL, Boggs CH, DiNardo GT. 2018. Towards Fishery-independent Biomass Estimation for Hawaiian Deep 7 Bottomfish. NOAA Tech Memo NMFS-PIFSC-67.:29. http://hawaiibottomfish.info/wp-content/uploads/2018/02/2018-BF-IndpendSurvey-Rpt-pdf.pdf.

Bak RPM, Joenje M, De Jong I, Lambrechts DYM, Nieuwland G. 1999. Bacterial suspension feeding by coral reef benthic organisms. Mar Ecol Prog Ser. 175:285–288.

Baker J. 2016. Hawaiian monk seal stock assessment report. In: Carretta J V, editor. Pacific Marine Mammal Stock Assessments:2016. p. 41–48.

Baker JD, Johanos TC, Wurth TA, Littnan CL. 2014. Body growth in Hawaiian monk seals. Mar Mammal Sci. 30(1):259–271.

Baldwin CC, Tornabene L, Robertson DR. 2018. Below the Mesophotic. Sci Rep. 8(1):4920. doi:10.1038/s41598-018-23067-1. http://www.nature.com/articles/s41598-018-23067-1.

Battista T, Costa B, Anderson S. 2007. Benthic habitats of the main Hawaiian Islands. Silver Spring, MD.

Bearzi M. 2005. Dolphin sympatric ecology. Mar Biol Res. 1(3):165–175.

Bell J. 2008. Feeding preferences of the Cushion Star Culcita novaeguineae in the presence of the Crown of Thorns Starfish Acanthaster planci.

Benoit-Bird K, Au WWL, Brainard RE, Lammers MO. 2001. Diel horizontal migration of the Hawaiian mesopelagic boundary community observed acoustically. Mar Ecol Prog Ser. 217(1991):1–14. doi:10.3354/meps217001. http://www.int-res.com/abstracts/meps/v217/p1-14/.

Benoit-Bird KJ. 2004. Prey caloric value and predator energy needs : foraging predictions for wild spinner dolphins. Martine Biol. 145:435–444. doi:10.1007/s00227-004-1339-1.

Benoit-Bird KJ, Au WWL. 2003. Prey dynamics affect foraging by a pelagic predator (Stella longirostris) over a range of spatial and temporal scales. Behav Ecol Sociobiol. 53:364–373. doi:10.1007/s00265-003-0585-4. http://people.oregonstate.edu/~BENOITBK/reprints/spinner foraging bes.pdf.

Benson AJ, Stephenson RL. 2018. Options for integrating ecological, economic, and social objectives in evaluation and management of fisheries. Fish Fish. 19:40–56. doi:10.1111/faf.12235.

Bernal A, Olivar MP, Maynou F, Fernández ML, Puelles D. 2015. Progress in Oceanography Diet and feeding strategies of mesopelagic fishes in the western Mediterranean. Prog Oceanogr. 135:1–17. doi:10.1016/j.pocean.2015.03.005. http://dx.doi.org/10.1016/j.pocean.2015.03.005.

Berumen ML. 2005. The importance of juveniles in modelling growth: Butterflyfish at Lizard Island. Environ Biol Fishes. 72(4):409–413. doi:10.1007/s10641-004-2595-0.

Borenstein M, Cooper H, Hedges L, Valentine J. 2009. Effect sizes for continuous data. Handb Res Synth meta-analysis. 2:221–235.

Bozec Y, Alvarez-Filip L, Mumby PJ. 2015. The dynamics of architectural complexity on coral reefs under climate change. Glob Chang Biol. 21(1):223–235.

Bracis C, Lehuta S, Savina-Rolland M, Travers-Trolet M, Girardin R. 2020. Improving confidence in complex ecosystem models: The sensitivity analysis of an Atlantis ecosystem model. Ecol Modell. 431:109133.

Breslow SJ, Sojka B, Barnea R, Basurto X, Carothers C, Charnley S, Coulthard S, Dolšak N, Donatuto J, García-Quijano C, et al. 2016. Conceptualizing and operationalizing human wellbeing for ecosystem assessment and management. Environ Sci Policy. 66:250–259. doi:10.1016/j.envsci.2016.06.023.

Brey T. 2001. Population dynamics in benthic invertebrates. A virtual handbook.

Broom MJ. 1982. Analysis of the Growth of Anadara granosa(Bivalvia: Arcidae) in Natural, Artificially Seeded and Experimental Populations. Mar Ecol Prog Ser. 9(1):69–79.

Bruggemann JH, Kuyper MWM, Breeman a M. 1994. Comparative-Analysis of Foraging and Habitat Use By the Sympatric Caribbean Parrotfish Scarus-Vetula and Sparisoma-Viride (Scaridae). Mar Ecol Ser. 112:51–66. doi:10.3354/meps112051.

Busch DS, McElhany P. 2016. Estimates of the Direct Effect of Seawater pH on the Survival Rate of Species Groups in the California Current Ecosystem. PLoSOne. 11(8):e0160669. doi:10.1371/journal.pone.0160669.

Bustamante R. 2010. Effects of trawling on the benthos and biodiversity : Development and delivery of a Spatially-explicit Management Framework for the Northern Prawn Fishery. (2005).

Cahoon M. 2011. The foraging ecology of monk seals in the main Hawaiian Islands. University of Hawaii at Manoa.

Cahoon MK, Littnan CL, Longenecker K, Carpenter JR. 2013. Dietary comparison of two Hawaiian monk seal populations: the role of diet as a driver of divergent population trends. Endanger Species Res. 20(2):137–146.

Cammen LM. 1979. Ingestion rate: An empirical model for aquatic deposit feeders and detritivores. Oecologia. 44(3):303–310. doi:10.1007/bf00545232. http://dx.doi.org/10.1007/BF00545232.

Carretta J V, Forney KA, Oleson EM (Erin M, Weller 1963- DW, Lang AR, Baker JD, Muto M (Marcia), Hanson B, Orr AJ, Huber HR, et al. 2019. U.S. Pacific Marine Mamal Stock Assessments: 2018. (U.S.) SFSC, editor. doi:https://doi.org/10.25923/x17q-2p43. https://repository.library.noaa.gov/view/noaa/20266.

Carrillo JH, Hastings MG, Sigman DM, Huebert BJ. 2002. Atmospheric deposition of inorganic and organic nitrogen and base cations in Hawaii. Global Biogeochem Cycles. 16(4):24-1-24–16. doi:10.1029/2002GB001892. http://doi.wiley.com/10.1029/2002GB001892.

Cartes JE, Brey T, Sorbe JC, Maynou F. 2002. Comparing production-biomass ratios of benthos and suprabenthos in macrofaunal marine crustaceans. Can J Fish Aquat Sci. 59(10):1616–1625.

Cesar HS, Van Beukering PJ. 2004. Economic valuation of the coral reefs of Hawai'i. Pacific Sci. 58(2):231–242.

Chaloupka M, Balazs G. 2007. Using Bayesian state-space modelling to assess the recovery and harvest potential of the Hawaiian green sea turtle stock. Ecol Modell. 205(1):93–109.

Chen L. 2002. Post-settlement diet dhit of Chorurus sordidus and Scarus schlegeli (Pices: Scaridae). Zool Stud. 41(1):47–58.

Choat J, Clements K, Robbins W. 2002. The trophic status of herbivorous fishes on coral reefs. Mar Biol. 140(3):613–623.

Choat JH, Robertson DR. 2002. Age-based studies on coral reef fishes. In: Coral reef fishes: dynamics and diversity in a complex ecosystem. San Diego: Academic Press. p. 57–80.

Choy CA, Haddock SHD, Robison BH. 2017. Deep pelagic food web structure as revealed by in situ feeding observations. Proc R Soc B Biol Sci. 284(1868):20172116. doi:10.1098/rspb.2017.2116. http://rspb.royalsocietypublishing.org/lookup/doi/10.1098/rspb.2017.2116.

Choy CA, Wabnitz CCC, Weijerman M, Woodworth-jefcoats PA, Polovina JJJ. 2016. Finding the way to the top: How the composition of oceanic mid-trophic micronekton groups determines apex predator biomass in the central North Pacific. Mar Ecol Prog Ser. 549(2006):1–15. doi:10.3354/meps11680.

Choy SC. 1986. Natural diet and feeding habits of the crabs Liocarcinus puber and L. holsatus (Decapoda, Brachyura, Portunidae). Mar Ecol Prog Ser. 31:87–99.

Christensen V, Walters CJ. 2004. Ecopath with Ecosim: methods, capabilities and limitations. Ecol Modell. 172(2–4):109–139. doi:10.1016/j.ecolmodel.2003.09.003. [accessed 2015 Nov 23]. http://www.sciencedirect.com/science/article/pii/S030438000300365X.

Clarke KR, Somerfield PJ, Gorley RN. 2008. Testing null hypotheses in exploratory community analyses: similarity profiles and biota-environmental linkage. J Exp Mar Bio Ecol.:56–69.

Clarke TA, Privitera LA. 1995. Reproductive biology of two Hawaiian pelagic carangid fishes, the bigeye scad, Selar crumenophthalmus, and the round scad, Decapturus macarellus. Bull Mar Sci. 56(1):33–47.

Cortés E. 2000. Life history patterns and correlations in sharks. Rev Fish Sci. 8(4):299–344.

Cox EF, Ward S. 2002. Impact of elevated ammonium on reproduction in two Hawaiian scleractinian corals with different life history patterns. Mar Pollut Bull. 44(11):1230–1235. doi:http://dx.doi.org/10.1016/S0025-326X(02)00213-8. http://www.sciencedirect.com/science/article/pii/S0025326X02002138.

Cullen JJ. 1982. The deep chlorophyll maximum: comparing vertical profiles of chlorophyll a. Can J Fish Aquat Sci. 39:791–801.

Dale JJ, Holland KN. 2012. Age, growth and maturity of the brown stingray (Dasyatis lata) around Oahu, Hawai'i. Mar Freshw Res. 63(6):475–484.

Darling ES, Graham NAJ, Januchowski-Hartley FA, Nash KL, Pratchett MS, Wilson SK. 2017. Relationships between structural complexity, coral traits, and reef fish assemblages. Coral Reefs. 36(2). doi:10.1007/s00338-017-1539-z.

DeMartini E, Landgraf K, Ralston S. 1994. A recharacterization of the age-length and growth relationships of hawaiian snapper. Honolulu, Hawai'i: Technical Report NOAA-TM-NMFS-SWFSC-199 ….

DeMartini EE, Parrish FA, Ellis DM. 1996. Barotrauma-associated regurgitation of food: Implications for diet studies of Hawaiian pink snapper, Pristipomoides filamentosus (family Lutjanidae). Fish Bull. 94(2):250–256.

Domokos R, Pakhomov EA, Suntsov A V, Seki MP, Polovina JJ. 2010. 2.2 Acoustic Characterization of the Mesopelagic Community off the Leeward Coast of Oahu Island, Hawaii. In: Pakhomov E, Yamamura O, editors. Report of the Advisory Panel on Micronekton Sampling Intercalibration Experiment. Sidney, BC. Canada. p. 19–26.

Dove D, Weijerman M, Grüss A, Acoba T, Smith JR. 2019. Substrate mapping to inform ecosystem science and marine spatial planning around the Main Hawaiian Islands. In: Seafloor Geomorphology as Benthic Habitat: GeoHab Atlas of seafloor geomorphic features and benthic habitat -2nd Edition. Elsevier. https://elseviermpsops.mpslimited.com/books/authorproofs/Harris-SGBH-1631797/32c7d7c3ef4f9b62435d04dd0c1d441e.

Drazen JC, Sutton TT. 2017. Dining in the Deep: The Feeding Ecology of Deep-Sea Fishes. Ann Rev Mar Sci. 9(1):337–366. doi:10.1146/annurev-marine-010816-060543. http://www.annualreviews.org/doi/10.1146/annurev-marine-010816-060543.

Dunic JC, Baum JK. 2017. Size structuring and allometric scaling relationships in coral reef fishes. J Anim Ecol. 86:577–589. doi:10.1111/1365-2656.12637.

Edwards DC, Huebner JD. 1977. Feeding and growth rates of Polinices duplicatus preying on Mya arenaria at Barnstable Harbor, Massachusetts. Ecology. 58:1218–1236.

Enochs IC. 2012. Motile cryptofauna associated with live and dead coral substrates: Implications for coral mortality and framework erosion. Mar Biol. 159(4):709–722. doi:10.1007/s00227-011-1848-7.

Enochs IC, Manzello DP. 2012. Species richness of motile cryptofauna across a gradient of reef framework erosion. Coral Reefs. 31(3):653–661. doi:10.1007/s00338-012-0886-z.

Fowler AJ. 1990. Validation of annual growth increments in the otoliths of a small, tropical coral reef fish. Mar Ecol Prog Ser. 64(March 1988):25–38. doi:10.3354/meps064025.

Fulton EA, Link JS, Kaplan IC, Savina-Rolland M, Johnson P, Ainsworth C, Horne P, Gorton R, Gamble RJ, Smith ADM, et al. 2011. Lessons in modelling and management of marine ecosystems: the Atlantis experience. Fish Fish. 12:no. doi: 10.1111/j.1467-2979.2011.00412.x. doi:10.1111/j.1467-2979.2011.00412.x. http://dx.doi.org/10.1111/j.1467-2979.2011.00412.x.

Fulton EA, Smith ADM, Johnson CR. 2004. Biogeochemical marine ecosystem models I: IGBEM--a model of marine bay ecosystems. Ecol Modell. 174(3):267–307. doi:DOI: 10.1016/j.ecolmodel.2003.09.027. http://www.sciencedirect.com/science/article/B6VBS-4BGW2X2-2/2/b106ddcf67eed6d7be1bc814296fe8bd.

Fulton EA, Smith ADM, Smith DC. 2007. Alternative management strategies for Southeast Australian Commonwealth Fisheries: Stage 2: Quantitative management strategy evaluation. Deakin West, ACT: Fisheries Research and Development Corp.

Gartner Jr J V, Crabtree RE, Sulak KJ. 1997. 4 Feeding At Depth. In: Randall D, Farrell A, editors. Deep-Sea fishes. Vol. 16. San Diego, CA: Academic Press. p. 115–193.

Gloeckler K, Choy CA, Hannides CCS, Close HG, Goetze E, Popp BN, Drazen JC. 2018. Amino acid – compound specific stable isotope analysis of micronekton around Hawaii reveals the importance of suspended particles as an important nutritional source in the meso/bathypelagic. Limnol Oceanogr. 63(3):1168–1180. doi:10.1002/lno.10762. http://doi.wiley.com/10.1002/lno.10762.

Glynn PW. 2004. High complexity food webs in low-diversity eastern Pacific reef-coral communities. Ecosystems. 7(4):358–367. doi:10.1007/s10021-004-0184-x.

González-Rivero M, Harborne AR, Herrera-Reveles A, Bozec YM, Rogers A, Friedman A, Ganase A, Hoegh-Guldberg O. 2017. Linking fishes to multiple metrics of coral reef structural complexity using three-dimensional technology. Sci Rep. 7(1). doi:10.1038/s41598-017-14272-5.

Grafeld S, Oleson KLL, Teneva L, Kittinger JN. 2017. Follow that fish : Uncovering the hidden blue economy in coral reef fisheries. PLoSOne. 12(8):e0182104. doi:10.1371/journal.pone.0182104. https://doi.org/10.1371/journal. pone.0182104.

Graham NAJ, Wilson SK, Jennings S, Polunin NVC, Bijoux JP, Robinson J. 2006. Dynamic fragility of oceanic coral reef ecosystems. Proc Natl Acad Sci U S A. 103(22):8425–8429. doi:10.1073/pnas.0600693103.

Gribble NA. 2007. Ecosystem Based Management: Linked-ecosystem modelling of the Great Barrier Reef. In: MODSIM 2007 International Congress on Modelling and Simulation. p. 315–321.

Haight WR, Parrish JD, Hayes TA. 1993. Feeding Ecology of Deepwater Lutjanid Snappers at Penguin Bank, Hawaii. Trans Am Fish Soc. 122(3):328–347. doi:10.1577/1548-8659(1993)122<0328:FEODLS>2.3.CO;2. http://doi.wiley.com/10.1577/1548-8659(1993)122%3C0328:FEODLS%3E2.3.CO;2.

Hansen C, Drinkwater KF, Jähkel A, Fulton EA, Gorton R, Skern-Mauritzen M. 2019. Sensitivity of the Norwegian and Barents Sea Atlantis end-to-end ecosystem model to parameter perturbations of key species. PLoS One. 14(2):e0210419.

Harikrishnan M, Unnikrishnan U, Maju MS, Greeshma ARR, Kurup BM. 2010. Size at sexual maturity, egg number and reproductive output of the snapping shrimp Alpheus euphrosyne euphrosyne De Man, 1897. Invertebr Reprod Dev. 54(4):195–202.

Harvey CJ, Kelble CR, Schwing FB. 2017. Implementing "the IEA": Using integrated ecosystem assessment frameworks, programs, and applications in support of operationalizing ecosystem-based management. ICES J Mar Sci. 74(1):398–405. doi:10.1093/icesjms/fsw201.

Hawn AT, Martin GB, Sandin S a, Hare J a. 2005. Early juvenile mortality in the coral reef fish. Bull Mar Sci. 77(2):309–318.

Heikoop JM, Risk MJ, Lazier A V., Edinger EN, Jompa J, Limmon G V., Dunn JJ, Browne DR, Schwarcz HP. 2000. Nitrogen-15 signals of anthropogenic nutrient loading in reef corals. Mar Pollut Bull. 40(7):628–636. doi:10.1016/S0025-326X(00)00006-0.

Van Heukelem WF. 1976. Growth, bioenergetics and life-span of Octopus cyanea and Octopus maya. University of Hawaii at Manoa.

van Hooidonk RJ, Maynard J, Tamelander J, Gove JM, Ahmadia G, Raymundo L, Williams GJ, Heron SF, Planes S. 2016. Local-scale projections of coral reef futures and implications of the Paris Agreement. Sci Rep. 6. doi:10.1038/srep39666. [accessed 2017 Jun 14]. https://www.ncbi.nlm.nih.gov/pmc/articles/PMC5175274/.

Hopkins TL, Gartner J V. 1992. Resource-partitioning and predation impact of a low-latitude myctophid community. Mar Biol. 114(2):185–197.

Horne PP, Kaplan IC, Marshall K, Levin P, Harvey C, Hermann A, Fulton E. 2010. Design and parameterization of a spatially explicit ecosystem model of the central California Current. Technical Memo, NMFS-NWFSC-104, Dept. of Commerce, NOAA. http://www.nwfsc.noaa.gov/publications/scientificpubs.cfm.

Houlbrèque F, Tambutté E, Richard C, Ferrier-pagès C. 2004. Importance of a micro-diet for scleractinian corals. Mar Ecol Prog Ser. 282:151–160.

Van Houtan KS, Andrews AH, Jones TT, Murakawa SKK, Hagemann ME. 2016. Time in tortoiseshell: a bomb radiocarbon-validated chronology in sea turtle scutes. Proc R Soc B. 283:20152220. doi:10.1098/rspb.2015.2220. http://www.seaturtle.org/PDF/VanHoutanKS_2016_ProcRSocB.pdf.

Humphreys RL, Kramer SH. 1984. Ciguatera and the feeding habits of the greater amberjack, Seriola dumerili, in the Hawaiian Archipelago. In: Proceedings of the 2nd Symposium on Resource Investigations in the Northwestern Hawaiian Islands. Vol. 2. University of Hawa'i. p. 179–191.

Ingram RJ, Oleson KLL, Gove JM. 2018. Revealing complex social-ecological interactions through participatory modeling to support ecosystem-based management in Hawai‘i. Mar Policy. 94(December 2017):180–188. doi:10.1016/j.marpol.2018.05.002. https://doi.org/10.1016/j.marpol.2018.05.002.

Ishihara T, Tachihara K. 2011. Pelagic larval duration and settlement size of Apogonidae, Labridae, Scaridae, and Tripterygiidae species in a coral lagoon of Okinawa Island, Southern Japan. Pacific Sci. 65(1):87–93. doi:10.2984/65.1.087.

Iverson S, Piche J, Blanchard W, U.S. Dep. Commer. NTM. 2011. Hawaiian Monk Seals and Their Prey: Assessing Characteristics of Prey Species Fatty Acid Signatures and Consequences for Estimating Monk Seal Diets Using Quantitative Fatty Acid Signature Analysis. NOAA-TM-NMFS-PIFSC-23.:114 + Appendices.

Jennings S, Oliveira JA, Warr KJ. 2007. Measurement of body size and abundance in tests of macroecological and food web theory. J Anim Ecol. 76(1):72–82.

Johnson DS. 2015. crawl: Fit Continuous-Time Correlated Random Walk Models to Animal Movement Data 2016. R Packag version 2.

Jokiel PL, Coles SL. 1990. Response of Hawaiian and other Indo-Pacific reef corals to elevated temperature. Coral Reefs. 8(4):155–162. doi:10.1007/BF00265006.

Kahng SE, Copus JM, Wagner D. 2014. Recent advances in the ecology of mesophotic coral ecosystems (MCEs). Curr Opin Environ Sustain. 7:72–81. doi:10.1016/j.cosust.2013.11.019. http://dx.doi.org/10.1016/j.cosust.2013.11.019.

Kawamoto PY. 1973. Management investigation of the akule or big-eye scad, Trachurops crumenophthalmus (Bloch). Hawaii Div Fish Game, Proj Rep No H-4-r, Honolulu, Hawaii. 28.

Kelley C, Moffitt R, Smith JR. 2006. Mega-to micro-scale classification and descriptio of bottomfish Essential Fish Habitat on four banks in the Northwestern Hawaiian Islands. Atoll Res Bull. 543:319–332.

Kelly ELA, Eynaud Y, Clements SM, Gleason M, Sparks RT, Williams ID, Smith JE. 2016. Investigating functional redundancy versus complementarity in Hawaiian herbivorous coral reef fishes. Oecologia.(September). doi:10.1007/s00442-016-3724-0. http://link.springer.com/10.1007/s00442-016-3724-0.

Kittinger JN, Teneva LT, Koike H, Stamoulis KA, Kittinger DS, Oleson KLL, Conklin E, Gomes M, Wilcox B, Friedlander AM. 2015. From Reef to Table: Social and Ecological Factors Affecting Coral Reef Fisheries, Artisanal Seafood Supply Chains, and Seafood Security. PLoS One. 10(8):e0123856. doi:10.1371/journal.pone.0123856. http://dx.doi.org/10.1371%2Fjournal.pone.0123856.

Kohn AJ, Helfrich P. 1957. Primary organic productivity of a Hawaiian coral reef. Limnol Oceanogr.:241–251.

Kohn AJ, White JK. 1977. Polychaete annelids of an intertidal reef limestone platform at Tanguisson, Guam. Micronesica. 13(2):199–215.

Kolding J, Bundy A, van Zwieten PAM, Plank MJ. 2016. Fisheries, the inverted food pyramid. ICES J Mar Sci. 73(6):1697–1713.

Kolinski SP, Cox EF. 2003. An update on modes and timing of gamete and planula release in Hawaiian scleractinian corals with implications for conservation and management. Pacific Sci. 57(1):17–27. doi:10.1353/psc.2003.0005.

Kroeker KJ, Kordas RL, Crim R, Hendriks IE, Ramajo L, Singh GS, Duarte CM, Gattuso J-P. 2013. Impacts of ocean acidification on marine organisms: quantifying sensitivities and interaction with warming. Glob Chang Biol. 19(6):1884–1896. doi:10.1111/gcb.12179. http://dx.doi.org/10.1111/gcb.12179.

Kulbicki M, Bozec YM, Labrosse P, Letourneur Y, Mou-Tham G, Wantiez L. 2005. Diet composition of carnivorous fishes from coral reef lagoons of New Caledonia. Aquat Living Resour. 18(03):231–250.

Langdon C, Atkinson MJ. 2005. Effect of elevated pCO2 on photosynthesis and calcification of corals and interactions with seasonal change in temperature/irradiance and nutrient enrichment. J Geophys Res Ocean. 110(C9):C09S07. doi:10.1029/2004jc002576. http://dx.doi.org/10.1029/2004JC002576.

Langseth B, Syslo J, Yau A, Kapur M, Brodziak J. 2018. Stock assessment for the Main Hawaiian Islands Deep 7 bottomfish complex in 2018, with catch projections through 2022. Honolulu, Hawai'i.

Leong KM, Wongbusarakum S, Ingram RJ, Mawyer A, Poe MR. 2019. Improving Representation of Human Well-Being and Cultural Importance in Conceptualizing the West Hawai'i Ecosystem. Front Mar Sci. 6:231. https://www.frontiersin.org/article/10.3389/fmars.2019.00231.

Link JS. 2010. Adding rigor to ecological network models by evaluating a set of pre-balance diagnostics: a plea for PREBAL. Ecol Modell. 221(12):1580–1591. doi:10.1016/j.ecolmodel.2010.03.012. http://dx.doi.org/10.1016/j.ecolmodel.2010.03.012.

Link JS, Browman HI. 2017. Operationalizing and implementing ecosystem-based management. ICES J Mar Sci. 74(1):379–381. doi:10.1093/icesjms/fsw247.

Longenecker K, Langston R. 2008. Life History Compendium of Exploited Hawaiian Fishes. Honolulu, HI.

Di Lorenzo E, Schneider N, Cobb KM, Franks PJS, Chhak K, Miller AJ, McWilliams JC, Bograd SJ, Arango H, Curchitser E, et al. 2008. North Pacific Gyre Oscillation links ocean climate and ecosystem change. Geophys Res Lett. 35(8):n/a-n/a. doi:10.1029/2007GL032838. http://dx.doi.org/10.1029/2007GL032838.

Luers MA, DeMartini EE, Humphreys RL. 2018. Seasonality, sex ratio, spawning frequency and sexual maturity of the opakapaka Pristipomoides filamentosus (Perciformes: Lutjanidae) from the Main Hawaiian Islands: fundamental input to size-at-retention regulations. Mar Freshw Res. 69(2):325–335.

MacDonald CD. 1981. Reproductive strategies and social organization in damselfishes. [Honolulu]: University of Hawaii.

McCarthy DA, Young CM, Emson RH. 2003. Influence of wave-induced disturbance on seasonal spawning patterns in the sabellariid polychaete Phragmatopoma lapidosa. Mar Ecol Prog Ser. 256:123–133.

McCoy KS, Williams ID, Friedlander AM, Hongguang M, Teneva LT, Kittinger JN. 2018. Estimating nearshore coral reef-associated fisheries production from the main Hawaiian Islands using commercial and non-commercial data. PLoS One.:1–13. doi:10.1371/journal.pone.0195840.

Meyer CG, Holland KN, Wetherbee BM, Lowe CG. 2001. Diet, resource partitioning and gear vulnerability of Hawaiian jacks captured in fishing tournaments. Fish Res. 53(2):105–113.

Mladenov P V, Emson RH. 1984. Divide and broadcast: sexual reproduction in the West Indian brittle star Ophiocomella ophiactoides and its relationship to fissiparity. Mar Biol. 81(3):273–282.

Moffitt RB, Parrish FA. 1996. Habitat and life history of juvenile Hawaiian pink snapper, Pristipomoides filamentosus. Pacific Sci. 50(4):371–381.

Moore C, Drazen JC, Radford BT, Kelley C, Newman SJ. 2016. Improving essential fish habitat designation to support sustainable ecosystem-based fisheries management. Mar Policy. 69:32–41. doi:10.1016/j.marpol.2016.03.021. http://dx.doi.org/10.1016/j.marpol.2016.03.021.

Moriarty DJW. 1982. Feeding of Holothuria atra and Stichopus chloronotus on bacteria, organic carbon and organic nitrogen in sediments of the Great Barrier Reef. Mar Freshw Res. 33(2):255–263. doi:http://dx.doi.org/10.1071/MF9820255. http://www.publish.csiro.au/paper/MF9820255.

Morton B. 1990. The physiology and feeding behaviour of two marine scavenging gastropods in Hong Kong: the subtidal Babylonia lutosa (Lamarck) and the intertidal Nassarius festivus (Powys). J Molluscan Stud. 56(2):275–288.

Nadon MO, Ault JS, Williams ID, Smith SG, DiNardo GT. 2015. Length-Based Assessment of Coral Reef Fish Populations in the Main and Northwestern Hawaiian Islands. PLoS One. 10(8):e0133960. doi:10.1371/journal.pone.0133960. http://dx.plos.org/10.1371/journal.pone.0133960.

Nadon MO, Sculley M, Carvalho F. 2020. Stock assessment of Uku (Aprion virescens) in Hawaii, 2020.

Nalley E. 2020. Picky eater or generalist feeder? Diet diversity and functional homogenization in herbivorous reef fishes. University of Hawaii at Manoa.

NOAA Fisheries. 2016. Ecosystem-Based Fisheries Management Road Map, Policy 01-120. https://www.st.nmfs.noaa.gov/Assets/ecosystems/ebfm/EBFM_Road_Map_final.pdf.

O'Malley JM, MacDonald CD. 2009. Preliminary growth estimates of Northwestern Hawaiian Islands spiny lobster (Panulirus marginatus): indications of spatiotemporal variability. Honolulu, HI 96822-2396: US Department of Commerce, National Oceanic and Atmospheric Administration, National Marine Fisheries Service, Pacific Islands Fisheries Science Center.

O'Malley JM, Walsh WA. 2013. Annual and long-term movement patterns of spiny lobster, Panulirus marginatus, and slipper lobster, Scyllarides squammosus, in the Northwestern Hawaiian Islands. Bull Mar Schience. 89(2):1–22.

Olesiuk PF. 1993. Annual prey consumption by harbor seals (Phoca vitulina) in the Strait of Georgia, British Columbia. Fish Bull. 91:491–515.

Olsen E, Fay G, Gaichas S, Gamble R, Lucey S, Link JS. 2016. Ecosystem model skill assessment. Yes we can! PLoS One. 11(1):e0146467.

Opitz S. 1996. Trophic interactions on a Caribbean coral reef. Tech. Rep. 43. Manila, Philippines: ICLARM.

Pakhomov EA, Suntsov A V, Seki MP, Brodeur RD, Domokos R, Pakhomova LG, Owen KR. 2010. 2 First Micronekton Inter-calibration Experiment, MIE-1. In: Pakhomov E, Yamamura O, editors. PICES SCIENTIFIC REPORT No. 38 2010. Sidney, BC. Canada. p. 3.

Papastamatiou YP, Meyer CG, Kosaki RK, Wallsgrove NJ, Popp BN. 2015. Movements and foraging of predators associated with mesophotic coral reefs and their potential for linking ecological habitats. Mar Ecol Prog Ser. 521:155–170. doi:10.3354/meps11110.

Parrish FA. 2006. Precious corals and subphotic fish assemblages. Atoll Res Bull. 543:425–438.

Parrish FA. 2009. Do monk seals exert top-down pressure in subphotic ecosystems ? Mar Mammal Sci. 25(January):91–106. doi:10.1111/j.1748-7692.2008.00245.x.

Parrish FA, Howell EA, Antonelis GA, Iverson SJ, Littnan CL, Parrish JD, Polovina JJ. 2011. Estimating the carrying capacity of French Frigate Shoals for the endangered Hawaiian monk seal using Ecopath with Ecosim. Mar Mammal Sci. 28(3):522–541.

Parrish FA, Howell EA, Antonelis GA, Iverson SJ, Littnan CL, Parrish JD, Polovina JJ. 2012. Estimating the carrying capacity of French Frigate Shoals for the endangered Hawaiian

monk seal using Ecopath with Ecosim. Mar Mammal Sci.:1–20. doi:10.1111/j.1748-7692.2011.00502.x.

Pauly D. 1980. On the interrelationships between natural mortality, growth parameters, and mean environmental temperature in 175 fish stocks. J du Cons. 39(2):175–192.

Pethybridge HR, Weijerman M, Perrymann H, Audzijonyte A, Porobic J, McGregor V, Girardin R, Bulman C, Ortega-Cisneros K, Sinerchia M, et al. 2019. Calibrating process-based marine ecosystem models: An example case using Atlantis. Ecol Modell. 412:108822. doi:10.1016/J.ECOLMODEL.2019.108822.

Piacenza SE, Balazs GH, Hargrove SK, Richards PM, Heppell SS. 2016. Trends and variability in demographic indicators of a recovering population of green sea turtles Chelonia mydas. Endanger Species Res. 31:103–117. doi:10.3354/esr00753.

Plagányi ÉE, Rademeyer RA, Butterworth DS, Cunningham CL, Johnston SJ. 2007. Making management procedures operational—innovations implemented in South Africa. ICES J Mar Sci J du Cons. 64(4):626.

Pyle RL, Boland R, Bolick H, Bowen BW, Bradley CJ, Kane C, Kosaki RK, Langston R, Longenecker K, Montgomery A, et al. 2016. A comprehensive investigation of mesophotic coral ecosystems in the Hawaiian Archipelago. PeerJ. 4:e2475. doi:10.7717/peerj.2475. [accessed 2016 Oct 4]. https://peerj.com/articles/2475.

Richards BL, Smith SG, Ault JS, DiNardo GT, Kobayashi DR, Domokos R, Anderson J, Taylor JC, Misa W, Giuseffi L, et al. 2016. Design and Implementation of a Bottomfish Fishery-Independent Survey in the Main Hawaiian Islands. NOAA Tech Memo NMFS-PIFSC-53.:66.

Richmond RH, Hunter CL. 1990. Reproduction and recruitment of corals: Comparisons among the Caribbean, the Tropical Pacific, and the Red Sea. Mar Ecol Prog Ser Oldend. 60(1):185–203.

Rogers A, Blanchard JL, Mumby PJ, Building AD, Bank W. 2014. Vulnerability of Coral Reef Fisheries to a Loss of Structural Complexity. Curr Biol. 24(9):1000–1005. doi:10.1016/j.cub.2014.03.026. http://dx.doi.org/10.1016/j.cub.2014.03.026.

Rooney J, Donham E, Montgomery A, Spalding H, Parrish F, Boland R, Fenner D, Gove J, Vetter O. 2010. Mesophotic coral ecosystems in the Hawaiian Archipelago. Coral Reefs. 29(2):361–367. doi:10.1007/s00338-010-0596-3.

Rossi S, Ribes M, Coma R, Gill J-M. 2004. Temporal variability in zooplankton prey capture rate of the passive suspension feeder Leptogorgia sarmentosa (Cnidaria : Octocorallia), a case study. Mar Biol. 144:89–99. doi:10.1007/s00227-003-1168-7.

Ruiz Sebastián C, McClanahan TR. 2013. Description and validation of production processes in the coral reef ecosystem model CAFFEE (Coral–Algae–Fish-Fisheries Ecosystem Energetics) with a fisheries closure and climatic disturbance. Ecol Modell. 263.

doi:10.1016/j.ecolmodel.2013.05.012. http://dx.doi.org/10.1016/j.ecolmodel.2013.05.012.

Safarik M, Redden AM, Schreider MJ. 2006. Density-dependent growth of the polychaete Diopatra aciculata. Sci Mar.

Sale T, Marko P, Oliver T, Hunter C. 2019. Assessment of acclimatization and subsequent survival of corals during repeated natural thermal stress events in Hawai‘i. Mar Ecol Prog Ser. 624:65–76. doi:https://doi.org/10.3354/meps13031. https://www.int-res.com/abstracts/meps/v624/p65-76.

Schluessel V. 2008. Life history, population genetics and sensory biology of the white spotted eagle ray Aetobatus narinari (Euphrasen, 1790) with emphasis on the relative importance of olfaction. The University of Queensland.

Schluessel V, Bennett MB, Collin SP. 2010. Diet and reproduction in the white-spotted eagle ray Aetobatus narinari from Queensland, Australia and the Penghu Islands, Taiwan. Mar Freshw Res. 61(11):1278–1289. doi:http://dx.doi.org/10.1071/MF09261. http://www.publish.csiro.au/paper/MF09261.

Seifert M, Rost B, Trimborn S, Hauck J. 2020. Meta-analysis of multiple driver effects on marine phytoplankton highlights modulating role of pCO2. Glob Chang Biol. n/a(n/a). doi:https://doi.org/10.1111/gcb.15341. https://doi.org/10.1111/gcb.15341.

Seki MP, Callahan MW. 1988. The feeding habits of two deep slope snappers, Pristipomoides zonatus and P. auricilla, at Pathfinder Reef, Mariana Archipelago. Fish Bull. 86(4):807–811.

Siegel DA, Deuser WG. 1997. Trajectories of sinking particles in the Sargasso Sea: modeling of statistical funnels above deep-ocean sediment traps. Deep Sea Res Part I Oceanogr Res Pap. 44(9):1519–1541. doi:https://doi.org/10.1016/S0967-0637(97)00028-9. http://www.sciencedirect.com/science/article/pii/S0967063797000289.

Simmonds J, MacLennan DN. 2008. Fisheries acoustics: theory and practice. John Wiley & Sons.

Smith JE, Smith CM, Hunter CL. 2001. An experimental analysis of the effects of herbivory and nutrient enrichment on benthic community dynamics on a Hawaiian reef. Coral Reefs. 19(4):332–342. doi:10.1007/s003380000124.

Steinberg DK, Cope JS, Wilson SE, Kobari T. 2008. Deep-Sea Research II A comparison of mesopelagic mesozooplankton community structure in the subtropical and subarctic North Pacific Ocean. 55:1615–1635. doi:10.1016/j.dsr2.2008.04.025.

Stimson J, Cunha T, Philippoff J. 2007. Food preferences and related behavior of the browsing sea urchin Tripneustes gratilla (Linnaeus) and its potential for use as a biological control agent. Mar Biol. 151(5):1761–1772.

Storlazzi CD, Reguero BG, Cole AD, Lowe E, Shope JB, Gibbs AE, Nickel BA, McCall RT, van Dongeren AR, Beck MW. 2019. Rigorously valuing the role of US coral reefs in coastal hazard risk reduction. US Geological Survey.

Stow CA, Jolliff J, McGillicuddy Jr DJ, Doney SC, Allen JI, Friedrichs MAM, Rose KA, Wallhead P. 2009. Skill assessment for coupled biological/physical models of marine systems. J Mar Syst. 76(1):4–15. doi:10.1016/j.jmarsys.2008.05.002.

Struhsaker P. 1973. A contribution to the systematics and ecology of Hawaiian bathyal fishes. University of Hawaii at Manoa.

Sudekum A, Parrish J, Radtke R, Ralston S. 1991. Life history and ecology of large jacks in undisturbed, shallow oceanic communities. Fish Bull. 89(3):493–513.

Tam JC, Fay G, Link JS. 2019. Better together: the uses of ecological and socio-economic indicators with end-to-end models in marine ecosystem based management. Front Mar Sci. 6:560. https://www.frontiersin.org/articles/10.3389/fmars.2019.00560/full.

Taylor BM. 2012. Life history assessment of commercially important and functionally diverse parrotfish species from Guam. Final Report to Guam Coral Reef Initiative and NOAA Pacific Islands Fisheries Science Center. Mangilao, Guam.

Thresher RE, Colin PL, Bell LJ. 1989. Planktonic Duration , Distribution and Population Structure of Western and Central Pacific damslefishes (Pomacentridae). Copeia. 2:420–434.

Tricas T. 1985. The economics of foraging in coral-feeding butterflyfishes of Hawaii. In: Fifth International Coral Reef Congress. Tahiti.

Trites AW, Pauly D. 1998. Estimating mean body masses of marine mammals from maximum body lengths. Can J Zool Can Zool. 76(5):886–896.

Tsehaye I, Nagelkerke LAJ. 2008. Exploring optimal fishing scenarios for the multispecies artisanal fisheries of Eritrea using a trophic model. Ecol Modell. 212(3–4):319–333. doi:DOI: 10.1016/j.ecolmodel.2007.10.044. http://www.sciencedirect.com/science/article/B6VBS-4RWC550-2/2/89f9a1972d709c1d64b3e83dc54a409d.

Ulanowicz RE. 1986. Growth and development: Ecosystem phenomenology. :203.

Veazey LM, Franklin EC, Kelley C, Rooney J, Frazer LN, Toonen RJ. 2016. The implementation of rare events logistic regression to predict the distribution of mesophotic hard corals across the main Hawaiian Islands. PeerJ. 4:e2189. doi:10.7717/peerj.2189. https://peerj.com/articles/2189.

Veron JEN, Stafford-Smith MG. 2002. Australian Institute of Marine Science. Coral ID.

Wabnitz CCC, Balazs G, Beavers S, Bjorndal KA, Bolten AB, Christensen V, Hargrove S, Pauly D. 2010. Ecosystem structure and processes at Kaloko Honoko–hau, focusing on the role of herbivores, including the green sea turtle Chelonia mydas, in reef resilience. Mar Ecol Prog Ser. 420:27–44. doi:10.3354/meps08846.

Wedding LMLM, Lecky JH, Gove J, Walecka HRHR, Donovan MKMK, Williams GJGJGJ, Jouffray J, Crowder LBLBLBLB, Erickson A, Kim F, et al. 2017. Advancing the Integration of Spatial Data to Map Human and Natural Drivers on Coral Reefs. PLoS One.:1–29. doi:10.1371/journal.pone.0189792.

Weijerman M. 2017. Report of the Hawaii Atlantis Ecosystem Model Planning Workshop held in January 2017 in Honolulu. (U.S.) PIFSC, editor. doi:http://doi.org/10.7289/V5/AR-PIFSC-H-17-03. https://repository.library.noaa.gov/view/noaa/14439.

Weijerman M, Fulton EA, Kaplan IC, Gorton R, Leemans R, Mooij WM, Brainard RE. 2015. An integrated coral reef ecosystem model to support resource management under a changing climate. PLoS One. 10(12):e0144165. doi:10.1371/journal.pone.0144165. http://dx.doi.org/10.1371%2Fjournal.pone.0144165.

Weijerman M, Fulton EA, Parrish FA. 2013. Comparison of coral reef ecosystems along a fishing pressure gradient. PLoS One. 8(5):e63797. doi:10.1371/journal.pone.0063797. http://dx.doi.org/10.1371%2Fjournal.pone.0063797.

Weijerman M, Gove JM, Williams ID, Walsh WJ, Minton D, Polovina JJ. 2018. Evaluating management strategies to optimise coral reef ecosystem services. J Appl Ecol. 55(4):1823–1833. doi:10.1111/1365-2664.13105. http://dx.doi.org/10.1111/1365-2664.13105.

Weijerman M, Grüss A, Dove D, Asher J, Williams ID, Kelley C, Drazen JC. 2019. Shining a light on the composition and distribution patterns of mesophotic and subphotic fish communities in Hawai'i. Mar Ecol Prog Ser. 630:161–182. doi:10.3354/meps13135.

Weijerman M, Leong KM, Wongbusarakum S. 2019. Second Hawai'i Atlantis Ecosystem Model Planning Workshop: Where is the "S" in EBFM? doi:https://doi.org/10.25923/bfwa-7084. https://repository.library.noaa.gov/view/noaa/21425.

Weijerman M, Link JSS, Fulton EAA, Olsen E, Townsend H, Gaichas S, Hansen C, Skern-Mauritzen M, Kaplan ICC, Gamble R, et al. 2016. Atlantis Ecosystem Model Summit: Report from a workshop. Ecol Modell. 335:35–38. doi:10.1016/j.ecolmodel.2016.05.007.

Weijerman, M., Oyafuso, Z., Leong, K. M., Oleson, K. L. L., & Winston, M. 2020. Supporting Ecosystem-Based Fisheries Management in meeting multiple objectives for sustainable use of coral reef ecosystems. ICES Journal of Marine Science.

Weijerman M, Robinson S, Parrish F, Polovina J, Littnan C. 2017. Comparative application of trophic ecosystem models to evaluate drivers of endangered Hawaiian monk seal populations. Mar Ecol Prog Ser. 582:215–229. doi:10.3354/meps12320.

Welch A, Hoenig R, Stieglitz J, Daugherty Z, Sardenberg B, Miralao S, Farkas D, Benetti D. 2013. Growth rates of larval and juvenile bigeye scad Selar crumenophthalmus in captivity. Springerplus. 2(1):634.

Weng KCM, Sibert JR. 2004. Analysis of the Fisheries for two pelagic carangids in Hawaii. Honolulu, Hawaii: University of Hawaii, Joint Institute for Marine and Atmospheric Research.

Werding B. 1990. Alpheus schmitti Chace, 1972, a coral rock boring snapping-shrimp of the tropical western Atlantic (Decapoda, Caridea). Crustaceana. 58:88–96.

Wilkinson CR, Cheshire AC. 1990. Comparisons of sponge populations across the Barrier Reefs of Australia and Belize: Evidence for higher productivity in the Caribbean. Mar Ecol Prog Ser. 67(3):285–294.

Williams I, Ma H. 2013. Estimating catch weight of reef fish species using estimation and intercept data from the Hawaii Marine Recreational Fishing Survey. Honolulu, Hawai'i.

Wilson DT, McCormick MI. 1999. Microstructure of settlement-marks in the otoliths of tropical reef fishes. Mar Biol. 134(1):29–41.

Wilson K, Littnan C, Read AJ. 2017. Movements and home ranges of monk seals in the main Hawaiian Islands. Mar Mammal Sci. 33(4):1080–1096.

Winship AJ, Trites AW, Calkins DG. 2001. Growth in body size of the Steller sea lion (Eumetopias jubatus). J Mammal. 82(2):500–519.

Appendix A: Characteristics of spatial areas in Atlantis

Table A1 shows the number of the spatial area (BoxID), the (modeled) area of that box in m^2, the number of vertical water layers in that box, the maximum depth for the box and the percentage hard and soft substrate.

Table A1. Characteristics of the spatial areas in HI Atlantis

BoxID	Modeled Area (m^2)	# Water-column Layers	Max Depth (m)	Hardbottom (%)	Softbottom (%)
0	1000000000	3	-2000	NA	NA
1	86837950	3	-400	0.72	0.28
2	70314411	2	-150	0.62	0.38
3	20550660	1	-30	0.96	0.04
4	45565382	1	-30	0.86	0.14
5	98085777	2	-150	0.66	0.34
6	254311049	3	-400	0.64	0.36
7	1000000000	3	-2000	NA	NA
8	571491897	3	-400	0.23	0.77
9	134529397	2	-150	0.14	0.86
10	41544665	1	-30	0.52	0.48
11	44769089	1	-30	0.73	0.27
12	304230803	2	-150	0.74	0.26
13	344581628	3	-400	0.72	0.28
14	10000000000	3	-2000	NA	NA0
15	10000000000	3	-2000	NA	NA
16	54796911	3	-400	0.92	0.08
17	96074157	2	-150	0.66	0.34
18	28884198	1	-30	0.85	0.15
19	51587979	3	-400	0.60	0.40
20	100678121	2	-150	0.38	0.62
21	25334113	1	-30	0.84	0.16
22	9192920	1	-30	0.84	0.16
23	27258554	2	-150	0.66	0.34
24	28187831	1	-30	0.78	0.22
25	290936862	2	-150	0.37	0.63
26	40355117	1	-30	0.75	0.25
27	738431773	3	-400	0.31	0.69
28	474137398	2	-150	0.53	0.47
29	36519920	1	-30	0.57	0.43
30	55711796	1	-30	0.40	0.60
31	109103710	2	-150	0.33	0.67
32	170414432	3	-400	0.54	0.46

BoxID	Modeled Area (m^2)	# Water-column Layers	Max Depth (m)	Hardbottom (%)	Softbottom (%)
33	81283687	2	-150	0.11	0.89
34	13387472	1	-30	0.78	0.22
35	9324691	1	-30	0.88	0.12
36	76510477	2	-150	0.18	0.82
37	859092447	3	-400	0.46	0.54
38	111378576	2	-150	0.30	0.70
39	46808198	1	-30	0.68	0.32
40	8964789	1	-30	0.53	0.47
41	292676476	2	-150	0.51	0.49
42	51281407	2	-150	0.37	0.63
43	28296839	1	-30	0.72	0.28
44	43260763	1	-30	0.71	0.29
45	190212033	2	-150	0.45	0.55
46	155688989	3	-400	0.23	0.77
47	325411852	3	-400	0.46	0.54
48	1007017807	2	-150	0.56	0.44
49	46468590	1	-30	0.78	0.22
50	69618586	1	-30	0.72	0.28
51	10000000000	3	-2000	NA	NA
52	70598569	3	-400	0.79	0.21
53	98572918	2	-150	0.72	0.28
54	46144471	1	-30	0.88	0.12
55	115592299	1	-30	0.70	0.30
56	81960784	2	-150	0.65	0.35
57	84092178	3	-400	0.61	0.39
58	75651692	1	-30	0.88	0.12
59	195332834	2	-150	0.73	0.27
60	250847920	3	-400	0.78	0.22
61	138630762	3	-400	0.81	0.19
62	102303859	2	-150	0.75	0.25
63	45720462	1	-30	0.74	0.26
64	103824036	1	-30	0.76	0.24
65	33338683	3	-400	0.82	0.18
66	58885984	2	-150	0.33	0.67
67	65975190	1	-30	0.74	0.26
68	72306447	3	-400	0.51	0.49
69	128849063	2	-150	0.69	0.31
70	89814831	1	-30	0.76	0.24
71	86298312	1	-30	0.78	0.22
72	110958495	2	-150	0.79	0.21

BoxID	Modeled Area (m^2)	# Water-column Layers	Max Depth (m)	Hardbottom (%)	Softbottom (%)
73	69227275	3	-400	0.56	0.44
74	67686243	3	-400	0.69	0.31
75	79391217	2	-150	0.48	0.52
76	14365727	1	-30	0.73	0.27
77	17858498	1	-30	0.91	0.09
78	107580948	2	-150	0.60	0.40
79	64760693	3	-400	0.65	0.35
80	10000000000	3	-2000	NA	NA
81	island	0	0	0	0
82	island	0	0	0	0
83	island	0	0	0	0
84	island	0	0	0	0
85	island	0	0	0	0
86	island	0	0	0	0
87	island	0	0	0	0
88	island	0	0	0	0

Appendix B: Meta-analysis of sensitivities to pH and temperature of Hawaiian organisms

Contributor: Kaitlyn Lowder

From an initial screening of 1,543 full papers, we gathered and analyzed data from 334 papers of controlled experiments that exposed organisms from tropical Pacific or Indo-Pacific environments to either changes in pH or temperature. The database contains 2,561 responses of 243 unique species/genera belonging to 29 functional groups. Corals (PRM, PRM, MON, and POC) were most represented in the studies (Figure A1). Also, various life stages of small planktivorous fish species (aggregated in the functional group reef small planktivores, RSP; e.g., *Amphiprion ocellaris*, *Pomacetrus wardi*) were highly represented in the studies. We had no data on most of the fish species, deep sea corals in the genus *Leptoseris*, or manta rays.

As the Atlantis model can assimilate variables for growth, nutritional quality, reproduction, and predation vulnerability, responses of interest encompassed basic responses such as survival to behavioral responses like avoidance of predator cue. Yet, the majority of the studies explored the response in biomass growth, largely estimated through change in the rate of growth, calcification, consumption, mortality, and survival. Response values and sample sizes from individual studies were converted to effect size (log odds ratio or Hedges' g, depending on whether the data were continuous or binary), then related to changes in temperature or $[H^+]$. Likelihood ratio tests were used to compare and select intercept-only, linear, and quadratic models of best fit for each functional group and response.

In Atlantis, there can only be one relationship that describes the response of the four variables per functional group. To determine this relationship, we aggregated effect sizes for studies with multiple response measurements using Borenstein et al. (2009) procedures so meta-regression models were fit with independent data. Depending on the available data, in some cases we found both a continuous and binary model fit for the same group. In these cases, we chose the model fit with the lowest log likelihood. If the log likelihood was <10% different we chose the linear or quadratic fit over the intercept-only fit.

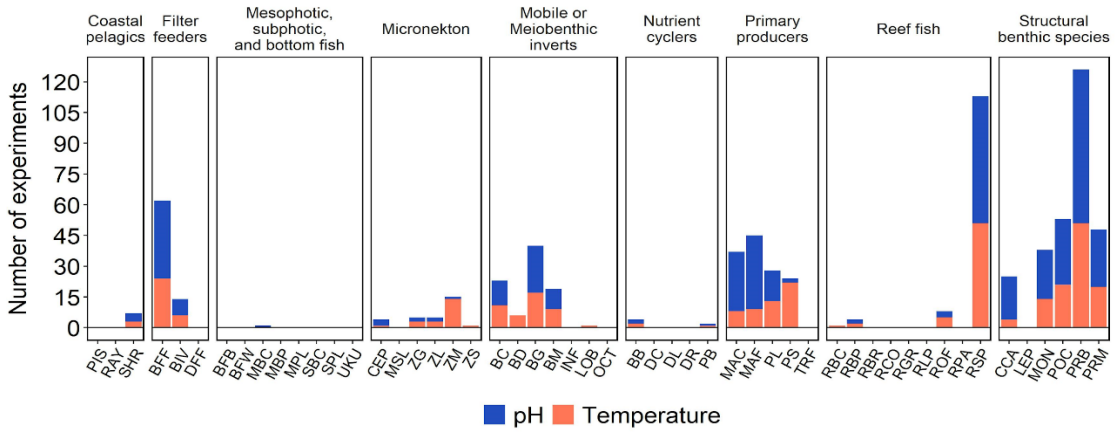

Figure A1. Number of experiments per Atlantis functional group for relationships of changes in pH (blue bar) and temperature (red bar).

pH relationships

For relationships with pH where the best fit was linear or quadratic, we developed a single pH sensitivity curve of pH against the functional group pH sensitivity factor (Busch and McElhany 2016). With a change in pH the survival of the group changes according to the corresponding value of this curve. To standardize these curves, we used the functional group that showed the most negatively responding relationship as a reference relationship. We scaled this relationship to a range of 1 at current pH (8.1) to 0 at pH=7.0 by setting the intercept at 1 for pH=8.1 and adjusting the slope so that the survival equals zero at pH=7.0. We then scaled the rest of the relationships to that reference curve by multiplying the slopes with the same value and setting all the intercepts to 1. This generated values of all the other functional groups proportionally less to pH.

For relationships where the best fit was an intercept model, we applied it as a piecewise function where at or above current pH, the sensitivity scalar is set to 1 and with a pH below 8.0 the scalar either step-increases or step-decreases and stays constant at further decreased pH values. All intercept values were standardized to a range of 0.1 and 1.3 assuming that under lower pH conditions the groups with a positive relationship with pH increased their survival with a maximum of 30% and those with a negative relationship decreased their survival to a minimum of 10%.

We looked for a natural break in pH and found one at around a pH value of 7. Therefore, we did not include any further decreases in pH (these results were often outliers addicting the curve of the shape disproportionately). Results showed that statistically the intercept model was in many cases the best fit, i.e., the data have no relationship to pH, and the effect size was for 8 groups positive and for 7 negative (Figure A2A). The pelagic bacteria (PB) and medium zooplankton (ZM) groups had the most positive and negative response and were set at 30% increase and 30% decrease with respect to the survival scalar, respectively. All other groups were scaled accordingly. For 8 functional groups the best fit was a linear relationship with pH and all groups showed a negative response with a decrease in pH (Figure A2B). The functional group with the most negative sensitivity was bivalves (BIV). This group served as the reference curve and all others were scaled accordingly.

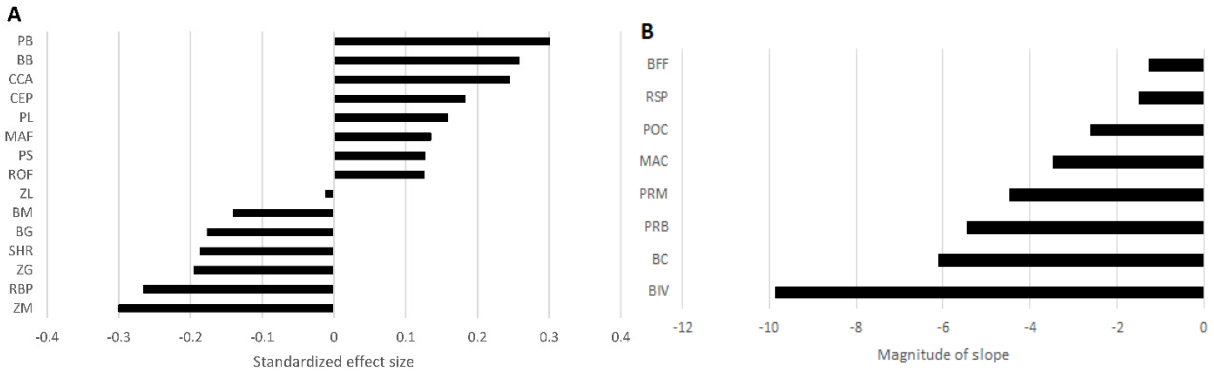

Figure A2. Relationship between a decrease in pH and survival of functional groups for (A) intercept only models and (B) linear models.

In correspondence with other studies (e.g., Kroeker et al., 2013), most calcareous groups (such as bivalves, corals, urchins, shrimps, calcareous algae, coccolithophores) decreased in biomass growth and plankton increased. However, contrary to Kroeker et al.'s finding, tropical crustose coralline algae actually increased its biomass growth under more acidic conditions.

Temperature relationships

For temperature sensitivity to growth related parameters, we calculated a single 'effect size' so with a change in temperature a functional group either increases its metabolic rate/growth when the effect size was >0 or decreases. Temperature can have a large influence on many biogeochemical and ecological processes. We only included results of studies where the temperature change was less than 5°C as higher increases are likely causing physiological responses. In Atlantis temperature effects are mostly applied through the "Tscalar" which is based on a set reference temperature of 15°C:

$$Tscalar = q10^{\frac{Tcurrent - Treference}{10}}$$

where q10 is a species-specific parameter the user needs to provide and is typically set to 2 which means that with an 10°C increase in ocean temperature, rate parameters will double (Tscalar=2).

Effect size ranged between -3.76 (n=19, AIC=185) for small phytoplankton, indicating that with an increase in temperature, growth decreases, and 3.24 (n=12, AIC=57) for benthic detritivores (Figure A3). We standardized these values so that an effect size of 2 resulted in a q10 of 2 and set the minimum to 0.1 (i.e., with a 10°C increase in ocean temperature, rate parameters will drop to 10%). This resulted in standardized values of q10 between 0.1, for sharks and small phytoplankton, and 3.52 for pelagic bacteria.

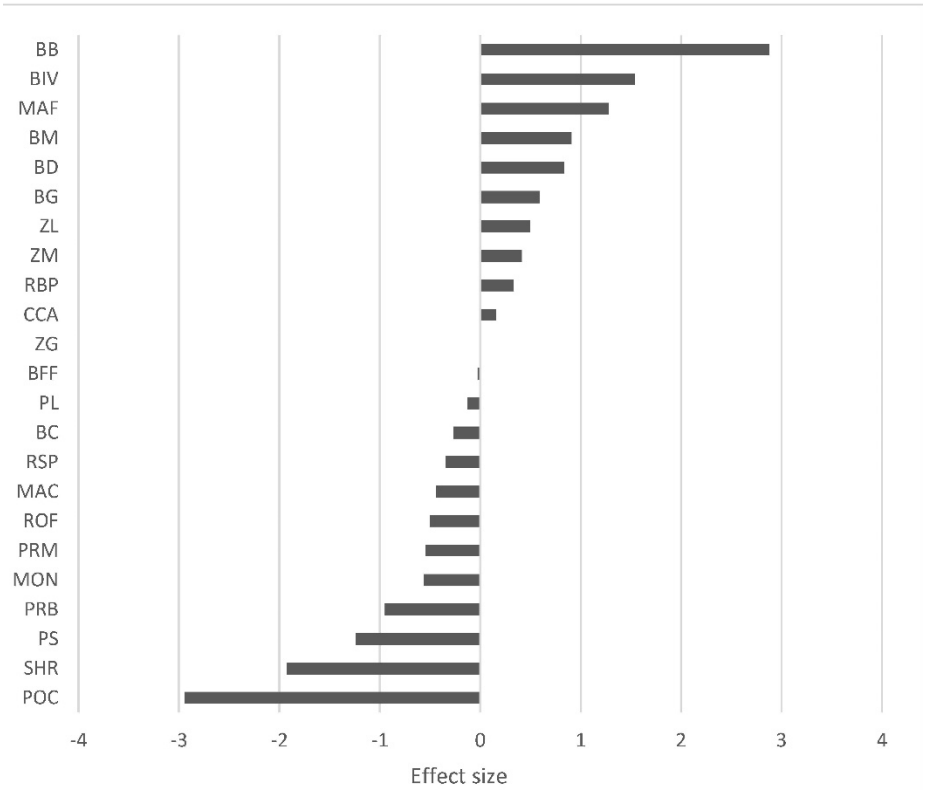

Figure A3. Effect size of the relationship between an increase in temperature and survival of functional groups.

Appendix C: Vertebrate species aggregated by functional groups

All species were aggregated in functional groups based on diet, habitat, life history parameters and social or economic importance. Table A2 shows the composition of each group with the code used throughout this report. For the reef fishes we only included the species that had a combined biomass and/or abundance proportion of approximately 85%.

Table A2. Species composition of the functional groups used in HI Atlantis. Purple lines are broad categories and other colors are the functional groups.

Code	Group	Family	Scientific Name
Reef Fishes			
RSP	**Small Planktivores**		
		Pomacentridae	*Chromis vanderbilti*
		Pomacentridae	*Chromis verater*
		Pomacentridae	*Dascyllus albisella*
		Chaetodontidae	*Heniochus diphreutes*
		Pomacentridae	*Abudefduf abdominalis*
		Acanthuridae	*Acanthurus thompsoni*
		Chaetodontidae	*Chaetodon kleinii*
		Pomacentridae	*Chromis hanui*
		Pomacentridae	*Abudefduf vaigiensis*
RLP	**Large Planktivores**		
		Balistidae	*Melichthys niger*
		Acanthuridae	*Naso hexacanthus*
		Acanthuridae	*Naso brevirostris*
		Holocentridae	*Myripristis berndti*
		Holocentridae	*Myripristis kuntee*
		Holocentridae	*Myripristis amaena*
RCO	**Corallivores**		
		Chaetodontidae	*Chaetodon ornatissimus*
		Chaetodontidae	*Chaetodon multicinctus*
		Chaetodontidae	*Chaetodon quadrimaculatus*
		Pomacentridae	*Plectroglyphidodon johnstonianus*
		Chaetodontidae	*Chaetodon unimaculatus*
		Chaetodontidae	*Chaetodon lunulatus*
ROF	**Invertivores**		
		Balistidae	*Sufflamen fraenatum*
		Balistidae	*Sufflamen bursa*
		Labridae	*Thalassoma duperrey*

Code	Group	Family	Scientific Name
		Balistidae	*Rhinecanthus rectangulus*
		Cirrhitidae	*Paracirrhites arcatus*
		Zanclidae	*Zanclus cornutus*
		Labridae	*Coris gaimard*
		Chaetodontidae	*Chaetodon lunula*
		Labridae	*Stethojulis balteata*
		Labridae	*Thalassoma ballieui*
		Tetraodontidae	*Canthigaster jactator*
		Labridae	*Coris venusta*
			Gomphosus varius
			Halichoeres ornatissimus
		Monacanthidae	*Cantherhines dumerilii*
			Forcipiger flavissimus
		Tetraodontidae	*Arothron meleagris*
RBC	**Target Benthic Carnivores**		
		Lutjanidae	*Lutjanus kasmira*
		Labridae	*Bodianus bilunulatus*
		Mullidae	*Parupeneus multifasciatus*
		Lutjanidae	*Lutjanus fulvus*
		Mullidae	*Parupeneus cyclostomus*
		Mullidae	*Mulloidichthys flavolineatus*
		Mullidae	*Mulloidichthys vanicolensis*
		Mullidae	*Parupeneus insularis*
		Labridae	*Coris flavovittata*
		Mullidae	*Parupeneus pleurostigma*
			Sargocentron diadema
RBR	**Target Browsers**		
		Acanthuridae	*Naso lituratus*
		Kyphosidae	*Kyphosus* sp
		Acanthuridae	*Naso unicornis*
		Scaridae	*Calotomus carolinus*
		Chanidae	*Chanos chanos*
RGR	**Target Grazers**		
		Acanthuridae	*Acanthurus olivaceus*
		Acanthuridae	*Acanthurus nigrofuscus*
		Acanthuridae	*Acanthurus dussumieri*
		Acanthuridae	*Acanthurus blochii*
		Acanthuridae	*Ctenochaetus strigosus*
		Balistidae	*Melichthys vidua*

Code	Group	Family	Scientific Name
		Acanthuridae	*Zebrasoma flavescens*
		Acanthuridae	*Acanthurus triostegus*
		Acanthuridae	*Acanthurus xanthopterus*
		Acanthuridae	*Acanthurus leucopareius*
		Acanthuridae	*Acanthurus nigroris*
		Pomacentridae	*Stegastes fasciolatus*
RPA	**Parrotfishes**		
		Scaridae	*Scarus rubroviolaceus*
		Scaridae	*Chlorurus spilurus*
		Scaridae	*Scarus psittacus*
		Scaridae	*Scarus dubius*
		Scaridae	*Chlorurus perspicillatus*
		Scaridae	*Scaridae*
RBP	**Benthic Piscivores**		
		Serranidae	*Cephalopholis argus*
		Muraenidae	*Gymnothorax flavimarginatus*
		Labridae	*Oxycheilinus unifasciatus*
		Muraenidae	*Gymnothorax meleagris*
		Cirrhitidae	*Paracirrhites forsteri*
		Aulostomidae	*Aulostomus chinensis*
		Muraenidae	*Gymnothorax javanicus*
PIS	**Roving Piscivores**		
		Carangidae	*Caranx melampygus*
		Carangidae	*Caranx ignobilis*
		Carangidae	*Seriola dumerili*
		Carangidae	*Seriola rivoliana*
		Lutjanidae	*Aphareus furca*
		Carangidae	*Carangoides ferdau*
		Carangidae	*Fistularia commersonii*
		Carangidae	*Carangoides orthogrammus*
		Carangidae	*Caranx ferdau*
		Fistulariidae	*Scomberoides lysan*
		Carangidae	*Elagatis bipinnulata*
		Belonidae	*Tylosurus crocodilus*
		Sphyraenidae	*Sphyraena barracuda*
		Gempylidae	*Rexea nakamurai*
		Berycidae	*Beryx decadactylus*
		Fistulariidae	*Fistularia petimba*

Code	Group	Family	Scientific Name
SHP	**Shallow Prey**		
		Carangidae	*Decapterus macarellus*
		Carangidae	*Selar crumenophthalmus*
		Carangidae	*Decapterus* sp.
Sharks and Rays			
SHR	**Sharks**		
		Squalidae	*Squalus mitsukurii*
		Carcharhinidae	*Carcharhinus plumbeus*
		Carcharhinidae	*Carcharhinus galapagensis*
		Carcharhinidae	*Carcharhinus amblyrhynchos*
		Carcharhinidae	*Triaenodon obesus*
		Carcharhinidae	*Carcharhinus altimus*
		Carcharhinidae	*Galeocerdo cuvier*
		Squalidae	*Squalus blainvillei*
		Cetorhinidae	*Selachii*
		Carcharhinidae	*Galeocerdo cuvier*
IVR	**Invertivorous Rays**		
		Myliobatidae	*Aetobatus narinari*
		Dasyatidae	*Bathytoshia lata*
		Plesiobatidae	*Plesiobatis daviesi*
		Dasyatidae	
		Batoidea	
RAY	**Manta Rays**	Mobulidae	*Mobula birostris*
Deep-water Fishes			
BFW	**Bottomfish—Water Column**		
		Lutjanidae	*Pristipomoides filamentosus*
		Lutjanidae	*Etelis coruscans*
		Lutjanidae	*Pristipomoides sieboldii*
		Lutjanidae	*Aphareus rutilans*
BFB	**Bottomfish—Bottom**		
		Lutjanidae	*Etelis carbunculus*
		Epinephelidae	*Hyporthodus quernus*
		Lutjanidae	*Pristipomoides zonatus*
UKU	**Uku**	Lutjanidae	*Aprion virescens*

Code	Group	Family	Scientific Name
Mesophotic Fishes			
MPL	**Mesophotic Planktivores**		
		Pomacentridae	*Chromis verater*
		Chaetodontidae	*Chaetodon miliaris*
		Chaetodontidae	*Heniochus diphreutes*
		Pomacentridae	*Chromis leucura*
		Acanthuridae	*Naso hexacanthus*
		Serranidae	*Pseudanthias Hawaiiensis*
		Pomacentridae	*Dascyllus albisella*
		Acanthuridae	*Naso* spp.
		Serranidae	*Luzonichthys earlei*
		Pomacentridae	*Chromis spp.*
		Acanthuridae	*Naso maculatus*
		Balistidae	*Melichthys niger*
		Pomacentridae	*Chromis ovalis*
		Holocentridae	*Myripristis berndti*
		Ostraciidae	*Lactoria diaphana*
MBC	**Mesophotic Benthic Carnivores**		
		Lutjanidae	*Lutjanus kasmira*
		Balistidae	*Sufflamen fraenatum*
		Mullidae	*Parupeneus multifasciatus*
		Zanclidae	*Zanclus cornutus*
		Pomacanthidae	*Apolemichthys arcuatus*
		Labridae	*Bodianus albotaeniatus*
		Holocentridae	*Myripristis chryseres*
		Acanthuridae	*Acanthurus* spp.
		Bothidae	Bothus thompsoni
		Tetraodontidae	*Sphoeroides cutaneus*
		Chaetodontidae	*Forcipiger flavissimus*
		Mullidae	*Parupeneus pleurostigma*
		Tetraodontidae	*Torquigener florealis*
		Chaetodontidae	*Forcipiger* spp.
		Mullidae	*Parupeneus chrysonemus*
		Labridae	*Pseudojuloides cerasinus*
		Apogonidae	*Ostorhinchus maculiferus*
		Acanthuridae	*Acanthurus* spp.
		Chaetodontidae	*Chaetodon kleinii*
MBP	**Meso and Subphotic Benthic Piscivores**		
		Scorpaenidae	
		Pontinus macrocephalus	*Pontinus macrocephalus*

Code	Group	Family	Scientific Name
		Chlorophthalmus proridens	*Chlorophthalmus proridens*
		Gymnothorax berndti	*Gymnothorax berndti*
		Polymixia berndti	*Polymixia berndti*
		Ariosoma marginatum	*Ariosoma marginatum*
		Gymnothorax spp.	*Gymnothorax* spp.
		Conger oligoporus	*Conger oligoporus*
		Synodus kaianus	*Synodus kaianus*
		Hoplichthys citrinus	*Hoplichthys citrinus*
		Trachinocephalus myops	*Trachinocephalus myops*
		Gymnothorax nuttingi	*Gymnothorax nuttingi*
		Chrionema spp.	*Chrionema* spp.
Subphotic Fishes			
SBC	**Subphotic Benthic Carnivores**		
		Ophichthidae	
		Monacanthidae	*Pervagor spilosoma*
		Synaphobranchidae	*Meadia abyssalis*
		Serranidae	*Zalanthias kelloggi*
		Percophidae	*Chrionema chryseres*
		Bothidae	*Poecilopsetta Hawaiiensis*
		Scorpaenidae	*Setarches guentheri*
		Chaunacidae	*Chaunax umbrinus*
		Bothidae	*Parabothus chlorospilus*
		Bothidae	*Taeniopsetta radula*
		Peristediidae	*Scalicus engyceros*
		Ogcocephalidae	*Halieutaea retifera*
		Pinguipedidae	*Parapercis roseoviridis*
		Chaetodontidae	*Chaetodon tinkeri*
		Tetraodontidae	*Canthigaster coronata*
		Congridae	*Gnathophis* spp.
		Moridae	*Laemonema rhodochir*
		Percophidae	*Chrionema squamiceps*
		Acropomatidae	*Parascombrops argyreus*
		Lophiidae	*Lophiodes miacanthus*
		Bothidae	*Arnoglossus debilis*
		Dactylopteridae	*Dactyloptena orientalis*
		Moridae	
		Lutjanidae	*Randallichthys filamentosus*
		Bothidae	*Parabothus coarctatus*
		Moridae	*Physiculus* spp.
		Cepolidae	*Owstonia Hawaiiensis*

Code	Group	Family	Scientific Name
		Aulopodidae	*Hime japonica*
		Bothidae	*Chascanopsetta prorigera*
		Bothidae	*Engyprosopon xenandrus*
		Ophichthidae	Myrophinae
		Chaetodontidae	*Forcipiger longirostris*
SPL	**Subphotic Planktivores**		
		Symphysanodontidae	*Symphysanodon maunaloae*
		Caproidae	*Antigonia* spp.
		Serranidae	*Odontanthias elizabethae*
		Chaetodontidae	*Roa excelsa*
		Symphysanodontidae	*Symphysanodon typus*
		Triacanthodidae	*Hollardia goslinei*
		Callanthiidae	*Grammatonotus* spp.
		Serranidae	*Odontanthias fuscipinnis*
		Caproidae	*Antigonia eos*
		Priacanthidae	*Priacanthus alalaua*
		Pomacentridae	*Chromis struhsakeri*
		Epigonidae	*Epigonus* spp.
		Callanthiidae	*Grammatonotus laysanus*
		Pinguipedidae	*Parapercis schauinslandii*
		Priacanthidae	*Cookeolus japonicus*
		Caproidae	*Antigonia steindachneri*
		Emmelichthyidae	*Erythrocles scintillans*
		Balistidae	*Xanthichthys auromarginatus*
		Serranidae	*Pseudanthias thompsoni*
		Priacanthidae	*Priacanthus meeki*
		Serranidae	*Pseudanthias fucinus*
		Argentinidae	*Glossanodon struhsakeri*
		Epigonidae	*Epigonus glossodontus*
Mesopelagic Scatter Layer			
MSL			
		Myctophidae	*Benthosema fibulatum*
		Myctophidae	*Idiolychnus urolampus*
		Myctophidae	
		Myctophidae	*Lampadena urophaos*
		Myctophidae	*Diaphus adenomus*
		Myctophidae	*Diaphus termophilus*
		Bregmacerotidae	*Bregmaceros* sp.
		Myctophidae	*Diaphus* spp.

Code	Group	Family	Scientific Name
Marine Reptiles			
GT		Cheloniodae	*Chelonia mydas*
HT		Cheloniodae	*Eretmochelys imbricata*
Marine Mammals			
MS		Phocidae	*Neomonachus schauinslandi*
SPD		Delphinidae	*Stenella longirostris longirostris*
BND		Delphinidae	*Tursiops truncatus truncatus*

Appendix D: Invertebrate data analysis

Contributor: Molly Timmers

Data collected from Autonomous Reef Monitoring Structures (ARMS)[17] by PIFSC's Reef Assessment and Monitoring Program were used for the shallow water (0–30 m) reef invertebrate groups. ARMS are long-term collecting devices that attract colonizing invertebrates. Designed to mimic, to some degree, the structural complexity of a coral reef, they are composed of 4 open and 4 semi-closed layers of 23×23 cm PVC plates. Up to 3 replicates were deployed at each site of similar depth and habitat type (fore reef 12–16 m) and remained on the benthos for 3 years. Mobile organisms 2 mm and greater from 37 ARMS units at 14 sites retrieved in 2013 and 2016 were examined. Given the device construction and the motile organismal focus, burrowing species, suspension feeders, and sessile organisms will be underrepresented in these data. All species were identified to species if possible or the next taxonomic level. Based on available literature, organisms were classified into the following trophic guilds: omnivores, carnivores, herbivores, suspension feeders, and detritivores.

Average density was 284 individuals per ARMS unit. Of the >400 identified species, the majority (70%) belonged to the phylum Arthropoda, 18% to Mollusca and 4.5% to Annelida (Figure A4). Annelids, which can make up 12% of the infaunal biomass and are extremely abundant with values up to 43,500 ind/m^2 (Kohn and White 1977), were underrepresented in part because an ARMS unit is likely not a suitable substrate for the burrowing marine worms. When partitioning these data by trophic guild, 40% were omnivorous (mostly crustaceans), 27% primarily detritus feeders, 15% carnivorous, 10% herbivorous and 8% suspension feeders (Figure A4).This distribution was similar as observed in the East Pacific (Enochs and Manzello 2012) and Guam (Weijerman et al. 2015).

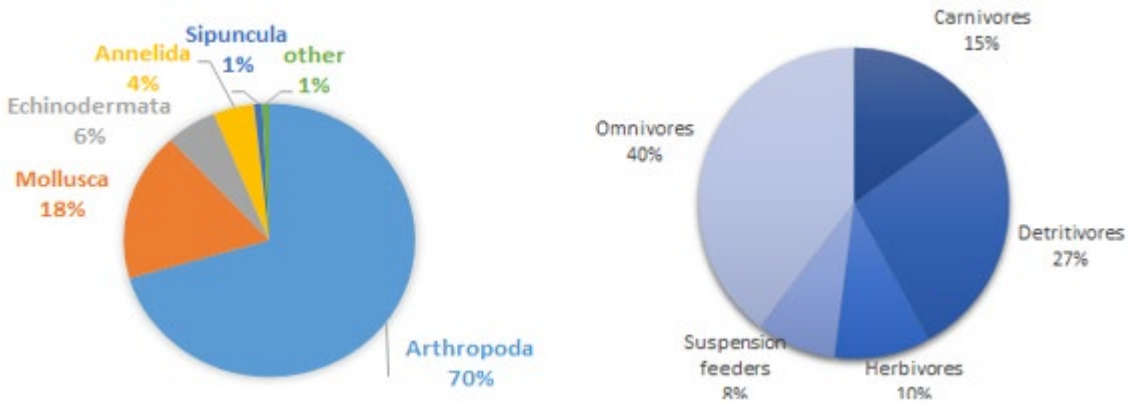

Figure A4. Composition of relative species count per (left panel) phylum and (right panel) trophic guild from 37 Autonomous Reef Monitoring Structure (ARMS) units.

Biomass estimates of crypto- and epifauna on reefs are difficult to obtain. Ainsworth et al. (Ainsworth et al. 2007) reported an infaunal biomass 27 g/m^2 and a total epifaunal biomass of

[17] https://www.pifsc.noaa.gov/cred/survey_methods/arms/

400 g/m^2 for a reef system in Indonesia. Bustamante (Bustamante 2010) reported an infaunal invertebrate biomass of 6 g/m^2 and a total epifauna excluding urchins, sea cucumbers, and sea stars of 9 g/m^2 for a subtropical bay in Australia. Enochs (Enochs 2012) estimated the total cryptofauna on dead coral for rubble, and high, medium and low degraded reefs as 3.5 AFDW/m^2, 6.2 AFDW/m^2, 11.0 AFDW/m^2 and 12.3 AFDW/m^2, respectively. I used the complexity estimates (PIFSC RAMP) as proxies for the degradation of a reef with a complexity of 2 corresponding to high degraded reef, 3 to medium degraded reef and a complexity of 4 and 5 to a low degraded reef. Using the trophic composition (Figure A4) and assuming omnivores to be the meiofauna groups, I could then estimate the biomass of each functional group. To account for the macroinvertebrates (e.g., urchins) in the benthic grazer groups, and the benthic detritivore group (e.g., sea cucumbers) and the underrepresented suspension feeders from ARMS data, I multiplied their biomass by 1.5. Further, I assumed a biomass of 30 g/m^2 for infauna (e.g., polychaetes).

I used the trophic composition of the ARMS data (Figure A4) for diet data of meiofauna, equally dividing the omnivores over the detritivores, carnivores, herbivores, and suspension feeders. Lobster and octopus biomass estimates were based on the assumption of a sustainable fishery (see main text). I then compared these values with values based on an Ecopath with Ecosim model developed for the same study site (Weijerman et al. In press).

Mean vital rate parameters were calculated based on the production:biomass ratios (P/B for growth rate) and consumption:biomass (Q/B for consumption rate) which came from literature or empirical relationships with values derived from literature (Table A3). The P/B depends highly on the mean annual temperature, mean individual weight, and swimming capacity of marine macroinvertebrates (Cartes et al. 2002); therefore, if I did not find any reported values in the literature I used an empirical relationship established by Brey (Brey 2001) that includes the following aspects:

Log (P/B) = 7.947 – 2.294 * log(M) – 2409.856 * 1/(T+273) + 0.168 * 1/D + 0.194 + 0.180 * Infauna/Epifauna + factor * taxon – 0.062 + 582.851 * log(M) * 1/(T+273)

where M is the mean individual body mass in kilojoules, D is the water depth in meter, infauna equals 1, epifauna equals 0. Motility and taxon are also taken into account with taxon being Annelida, Crustacea, Echinodermata or Insecta .For the Q/B ratio I used the empirical relationship established by Cammen (Cammen 1979):

$$C = 0.381*W^{0.742}$$

where C is the daily consumption in mg dry weight (DW), W is the mean body weight in mg DW.

Based on the species or family composition of the benthic small invertebrates derived from ARMS, we obtained a weighting factor for the calculation of P/B and Q/B per functional group of invertebrates (Table A3).

Table A3. The vital rate values, Production over Biomass (P/B) and Consumption over Biomass (Q/B) for species groups with their source.

Functional group	P/B	Source	Q/B	Source
Benthic Infauna: Fire worms, other polychaetes, flat worms, sipunculids (peanut worms), and nemerteans (ribbon worms)	3.9	(Brey 2001; McCarthy et al. 2003; Safarik et al. 2006; Gribble 2007)	10.0	(McCarthy et al. 2003; Safarik et al. 2006; Gribble 2007)
Benthic meiofauna: Xanthidae (pebble crabs), Pilumnidae (hairy crabs), Caridea (snapping shrimp, cleaner shrimp), and Stomatopoda (mantis shrimp)	2.64	(Werding 1990; Ainsworth et al. 2007; Harikrishnan et al. 2010)	10.52	(Cammen 1979; Werding 1990; Opitz 1996; Ainsworth et al. 2007; Harikrishnan et al. 2010)
Lobster and Large crabs	0.827	(Pauly 1980; Ainsworth et al. 2007; O'Malley and MacDonald 2009)	14.88	(Ainsworth et al. 2007)
Octopus	3.313	(Brey 2001; Tsehaye and Nagelkerke 2008)	8.0	(Van Heukelem 1976; Tsehaye and Nagelkerke 2008)
Benthic carnivores: triton, sea slugs, nudibranchs	3.344	(Edwards and Huebner 1977; Morton 1990; Brey 2001; Ainsworth et al. 2007)	11.34	(Edwards and Huebner 1977; Cammen 1979; Morton 1990; Opitz 1996)
Benthic Detritivores: Echinoderms (boring sea urchins, sea stars, sea cucumbers, crabs)	2.11	(Brey 2001; Ainsworth et al. 2007; Wabnitz et al. 2010; Weijerman et al. 2013)	16.13	(Cammen 1979; Ainsworth et al. 2007; Wabnitz et al. 2010; Weijerman et al. 2013)
Suspension feeders: Bivalves, brittle stars	3.722	(Broom 1982; Mladenov and Emson 1984; Ainsworth et al. 2007)	11.12	(Opitz 1996; Ainsworth et al. 2007)

Functional group	P/B	Source	Q/B	Source
Shallow filter feeders: sponges, soft corals	1.067	(Weijerman et al. 2013)	6.480	(Weijerman et al. 2013)
Deep filter feeders: soft corals, black corals, anemones	1.2		4.02	
Benthic Grazers: free-living urchins, sea hares, cowries, limpets, top snails, chitons	0.67	(Brey 2001)	8.56	(Cammen 1979; Wabnitz et al. 2010)

The annual Q/B values were then converted to daily consumption rates. Since Atlantis uses maximum consumption rates, these values were multiplied by 1.2.

Appendix E: Meso- and subphotic initial conditions

Benthic cover

Benthic cover was determined using mesophotic surveys (Pyle et al. 2016) conducted in areas east of Maui (Atlantis box 28) to get an indication what the percent cover is when *Leptoseris* and *Montipora* are present. We then used the predicted presence/absence of *Leptoseris* and *Montipora* maps for the entire inhabited Hawaiian Islands (Veazey et al. 2016) and estimated the percent cover by multiplying the likelihood estimate of *Leptoseris/Montipora* being present with the percent cover from the surveys. For turf algae, we assumed a cover of 1% at mesophotic depths. We further assumed that when substrate is suitable for *Leptoseris* growth, it is also suitable for crustose coralline algae (CCA) and multiplied the estimated *Leptoseris* cover with 0.5 to get an assumed CCA cover (Rhodolithophores) at mesophotic depths. For macroalgae (e.g., *Halimeda* beds) we calculated the ratio of macroalgae to *Leptoseris* cover from PISC surveys, which was 1.25 for calcareous macroalgae and 1 for fleshy macroalgae, and multiplied the *Leptoseris* cover with these ratios to get an estimate of macroalgal cover.

Invertebrates

Contributor: Elena Cosner

In the "twilight" zone, numerous species of structural corals and sponges foster rich and diverse ecosystems. We investigated community composition, abundance, and productivity of benthic macroinvertebrate communities along a depth gradient. Invertebrate data were obtained from 532 submarine dives conducted by the Hawai‘i Undersea Research Laboratory at the University of Hawai‘i at Mānoa in depths of 30–400 m. From these surveys, we focused on macroinvertebrate composition across the depth gradient in the model area, seeking to understand distinct depth zones as it relates to benthic macroinvertebrates.

A total of 17,367 observations of 462 species were analyzed using community ecology statistical methods. Using ArcMap point to line in WGS 1984 UTM Zone 4N projected coordinate system, the length of each submersible dive was determined in meters. Assuming a 3-m "view frame" from which the organisms were identified from the submersible, the total survey area was determined for each dive. For *Mokoli'i* dives, which were conducted before the advent of GPS, an average of the RCV dives was used as survey area. Any missing dive length data were filled in with average area from similar dives. From the area for each dive, the abundance per dive per square meter for each taxa was determined. Then, from the recorded depth, each observation was placed into a 10-m depth bin. Community structure was examined using the Bray-Curtis dissimilarity metric (also known as Sorenson index). Hierarchical clustering, using the clustsig package in R[18] was based on the complete-linkage method, which maximizing the distance between clusters to visualize the faunal breaks along the depth gradient (Clarke et al. 2008). The SIMPROF (Similarity Profile) analysis, with an alpha = 10^{-7} (source), determined the most significantly different clusters used to evaluate which depth bins act as a distinguishable community. A dendrogram from the hierarchical clustering created a visual of the zonation of depth in assemblage structure. The depth zones from the SIMPROF analysis were used with NMDS (non-metric multidimensional scaling) to visualize the community structure.

[18] https://cran.r-project.org/web/packages/clustsig/index.html

PERMANOVA (permutational analysis of variance; Anderson, 2017) identified the significance of the *a posteriori* depth zones based on SIMPROF results. Finally, SIMPER (similarity percentages) identified which species were responsible for the main differences within the depth zones.

Functional groupings for each species observed was determined from the existing literature based on diet, commercial importance, and habitat affinity (i.e., demersal vs pelagic). Many species did not have described diets and diet had to be inferred from species with similar lifestyles at similar depths. Due to the broad descriptions of the functional groups, related species are likely a good reference.

We found four distinct invertebrate community clusters along the depth gradient from 30–409 m: 30–89 m, 90–159 m, 160–279 m, 280–409 m. Two larger clusters, 30–159 m, and 160–409 m (Figure A5, Figure A6), were additionally more significantly different than the interior clusters. These two depth ranges can be broadly defined as the mesophotic and subphotic zones in Hawai‘i, with differentiations between upper and lower zones for each zone with an associated assemblage of macroinvertebrates.

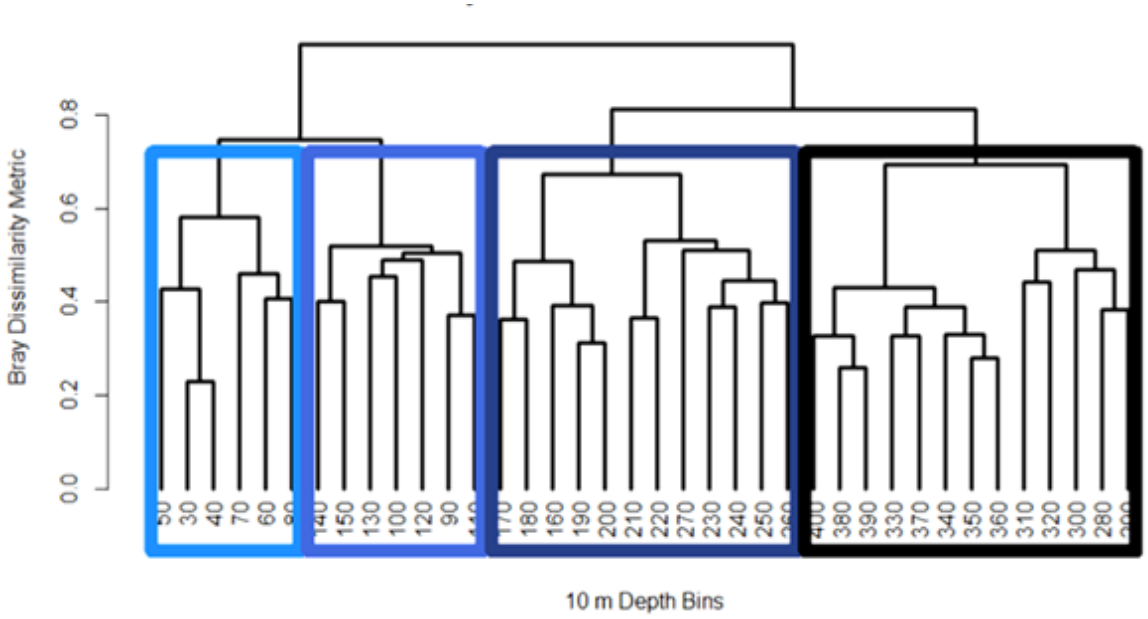

Figure A5. Hierarchical cluster dendogram using Bray-Curtis dissimilarity analysis of invertebrate presence/absence between 30 and 409 m. The colored boxes indicate groups that have significantly ($p < 0.00001$) distinct faunal communities based on the analysis of Similarity Profiles (SIMPROF). The values on the x-axis represent 10-m depth intervals (e.g., 30 refers to the 30–39 m depth interval).

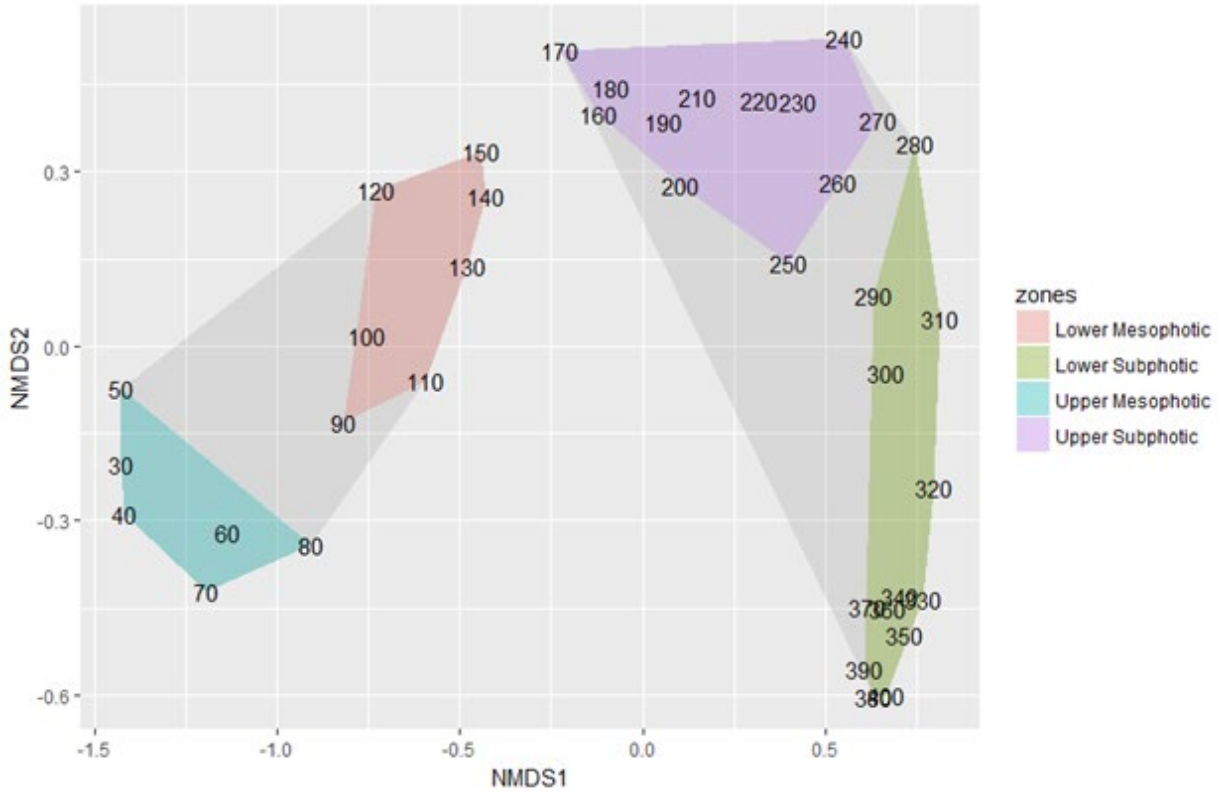

Figure A6. Non-metric multidimensional scaling (NMDS) ordination plot of faunal breaks along 10-m depth bins using *a priori* zones from the hierarchical clustering, (PERMANOVA; p<0.001). Colors represent distinct faunal depth zones. The values on the plot represent 10-m depth intervals (e.g., 30 refers to the 30–39 depth interval). The dark grey areas on the plot encompass the entire mesophotic (30–159 m) and subphotic (160–409 m) zones.

In these depth ranges, filter feeding invertebrates (chiefly cnidarians and sponges) dominated, whereas abundance of mobile invertebrates was relatively low. The mesophotic zone was dominated by hard corals and the subphotic zone was defined by soft corals. As depth increases, organisms dependent on photosynthesis, such as macroalgae and zooxanthellate corals, decrease in density with the scarcity of light. A shift from light-dependent to light-independent habitat builders occurs, changing the composition of reefs along this depth gradient. In the mesophotic zone, cnidarians were dominated by Scleractinia (hard corals) and Antipatharia (black corals; Figure A7). On the contrary, in the subphotic, Alcyonacea (soft corals) and Antipatharia were the dominant taxa. Furthermore, the subphotic zone had a wider abundance across taxa groups. In the mesophotic, taxa Zoantharia (zoanthids), Pennatualcea (sea pens), Corallimorphia (hydrozoans), Actiniaria (anemones), and Ceriantharia (tube-dwelling anemones) were absent or were only minor constituents of the cnidarian assemblage, whereas in the subphotic zone, these taxa had relatively higher abundances (Figure A7). Upper and lower mesophotic zones were distinctly different mainly due to the high abundance of hard corals (*Leptoseris* sp. *Montipora* sp. *Porites* sp and *Pocillopora* sp.), black corals (Anthipastes sp.) and the invasive coral species *Carijoa riisei* in the upper mesophotic and of sea urchins and a species of black coral (*Stichopathes* sp.) in the lower mesophotic. Differences between the upper and lower subphotic zones can be mostly attributed to black corals being mostly dominant in upper subphotic and

precious corals (e.g., the gold coral *Kulamanamana haumeaae*) abundant at lower subphotic depths.

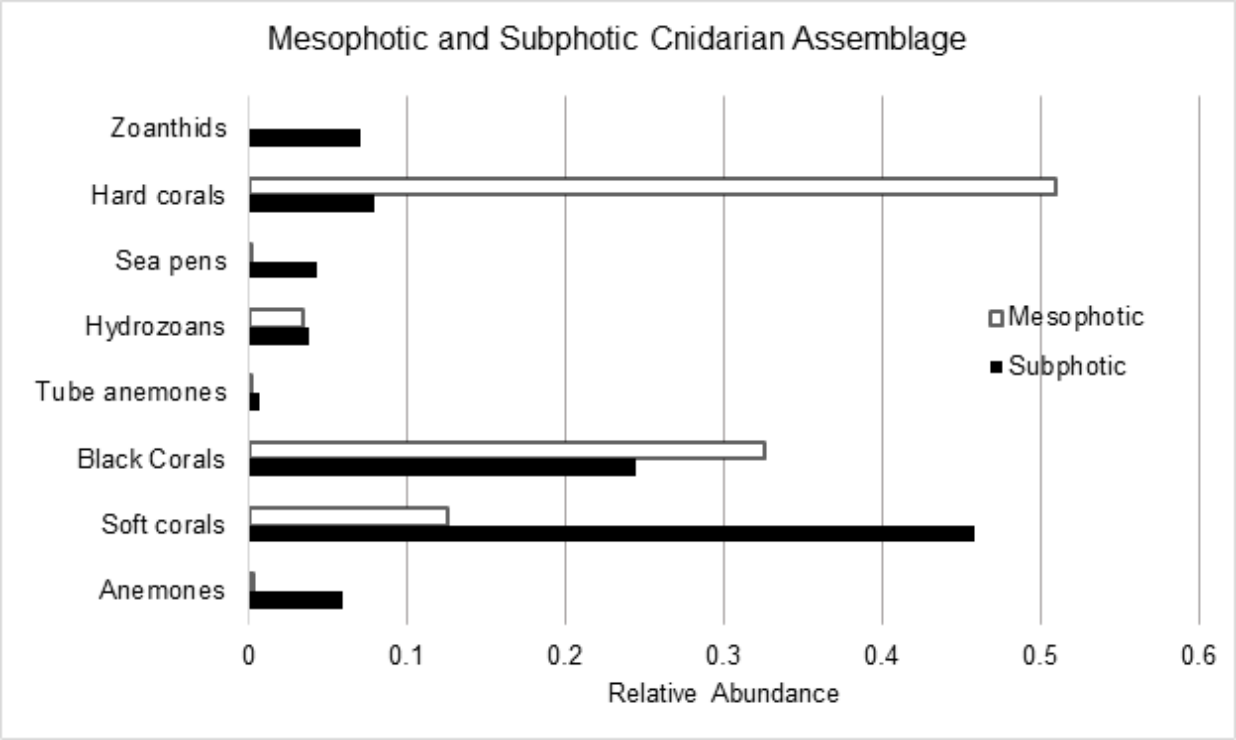

Figure A7. Cnidarian family assemblage differences by relative abundance between the mesophotic (open bars) and subphotic (black bars) zone.

Considering only mobile invertebrates, sea urchins were the most abundant, contributing around 14% of the mobile invertebrate relative abundance for both the mesophotic and the subphotic zones. Lobster were much more abundant in the mesophotic compared to the subphotic, contributing around 2% relative abundance, whereas in the subphotic, lobster rounded down to about 0%. Squat lobster, on the contrary, contributed to 7% of the relative abundance in the subphotic, and around 0% in the mesophotic. Shrimp, crabs, sea stars, and crinoids were as well more abundant in the subphotic compared to the mesophotic zone; however, sea cucumbers were more abundant in the mesophotic than the subphotic zone (Figure A8).

.

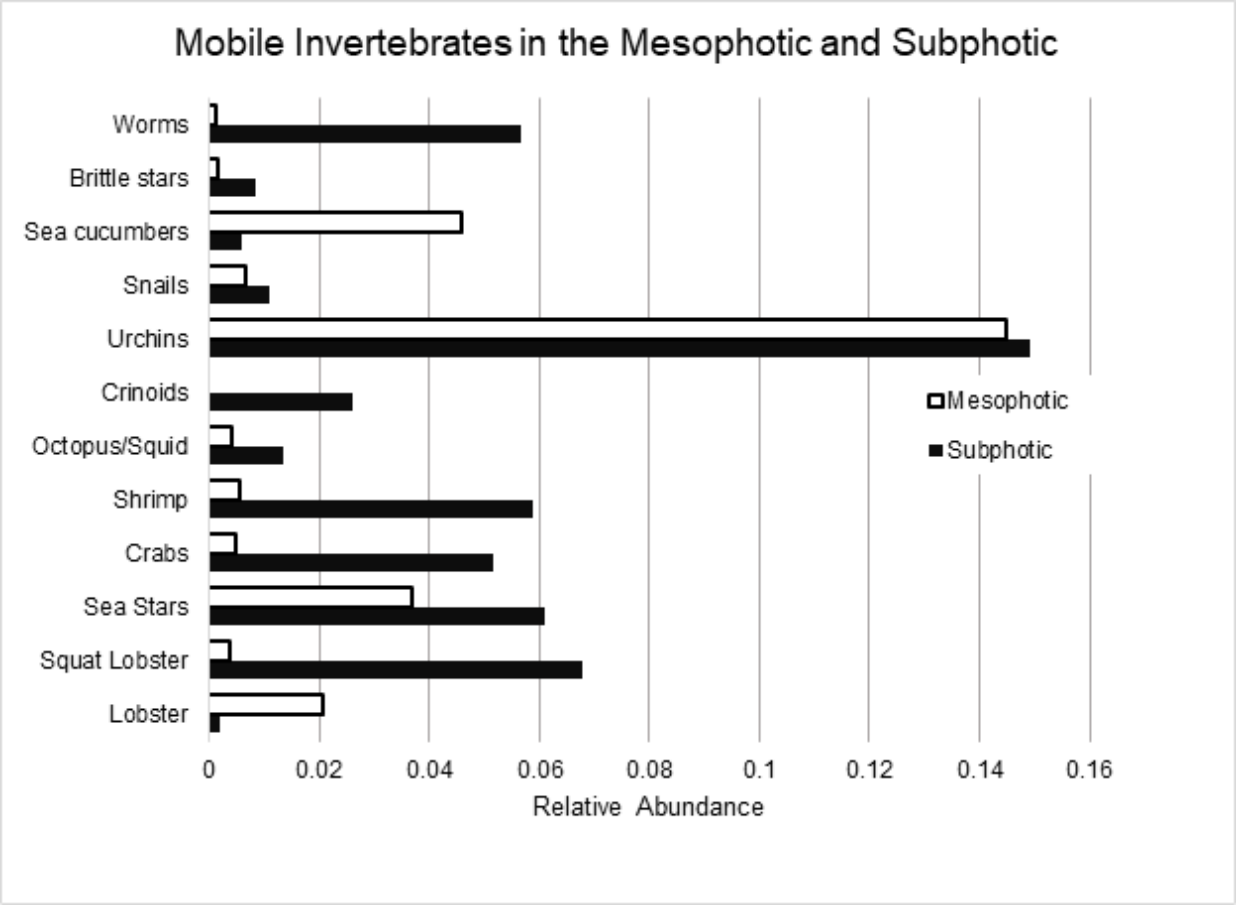

Figure A8. Comparison of mobile invertebrate relative abundance as a function of total invertebrates in the mesophotic (open bars) and the subphotic (black bars) zone.

Fishes

Fish abundance came from mesophotic surveys conducted by PIFSC (Asher et al. 2017, PIFSC unpublished data), Struhsaker (Struhsaker 1973), and the University of Hawai‘i at Mānoa (UH) Drazen lab (Moore et al. 2016) and Hawai‘i Underwater Research Lab (HURL). To allocate a biomass value to the MaxN values from the underwater baited camera surveys, we compared sites for which we had both shallow water coral reef surveys conducted by PIFSC[19] and underwater camera surveys (Asher et al. 2017) to calculate conversion factors for each functional group. These conversion factors were then used to calculate biomass values. HURL data had records of 237 surveys with species counts binned in quantity categories. We assumed the “1 or more” category was equal to 3, “1–5” was 3, “6–10” was 8 and “>10” was 15 unless the notes specified a group size. Where possible we used the average length and length-weight parameters from PIFSC or Struhsaker (1973) and if not available we took $^1/_2$ of the species-specific maximum length provided by fishBase[20] and the reported length-weight conversion factors to estimate biomass for each species. Track length of HURL surveys were estimated in ArcGIS and

[19] https://www.pifsc.noaa.gov/cred/pacific_ramp.php
[20] www.fishbase.org

multiplied with a field of view of 3 m to get survey area per survey. Where track lengths were absent we used a mean value from comparable dive durations. To get the total biomass estimate per functional group, we took the mean of the different survey estimates.

For the subphotic groups, data came from HURL, UH Drazen Lab, Struhsaker (1973), and PIFSC (PIFSC unpublished data). Struhsaker (1973) had data to calculate species-specific biomass per m^2. HURL data had records of 432 subphotic surveys and we estimated biomass for the mesophotic surveys using length data derived from field surveys (Parrish 2006) or fishBase. We used the conversion factors calculated for the mesophotic data to adjust the UH and PIFSC BotCam data. To obtain the final biomass value we took a mean of the different data sources. Bottomfish biomass was excluded from the previous survey data and came from the PIFSC stock assessment group who conducted underwater baited camera surveys to estimate spatial distribution and stock size (Richards et al. 2016; Ault et al. 2018).

Appendix F: Biomass of shallow prey fish and mesopelagic scatter layer

Contributors: Donald Kobayashi, Réka Domokos

Shallow prey fish biomass around the inhabited Hawaiian Islands was estimated from a multi-step process incorporating unpublished aerial survey data, high-resolution bathymetry, State of Hawai‘i commercial catch reports, dynamic production model stock assessment outputs, and numerous assumptions based on the published literature and expert opinion. Shallow prey fish were operationally assumed to be a coastal pelagic complex of 2 jacks (Carangidae): bigeye scad (*Selar crumenophthalmus*), henceforth akule, and mackerel scad (*Decapterus macarellus*), henceforth opelu. Biomass estimates for akule and opelu were accomplished separately, as described below.

Unpublished akule aerial survey data from collaborating scientific partner John Wiley (Poseidon Fisheries Research) from 2015 to 2016 was used to identify the location of akule schools around the island of O’ahu, and partnered fishing operations at the same time provided measures of akule school biomass. The survey swath of the aerial surveys was also calculated. Both the depth distribution of this survey area and the individual akule school locations were matched to a high-resolution (50 m) bathymetry database providing an estimate of biomass per square kilometer of area within 1-m depth bins. A modeled biomass function was created using an additive composite of 2 logistic curves which were able to account for the shape of the function and its asymmetry. This depth dependent akule biomass function was then used to estimate akule biomass in each of the Atlantis boxes with an assumed linearly proportional allocation scheme to each box using the minimum and maximum depths for that box and its total area. The akule biomass estimates were then scaled to match a total biomass as estimated from a dynamic production model stock assessment which used State of Hawai‘i commercial catch reports from 1966 to 1997 (Weng and Sibert 2004). The assumed biomass is taken from their estimate of carrying capacity K using what they called the “scalar K” approach and a conservative estimate of current biomass of 0.5 K (304,587 kg), assuming that there may have been slight declines in biomass since the time of that stock assessment which showed biomass to be somewhere in the interval between 0.6 K and 0.8 K. An examination of commercial catch data subsequent to that time period shows a slight decrease in akule landings over the immediately subsequent 20 years but akule landings have been generally stable over a multi-decadal time period from 1948 to 2018. The aerial biomass estimate was scaled by a factor of 4.5 to achieve a match to the Weng and Sibert (2004) biomass.

Opelu were assumed to occur at deeper depths than akule with a biomass function estimated from the shape parameters of the akule biomass function logistic curves and a depth offset. The opelu biomass function was further modified to incorporate a bimodal shape reflective of fisher and scientist observations of opelu schools in depths of 30–60 m and 90–120 m. These depths correspond to a day fishery and a night fishery, respectively. It is not well understood whether the fish move between the 2 areas over the course of a day/night or are spatially segregated based on size/age. Regardless, for purposes of Atlantis modeling a bimodal biomass function based on depth will capture the pertinent biomass patterns for this species as averaged over a block of time greater than or equal to 24 hours. The depth dependent opelu biomass function was then used to estimate opelu biomass in each of the Atlantis boxes in the same way as for the akule.

Micronekton biomass in the mesopelagic scatter layer around the inhabited Hawaiian islands was estimated from active acoustic data collected on the leeward side of Oahu in 2004 (Domokos et al. 2010). Since data on micronekton is severely limited, biomass estimates from this data set were assumed representative for the entire modeled area. To obtain micronekton density estimates, acoustic backscatter strength (S_v, in dB re 1 m^{-1}), proportional to density assuming the composition of organisms do not change (Simmonds and MacLennan 2008), was set at a threshold of -75 dB to contain only micronekton, such as small (2–20 cm) fish, squid, shrimp, or shrimp-like and gelatinous organisms. As micronekton form two ubiquitous horizontal scattering layers, S_v from the shallow (SSL) and deep scattering layers (DSL), were averaged and separated by day- and nighttime values. This step was necessary since most micronekton undergo diel migration from the daytime DSL to the nighttime SSL (Figure A9).

To calculate biomass, mean length of micronekton was assumed to be 5 cm. This value was based on sizes obtained during simultaneous micronekton tow samples and the fact that they made up most of the biomass of organisms (Pakhomov et al. 2010). Target Strength (TS, dB re 1 m^2) estimates were calculated from a TS vs. length relationship for myctophids (Simmonds and MacLennan 2008), then used in combination with the mean S_v values to obtain densities in units of number per m^2 per layer. Area densities were multiplied by the thickness of the layer (200 m) and by the area of the Atlantis box for biomass per box. Values only from the nighttime SSL were used since those values contained organisms that stayed in the SSL day and night and those that migrated to the DSL during daytime.

In lieu of an equation for weight and length relationship, the value of 1.82 g was used to convert the units from number to kg. This value was obtained as an average from tow samples collected in Hawaiian waters (John Denton, Florida Museum of Natural History, personal communication). Since the SSL, between 20 and 200 m depth, spread through all 3 Atlantis verticals depth layers (0–30, 30–150, and 150–400 m, respectively), values proportional to the thickness of the layers to that of the SSL were used. That is, for boxes with one, two, and three vertical layers, 15%, 75%, and 100% of the total biomass was used.

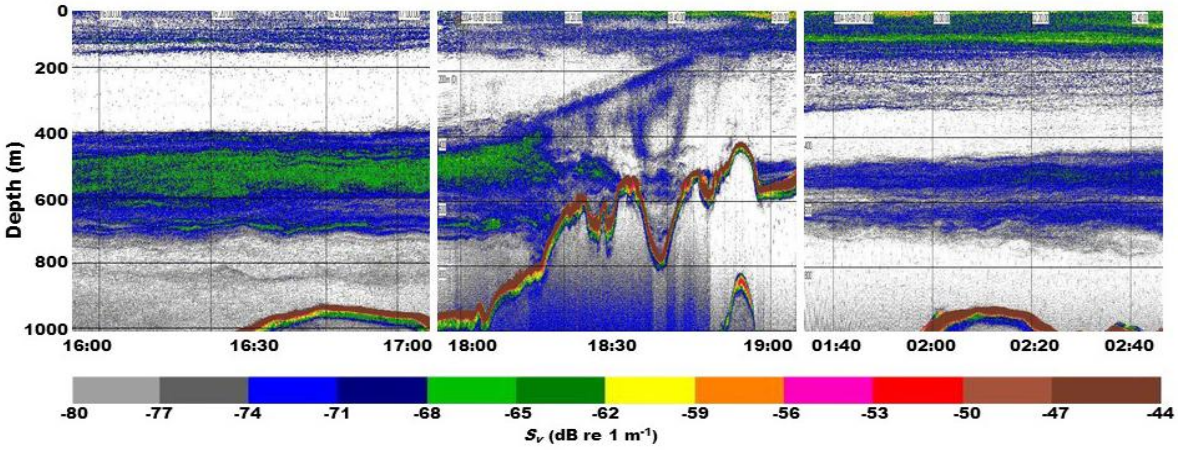

Figure A9. Acoustic backscatter during day (left panel), crepuscular (middle panel), and night (right panel) from the 2004 survey data. Red lines (>-47 dB) are backscatter from the ocean floor. The deep scatter layer can be seen between 450 m and 600 m during daytime (left panel), migrating upward around sunset, and in the 20–100 m layer during the night (right panel).

Appendix G: Allocation of Hawaiian monk seal biomass per model box

Contributor: Stacie Robinson

We used a stepwise process to determine the biomass of Hawaiian monk seal of each age class occupying each of the Atlantis model boxes:

1. Estimate total population of Hawaiian monk seals in the main Hawaiian Islands.
2. Allocate seals to age classes based on observed age distribution (based on size classes).
3. Multiply biomass by numbers per age/size class according to mass estimated for each.
4. Distribute biomass to boxes based on utilization distributions derived from satellite tags.

1. Population estimate

We based total monk seal biomass estimates on the annual population estimates for the inhabited Hawaiian Islands (Baker 2016). From Kauaʻi to Hawaiʻi the population estimate represents a minimum count based on seal sightings reports made either by NOAA staff, organized volunteer groups, or the general public (minimum number only, no confidence range available). For Niʻihau the population estimate is based on beach counts with a correction factor for the proportion of seals expected to be hauled out and available for sighting on a given survey day (mean estimated with 95% confidence intervals, we used the mean here). We based biomass calculations on the median of the yearly estimates from 2013 to 2016.

2. Age distribution

We calculated a single age distribution for the whole model area (Niʻihau and Kauaʻi-Hawaiʻi not separated). Ages were based on the ages noted for all seals included in the survey data. We included animals with know, estimated, and minimum ages:

- Known age – animals tagged in the year they were born, so exact age is known;
- Estimated age – animals tagged after their birth year, but typically while still juvenile (based on animal size), so that birth year/age can be reasonably estimated;
- Minimum age – animals first seen as adults (based on animal size) have a known minimum age (i.e., at least 5 years old in the year first seen), but not a precisely estimated age.

The Atlantis model allows ten age classes which are based on a consistent interval. Thus, we divided the total population into ten 2-year age classes (0–1 yr, –… 18–19 yrs). We chose a 2-year interval to mimic important natural patterns in the younger age classes; because immature seals are growing, we wanted narrow age classes so that mass estimates could accurately applied by class, also survival rates are most variable for youngest age classes. We recognize that monk seals are observed to live longer than 19 years; however, older seals would represent a very small proportion of the overall biomass, and there were 0 seals above 19 years old in the Hawaiʻi data used to calculate the age distributions. We multiplied the total population (median estimates) by the proportion in each age group to get the estimated numbers of animals per age group.

3. Biomass

Biomass estimates for each age class were based on (Baker et al. 2014), and correspond to the estimates used for juveniles/subadults/adults in previous ecosystem modeling (Parrish et al. 2011; Weijerman et al. 2017). Ages 0–1 yrs: 60 kg; Ages 2–3 yrs: 125 kg; Adults 5–6 yrs to 18–19 yrs: 170 kg.

Overall biomass per age group was calculated as:
Total population * proportion of population in age class X * estimated mass / seal of age class X

4. Utilization distribution

Monk seal biomass was allocated to model boxes within 400-m depth (within the typical foraging range of monk seals), deep water boxes far off shore (boxes 0, 7, 14, 15, 51, and 80) were considered transitory in the model, with biota passing through in transit to other boxes, but biomass and biological dynamics are not assigned to these boxes. All other boxes were assigned biomass of seals in proportion to the amount of time seals spent in those areas – according to satellite tracking data.

Our data set consisted of 24 seals tracked by Argos satellites for an average of 100 days. The study set included 17 males, 7 females; 12 were adults, 4 subadults, 5 juveniles, and 3 weaned pups. Tracked animals were captured and instrumented on Kauaʻi, Oahu, Molokaʻi, and Hawaiʻi. Animals were instrumented from 2004 to 2015 for foraging studies (Cahoon 2011; Wilson et al. 2017) as well as opportunistically (e.g., for tracking after health interventions; NMFS unpublished).

Because circumpolar Argos satellite coverage is sparse in the tropics, and because a seal must be wet but at the surface to get a satellite fix, Argos-based locations represent an incomplete sample of an animal's movement track. Thus, we used routines in the R package *crawl* to interpolate tracks, generating points at even intervals along each track (Johnson 2015). In this way, the number of points in a given area (e.g., Atlantis model box) can be used to represent the amount of its time an animal spent in that area. We calculated the proportion of each seal's points in each of the Atlantis model boxes, and then used the average proportion of points per box as the measure of the percent of total seal biomass that should be allocated to that box.

A substantial portion of the Hawaiʻi seal population inhabits Niʻihau, and is seldom seen elsewhere. Because research effort is limited at Niʻihau (privately owned island), no animals have been instrumented or satellite-tacked from there. Thus, to characterize this important part of the population, we had to estimate areas occupied by the Niʻihau portion of the seal population. Based on the number of seals estimated at Niʻihau, and the number of them seen on neighboring Kauaʻi is a given year, we estimated that Niʻihau seals spend 85% of their time in waters around Niihau, and 15% of their time around Kauaʻi. For the 15% of time around Kauaʻi, we allocated biomass in the same proportions that other Hawaiʻi seals used the boxes around Kauaʻi Island. For the 85% time allocated to Niʻihau boxes, we had to make our best guess, so we allocated time to boxes based on depth and area. We assumed seals would use boxes proportional to their area for shallow areas that make up the most frequent dive depths for monk seals (30-m deep).

For deeper boxes, we assumed that seal use was proportional to the box area, but discounted by a factor of 0.83 for boxes 31–150 m deep, and discounted by a factor of 0.66 for boxes 151–400 m deep.

Consumption rates and diet composition

Consumption

Previous research estimated that seals require 1364 Kcal/kg/day, and in captivity this caloric need could be satisfied by 1.5 kg of herring per day (Olesiuk 1993). We doubled the consumption rate of captive seals to account for the effort of foraging, thus assuming that wild seals require 3 kg of fish per day to satisfy their caloric needs (Parrish et al. 2012).

Diet Composition

Diet composition for Hawaiian monk seals varies considerably depending on the method of diet analysis (Table A4). For example, fatty acid analysis (Iverson et al. 2011) indicates that snapper and squid are major parts of the monk seal diet; however, fecal remains analysis (Heikoop et al. 2000; Cahoon et al. 2013) found these to be minor components, with triggerfishes and crustaceans being among most frequent diet items. Both methods found tang and surgeonfishes to be important diet items. Each method is subject to its own biases. Fecal analysis is highly dependent on digestion rates, and items eaten closest to shore may be more detectable in feces collected on beaches. Fatty acid analysis depends on models that can be influenced by model assumptions and the prey library used to parameterize them (although we expect our prey library represented most species in the prey base at various depth levels (Iverson et al. 2011; Parrish et al. 2012), and either is unlikely to provide the true/complete picture of the monk seal diet. Thus, for the diet in the Atlantis model, we included all prey items detected in either the fecal or fatty acid diet analyses. We assumed that the monk seal diet could include up to the highest proportion suggested by either analysis method.

Table A4. Monk seal diet composition based on the method of diet analyses.

	Family	(Subgroup if available, FA)	MAX% Diet
Minor Overall	Belonidae		0.06
	Callionymidae	(dragonet gurnard)	0.36
	Cheilodactylidae		0.37
	Xanthidae	(pebble crab)	0.37
	Lutjanidae	(pink snapper)	0.41
	Holocentridae	(squirrellfish)	0.06
	Acanthuridae	(unicornfish)	0.49
	Apogonidae		0.55
	Polymixiidae		0.55
	Diodontidae		0.61
	Carangidae		0.67
	Ammodytidae		0.60
	Cirrhitidae		0.73
	Kuhliidae		0.85
	Pentacerotidae	(armorhead)	0.87
	Ophichthidae	(cutthroat snake eel)	0.37
	Bothidae	(flounder)	0.55
	Pomacanthidae	(angel cardinalfish)	1.04
	Ophidiidae		1.16
	Chaetodontidae	(butterfly forcep pennant)	0.61
	Synodontidae	(lizard snakefish)	1.52
	Pandalidae	(shrimp)	1.68
	Kyphosidae		1.95
Important in Fecal Only	Crustaceans	(several spp)	13.16
	Scorpaenidae		2.35
	Ostraciidae		2.91
	Priacanthidae		2.44
	Monacanthidae		2.63
	Serranidae		7.30
	Congridae		9.81
	Labridae		11.82
	Balistidae		16.95
Important in Fatty Acid	Lithodidae	(box crab)	2.11
	Percophidae	(duckbill)	8.82
	Ommastrephidae	(squid)	11.01
	Pentacerotidae	(boarfish)	11.66
	Lutjanidae	(flower snapper)	23.35
Important in Fecal and Fatty Acid	Tetraodontidae	(toby)	2.50
	Mullidae	(goatfish)	3.53
	Pomacentridae	(sergeant)	2.68
	Scaridae	(parrotfish)	6.03
	Holocentridae	(soldierfish)	8.23
	Muraenidae	(moray)	10.81
	Acanthuridae	(tang surgeonfish)	11.40
	Octopodidae	(octopus)	17.67
	Lutjanidae	(squirrelfish snapper)	28.90

Appendix H: Mixed trophic impact analyses

Results of the mixed trophic impacts analyses (Figure A10) in the Ecopath model developed for the inhabited islands of Hawai‘i (Weijerman et al. In press).

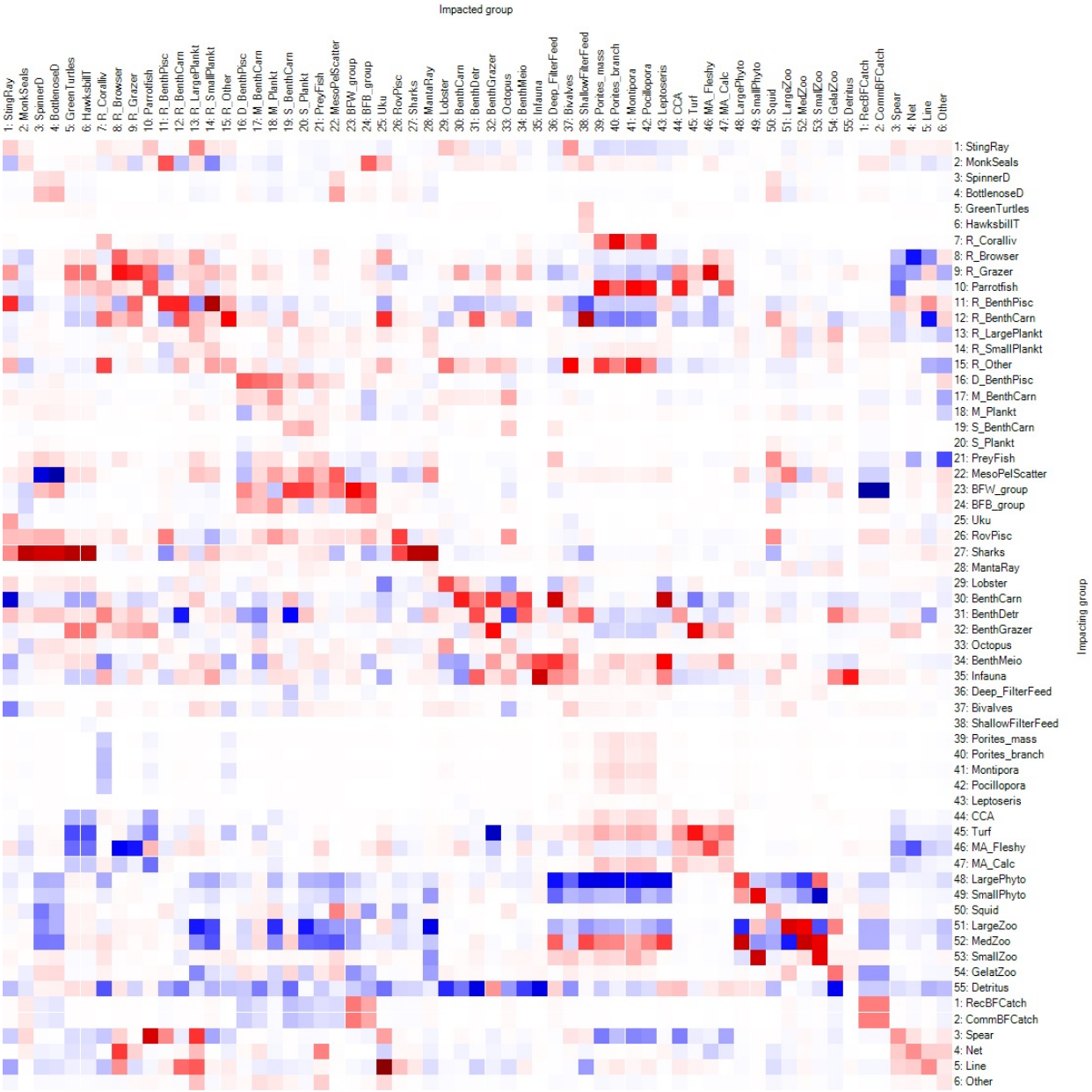

Figure A10. Mixed trophic impacts of impacted (columns) groups by impacting (rows) groups.

Red indicates negative impacts and blue positive impacts. The shading represents the value with harder colors representing higher values.

Appendix I: Calibration: No Fishing

For all the functional groups we show the trend line of the total biomass in the modeled area. The objective of this calibration exercise was to ascertain that no group becomes extinct or increases unrealistically. In the biomass plots the black line is the biomass trend and the dashed green line is the estimated biomass at carrying capacity or the initial biomass and is just for reference. For all vertebrate groups we also show the numbers and weight-at-age where the rainbow colors correspond to the age classes with red being age class 1 and violet age class 10. The objective was to have plausible numbers at the age classes (i.e., high numbers for the juveniles and low for the oldest age classes) and weight staying between 0.5 and 1.5 of the initial weight for each age class.

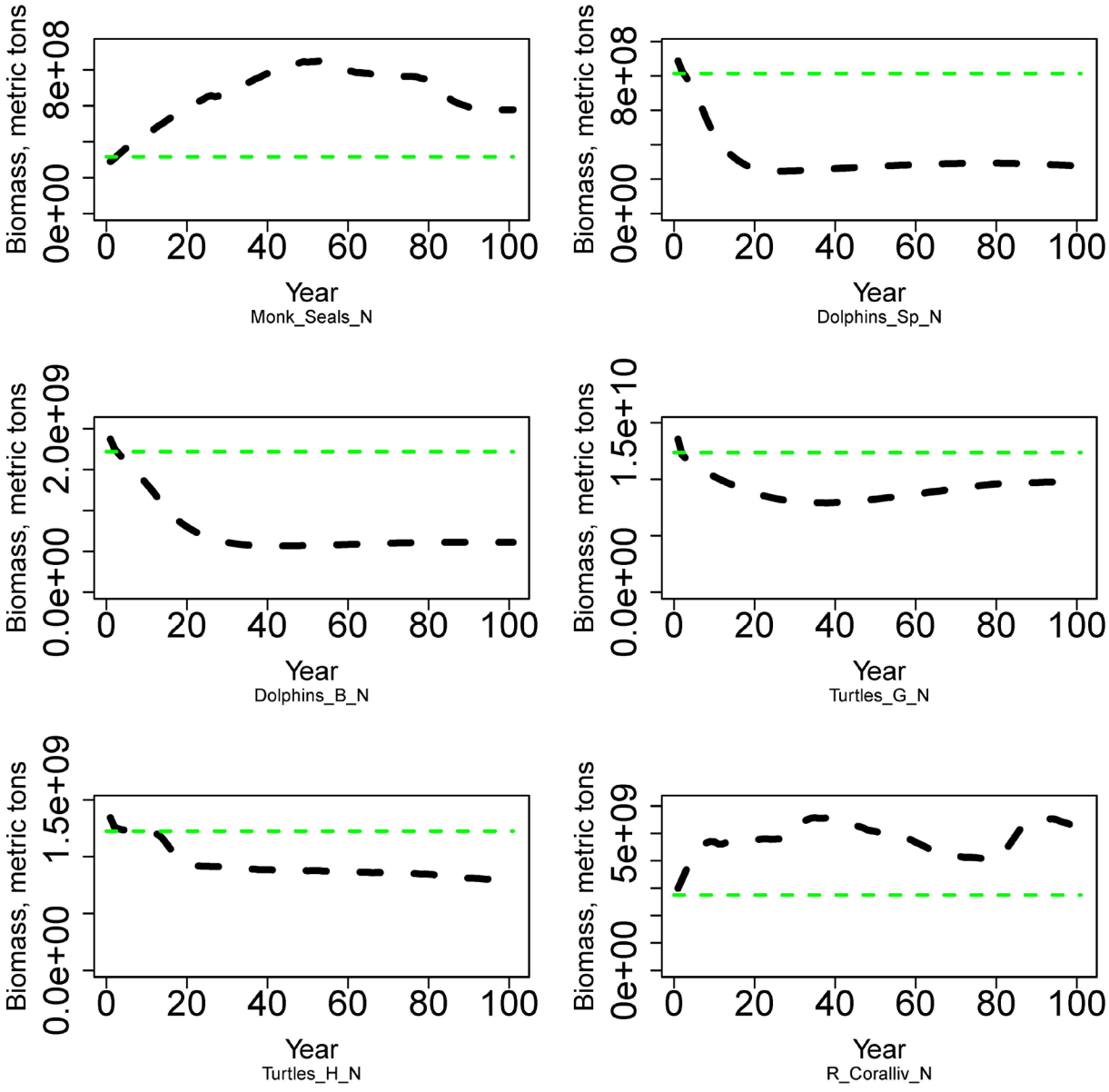

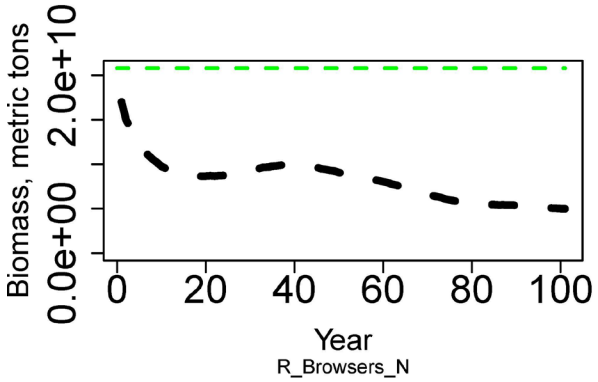
Biomass, metric tons
0.0e+00
2.0e+10
0
20
40
60
80
100
Year
R_Browsers_N

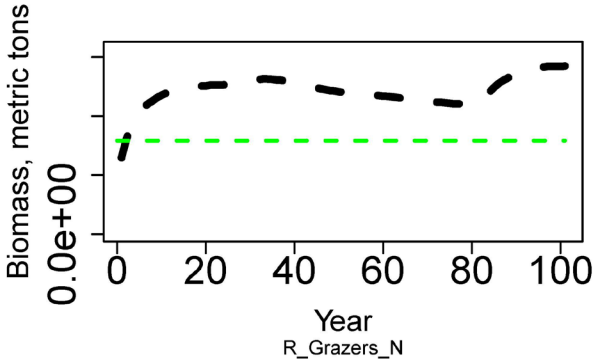
Biomass, metric tons
0.0e+00
0
20
40
60
80
100
Year
R_Grazers_N

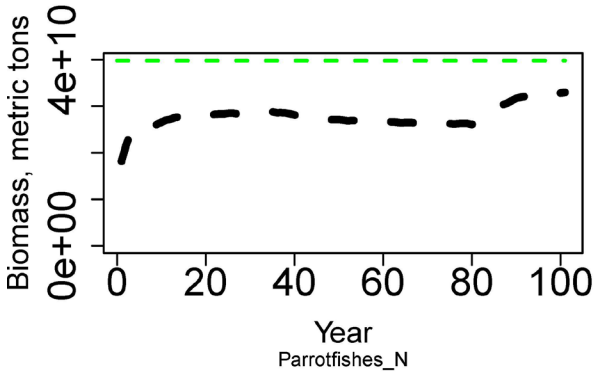
Biomass, metric tons
0e+00
4e+10
0
20
40
60
80
100
Year
Parrotfishes_N

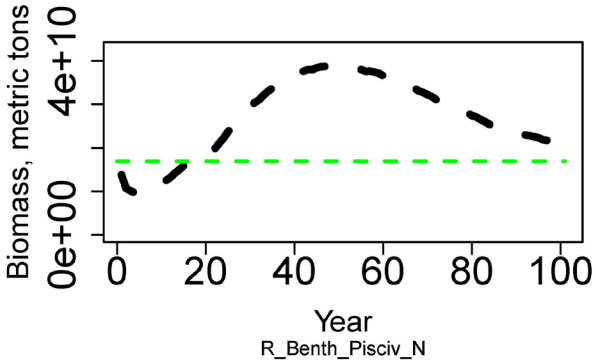
Biomass, metric tons
0e+00
4e+10
0
20
40
60
80
100
Year
R_Benth_Pisciv_N

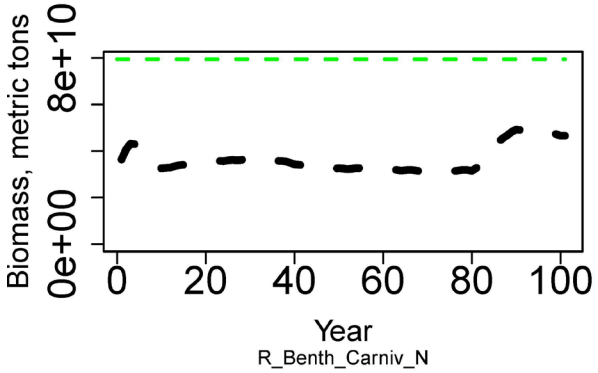
Biomass, metric tons
0e+00
8e+10
0
20
40
60
80
100
Year
R_Benth_Carniv_N

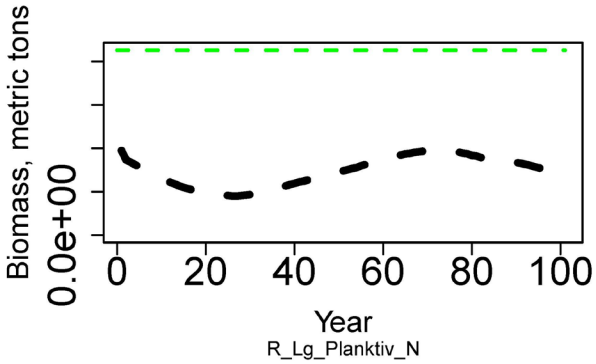
Biomass, metric tons
0.0e+00
0
20
40
60
80
100
Year
R_Lg_Planktiv_N

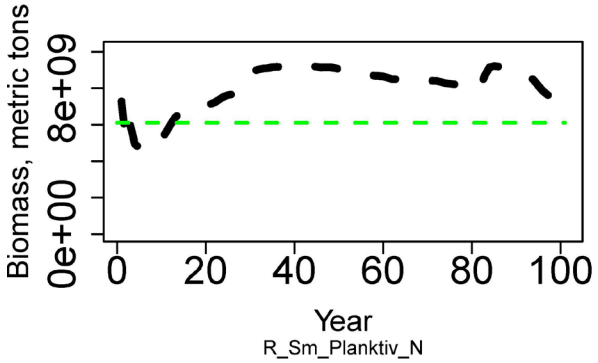
Biomass, metric tons
0e+00
8e+09
0
20
40
60
80
100
Year
R_Sm_Planktiv_N

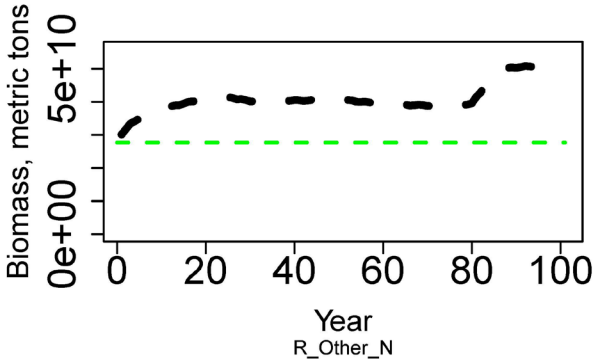
Biomass, metric tons
0e+00
5e+10
0
20
40
60
80
100
Year
R_Other_N

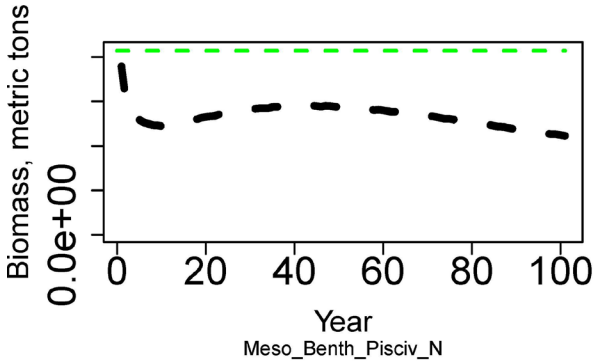
Biomass, metric tons
0.0e+00
0
20
40
60
80
100
Year
Meso_Benth_Pisciv_N

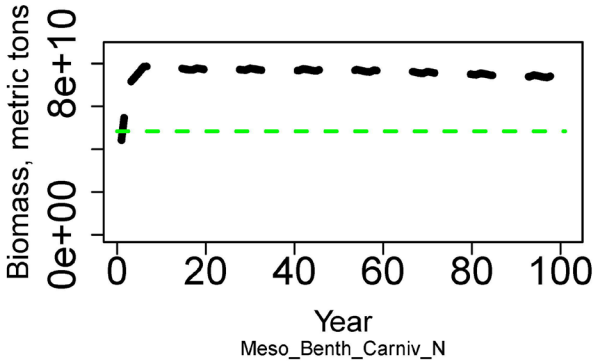
Biomass, metric tons
0e+00
8e+10
0
20
40
60
80
100
Year
Meso_Benth_Carniv_N

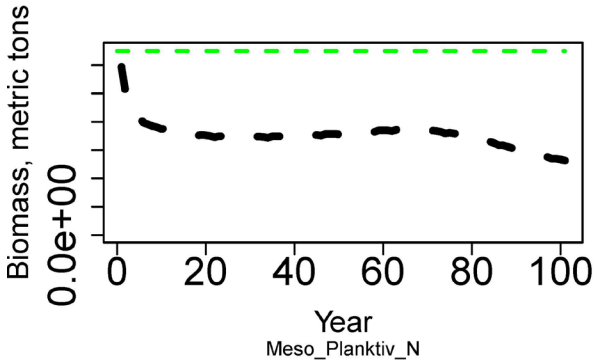
Biomass, metric tons
0.0e+00
0
20
40
60
80
100
Year
Meso_Planktiv_N

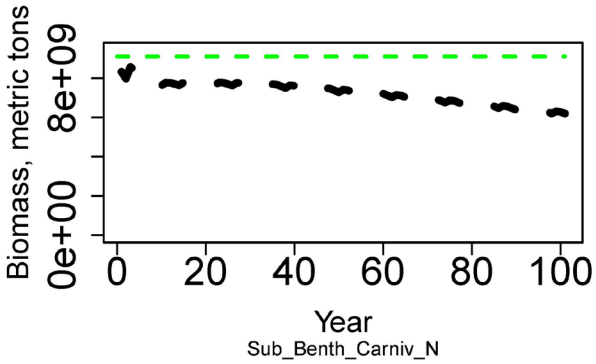
Biomass, metric tons
0e+00
8e+09
0
20
40
60
80
100
Year
Sub_Benth_Carniv_N

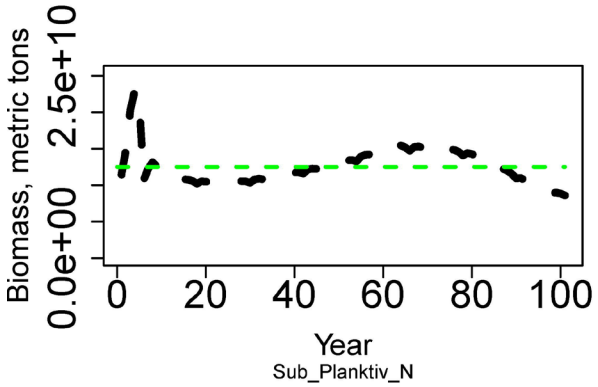
Biomass, metric tons
0.0e+00
2.5e+10
0
20
40
60
80
100
Year
Sub_Planktiv_N

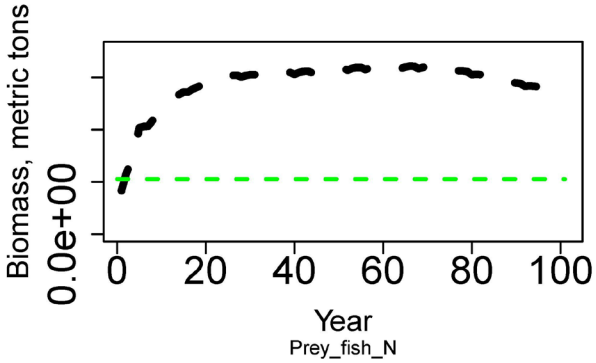
Biomass, metric tons
0.0e+00
0
20
40
60
80
100
Year
Prey_fish_N

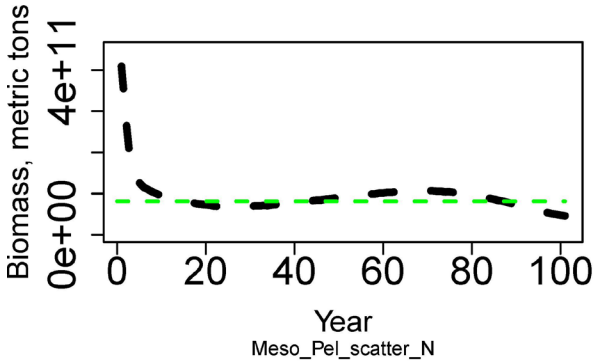
Biomass, metric tons
0e+00
4e+11
0
20
40
60
80
100
Year
Meso_Pel_scatter_N

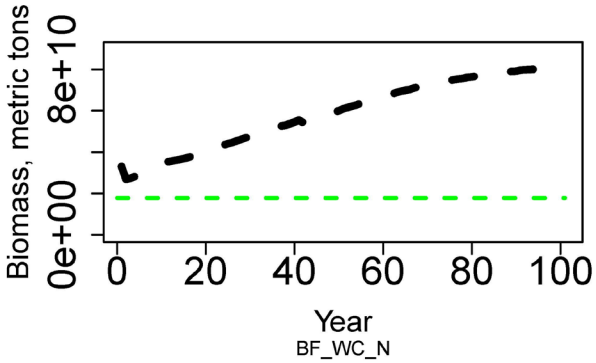
Biomass, metric tons
0e+00
8e+10
0
20
40
60
80
100
Year
BF_WC_N

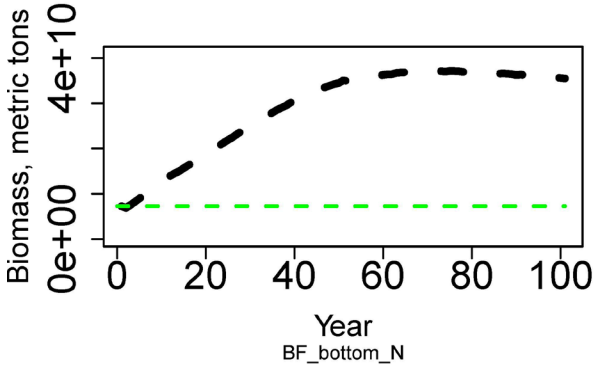
Biomass, metric tons
0e+00
4e+10
0
20
40
60
80
100
Year
BF_bottom_N

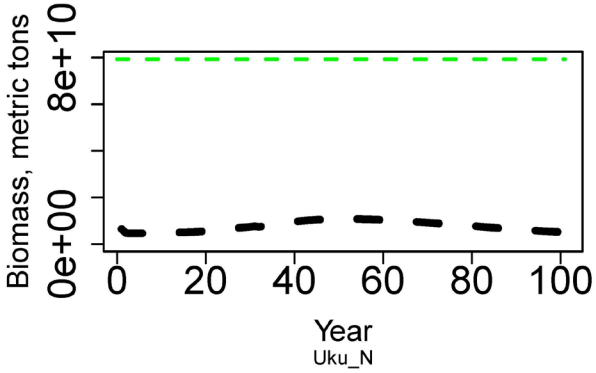
Biomass, metric tons
0e+00
8e+10
0
20
40
60
80
100
Year
Uku_N

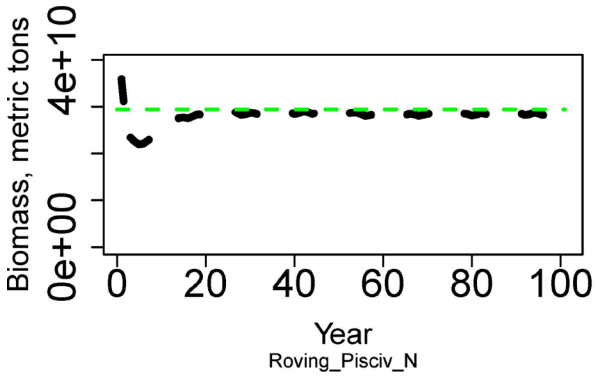
Biomass, metric tons
0e+00
4e+10
0
20
40
60
80
100
Year
Roving_Pisciv_N

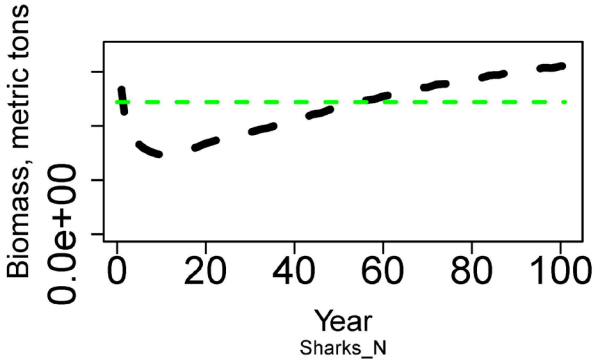
Biomass, metric tons
0.0e+00
0
20
40
60
80
100
Year
Sharks_N

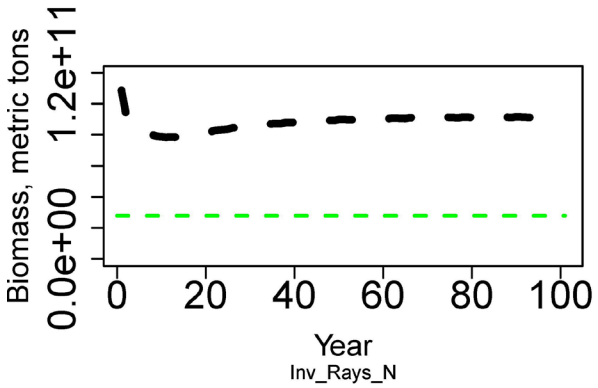
Biomass, metric tons
0.0e+00
1.2e+11
0
20
40
60
80
100
Year
Inv_Rays_N

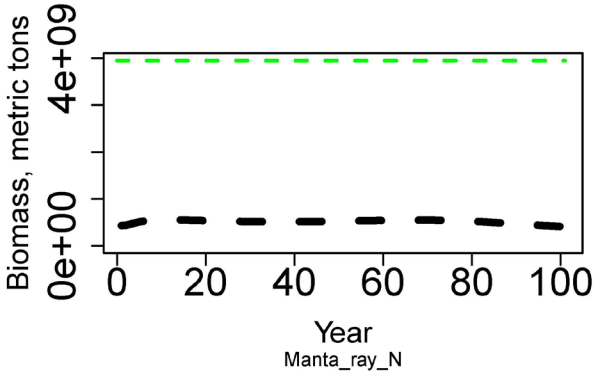
Biomass, metric tons
0e+00
4e+09
0
20
40
60
80
100
Year
Manta_ray_N

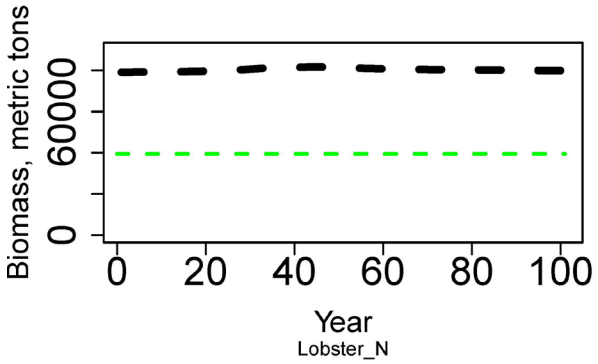
Biomass, metric tons
0
60000
0
20
40
60
80
100
Year
Lobster_N

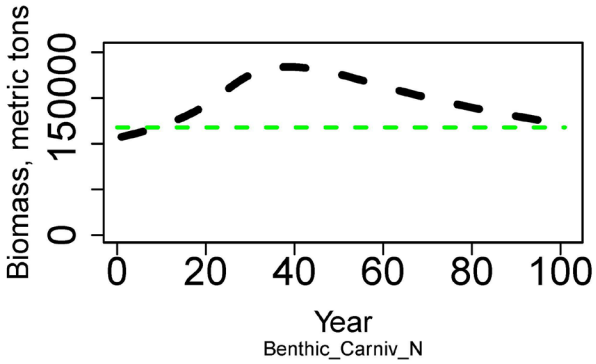
Biomass, metric tons
0
150000
0
20
40
60
80
100
Year
Benthic_Carniv_N

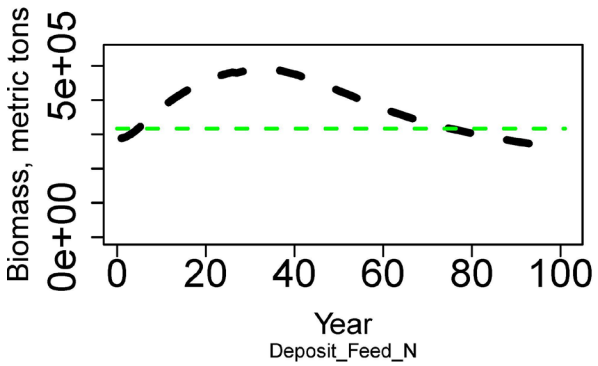
Biomass, metric tons
0e+00
5e+05
0
20
40
60
80
100
Year
Deposit_Feed_N

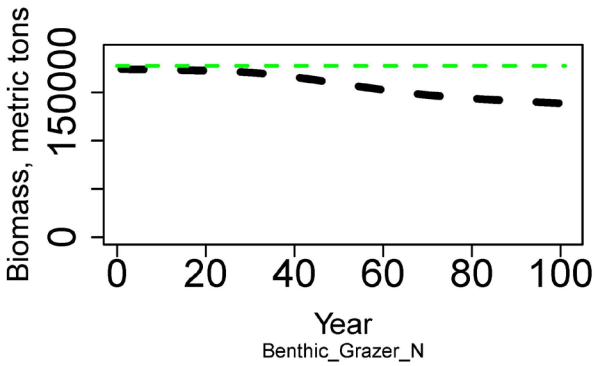
Biomass, metric tons
0
150000
0
20
40
60
80
100
Year
Benthic_Grazer_N

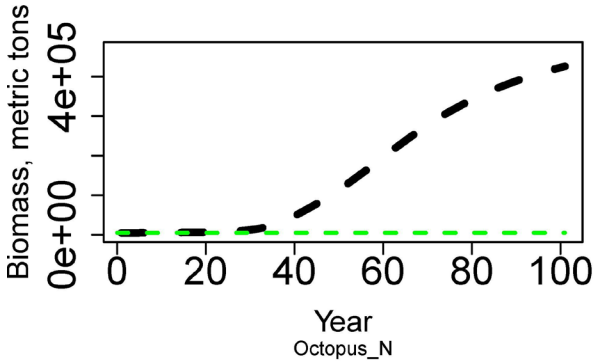
Biomass, metric tons
0e+00
4e+05
0
20
40
60
80
100
Year
Octopus_N

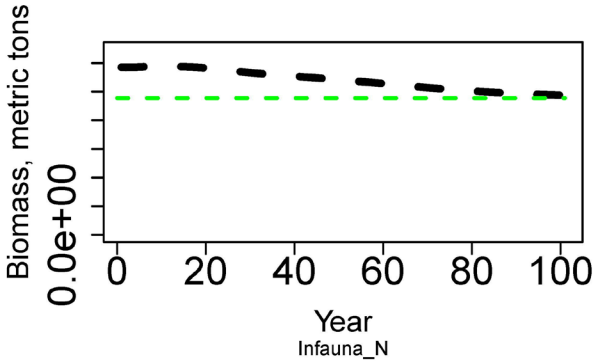
Biomass, metric tons
0.0e+00
0
20
40
60
80
100
Year
Infauna_N

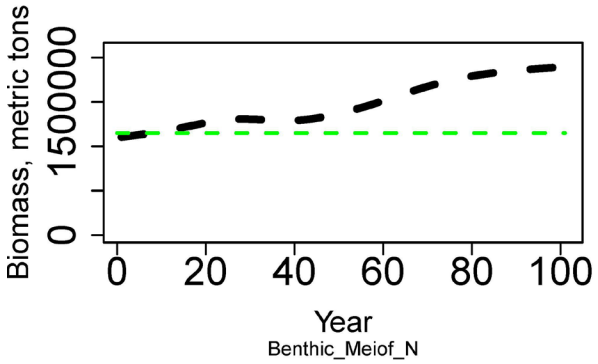
Biomass, metric tons
0
1500000
0
20
40
60
80
100
Year
Benthic_Meiof_N

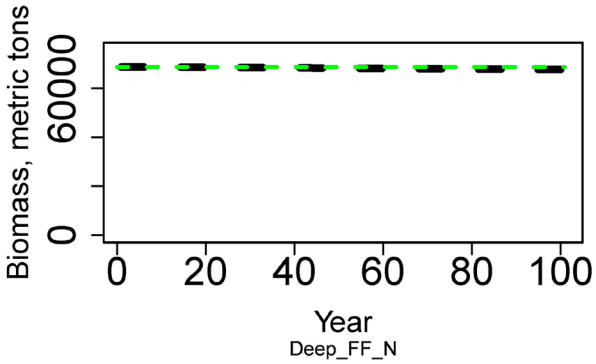
Biomass, metric tons
0
60000
0
20
40
60
80
100
Year
Deep_FF_N

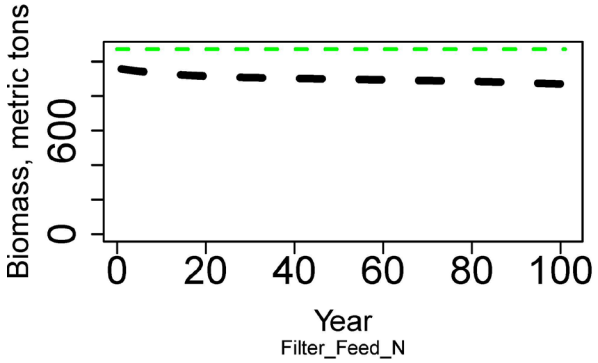
Biomass, metric tons
0
600
0
20
40
60
80
100
Year
Filter_Feed_N

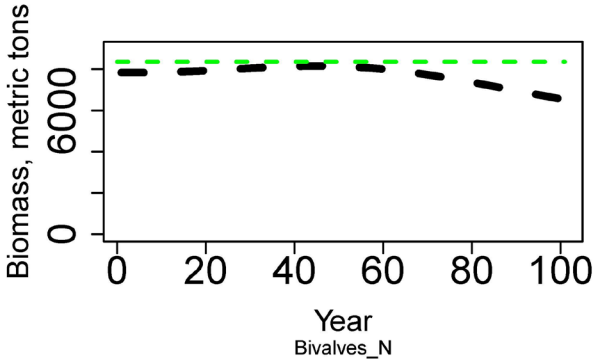
Biomass, metric tons
0
6000
0
20
40
60
80
100
Year
Bivalves_N

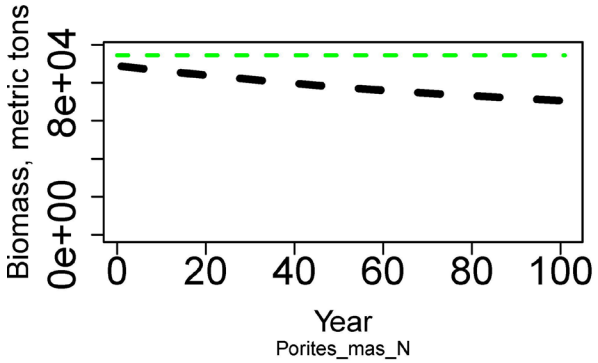
Biomass, metric tons
0e+00
8e+04
0
20
40
60
80
100
Year
Porites_mas_N

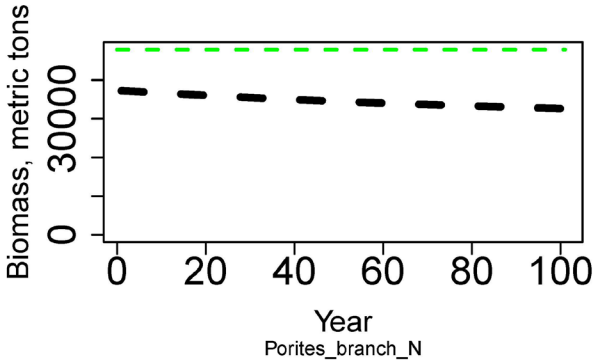
Biomass, metric tons
0
30000
0
20
40
60
80
100
Year
Porites_branch_N

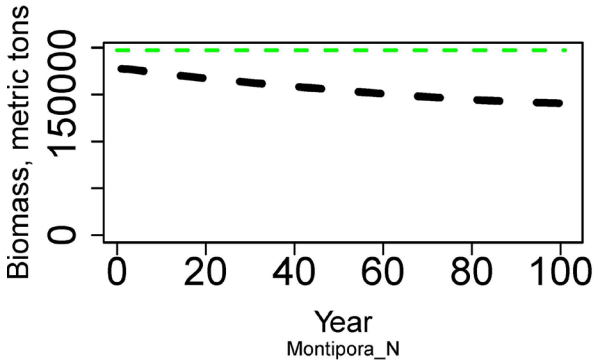
Biomass, metric tons
0
150000
0
20
40
60
80
100
Year
Montipora_N

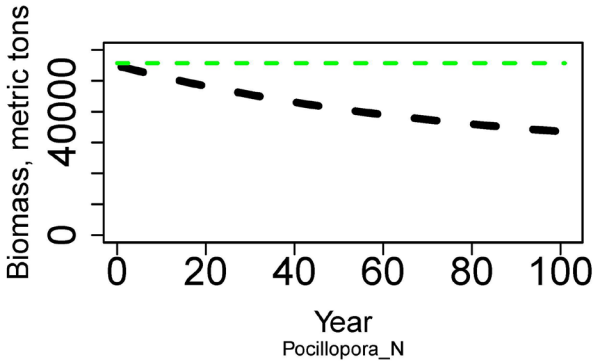
Biomass, metric tons
0
40000
0
20
40
60
80
100
Year
Pocillopora_N

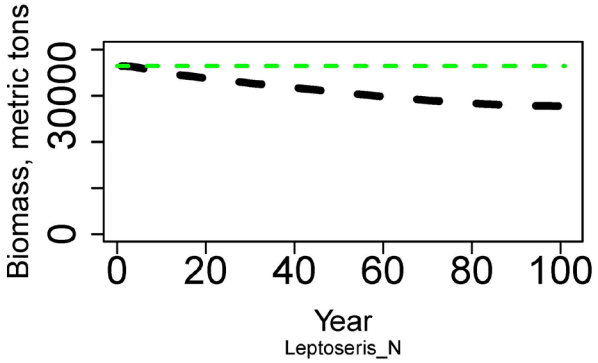
Biomass, metric tons
0
30000
0
20
40
60
80
100
Year
Leptoseris_N

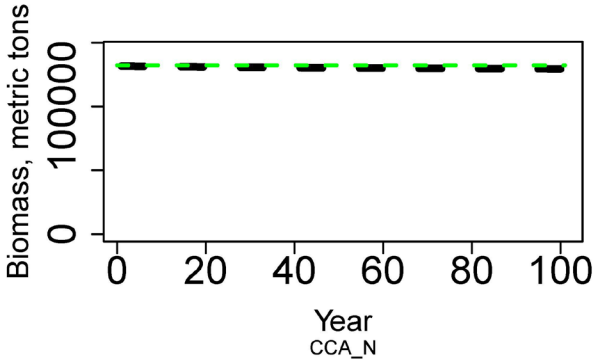
Biomass, metric tons
0
100000
0
20
40
60
80
100
Year
CCA_N

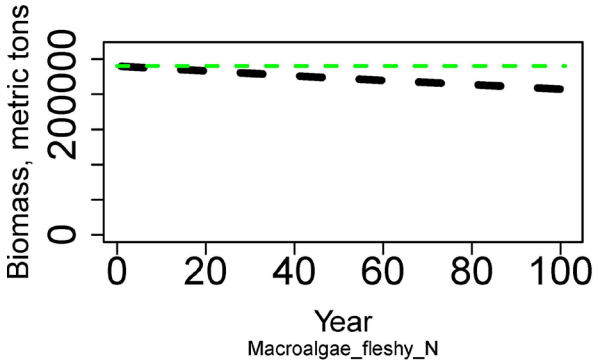
Biomass, metric tons
0
200000
0
20
40
60
80
100
Year
Macroalgae_fleshy_N

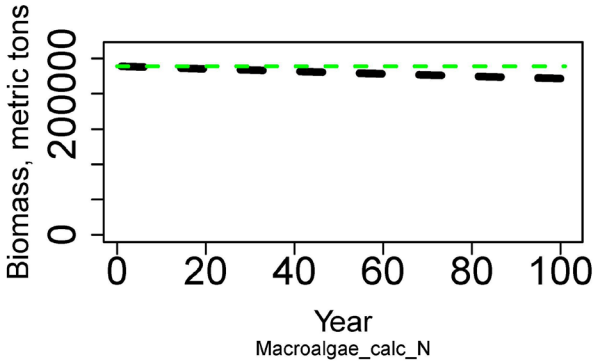
Biomass, metric tons
0
200000
0
20
40
60
80
100
Year
Macroalgae_calc_N

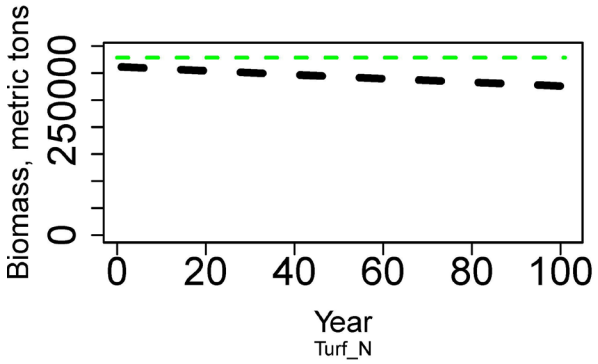
Biomass, metric tons
0
250000
0
20
40
60
80
100
Year
Turf_N

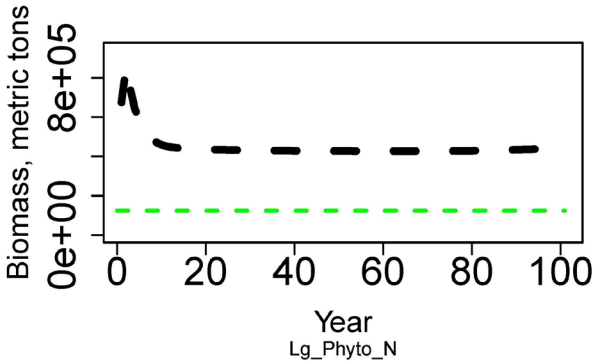
Biomass, metric tons
0e+00
8e+05
0
20
40
60
80
100
Year
Lg_Phyto_N

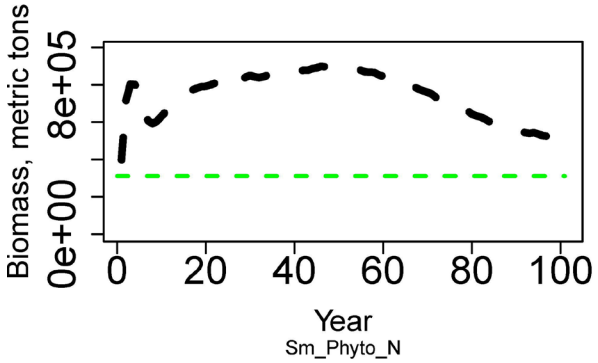
Biomass, metric tons
0e+00
8e+05
0
20
40
60
80
100
Year
Sm_Phyto_N

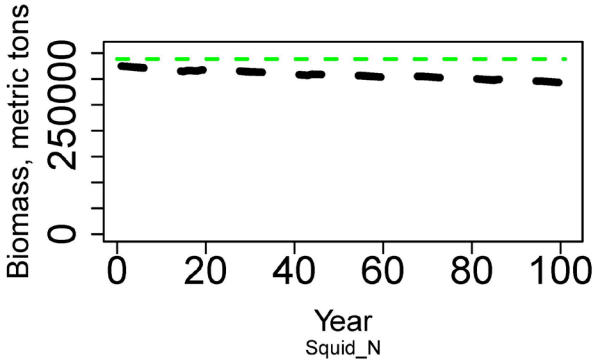
Biomass, metric tons
0
250000
0
20
40
60
80
100
Year
Squid_N

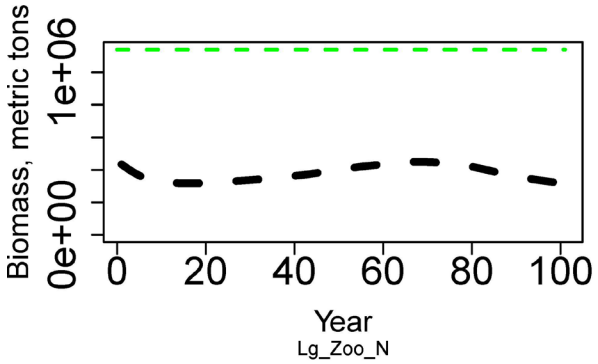
Biomass, metric tons
0e+00
1e+06
0
20
40
60
80
100
Year
Lg_Zoo_N

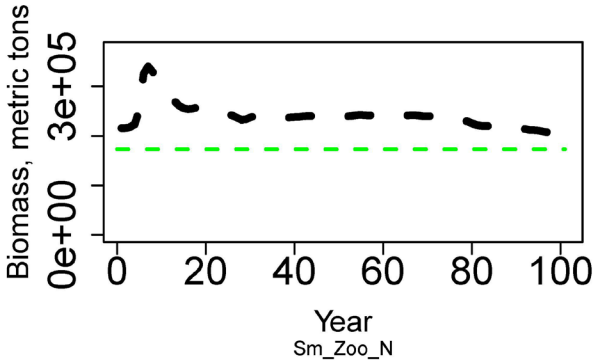
Biomass, metric tons
0e+00
3e+05
0
20
40
60
80
100
Year
Sm_Zoo_N

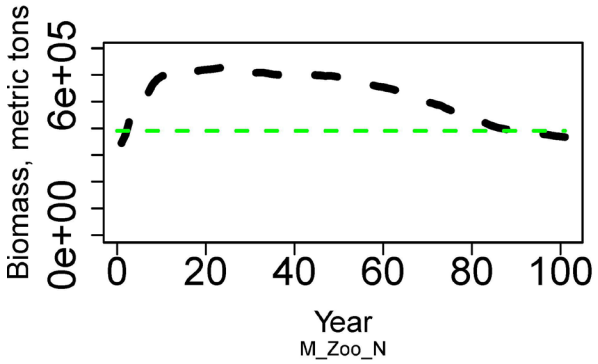
Biomass, metric tons
0e+00
6e+05
0
20
40
60
80
100
Year
M_Zoo_N

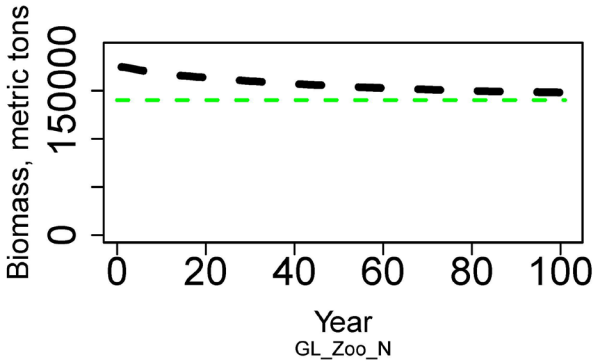
Biomass, metric tons
0
150000
0
20
40
60
80
100
Year
GL_Zoo_N

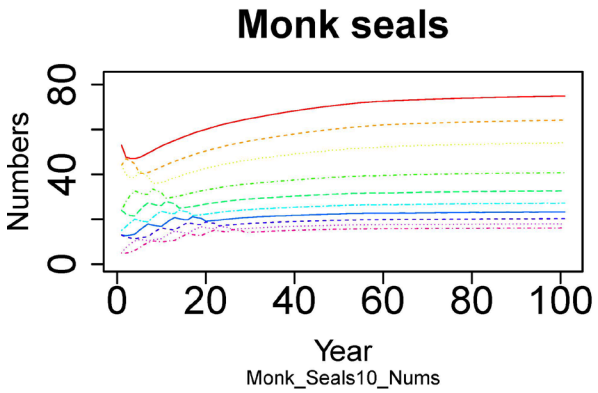
Monk seals
Numbers
0
40
80
0
20
40
60
80
100
Year
Monk_Seals10_Nums

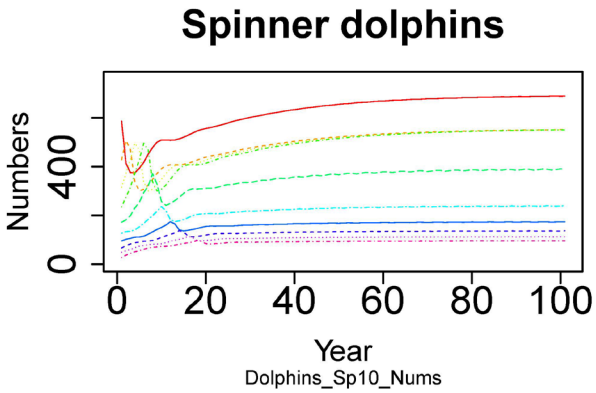
Spinner dolphins
Numbers
0
400
0
20
40
60
80
100
Year
Dolphins_Sp10_Nums

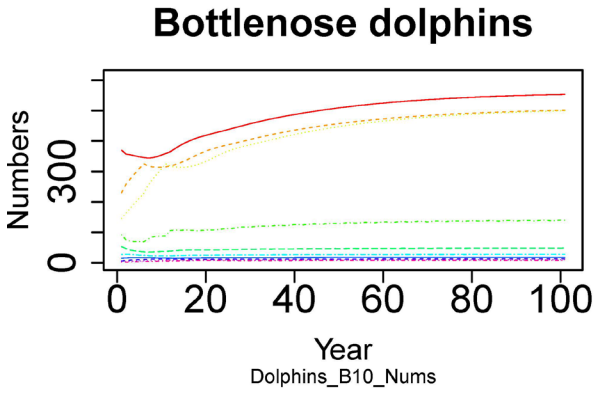
Bottlenose dolphins
Numbers
0
300
0
20
40
60
80
100
Year
Dolphins_B10_Nums

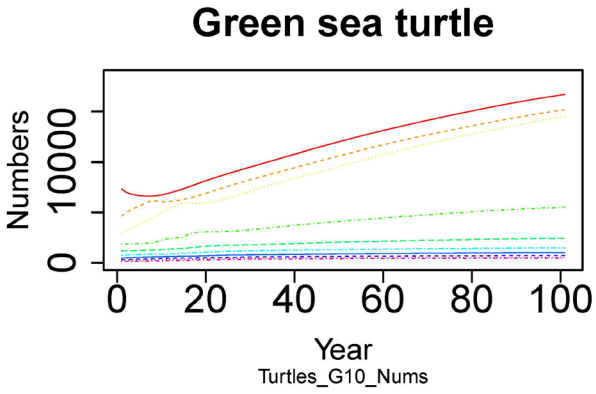
Green sea turtle
Numbers
0
10000
0
20
40
60
80
100
Year
Turtles_G10_Nums

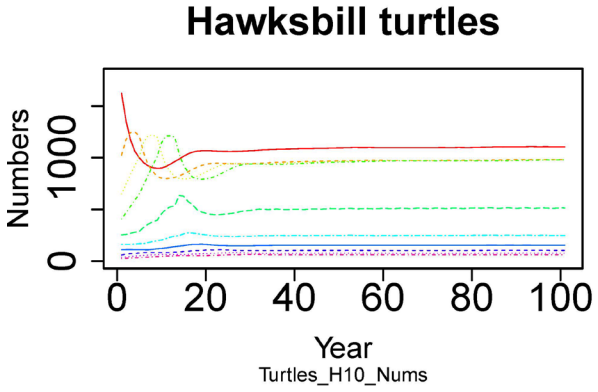
Hawksbill turtles
Numbers
0
1000
0
20
40
60
80
100
Year
Turtles_H10_Nums

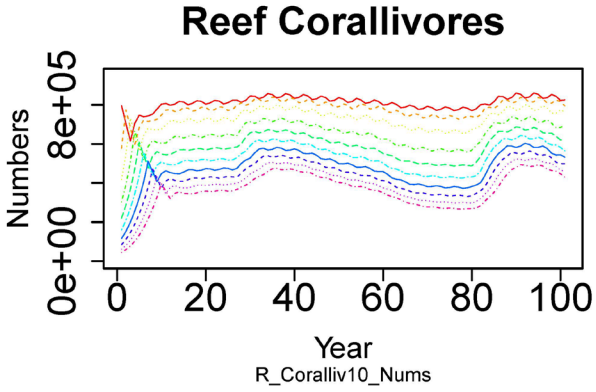
Reef Corallivores
Numbers
0e+00
8e+05
0
20
40
60
80
100
Year
R_Coralliv10_Nums

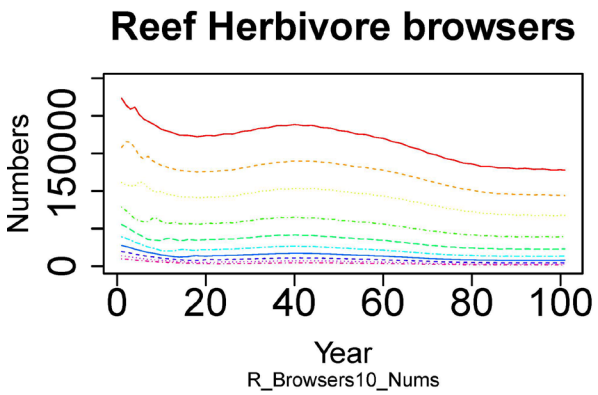
Reef Herbivore browsers
Numbers
0
150000
0
20
40
60
80
100
Year
R_Browsers10_Nums

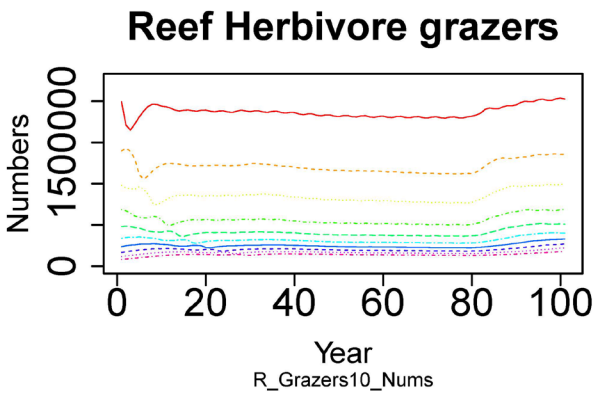
Reef Herbivore grazers
Numbers
0
1500000
0
20
40
60
80
100
Year
R_Grazers10_Nums

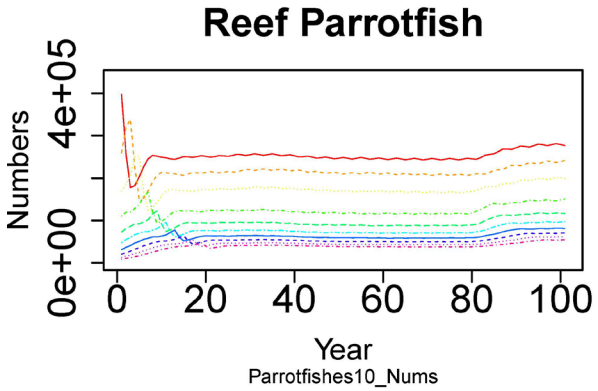
Reef Parrotfish
Numbers
0e+00
4e+05
0
20
40
60
80
100
Year
Parrotfishes10_Nums

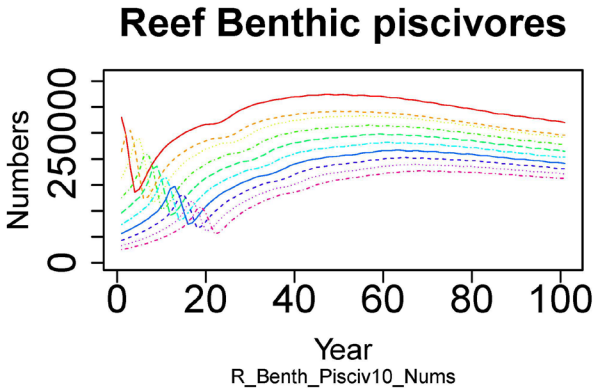
Reef Benthic piscivores
Numbers
0
250000
0
20
40
60
80
100
Year
R_Benth_Pisciv10_Nums

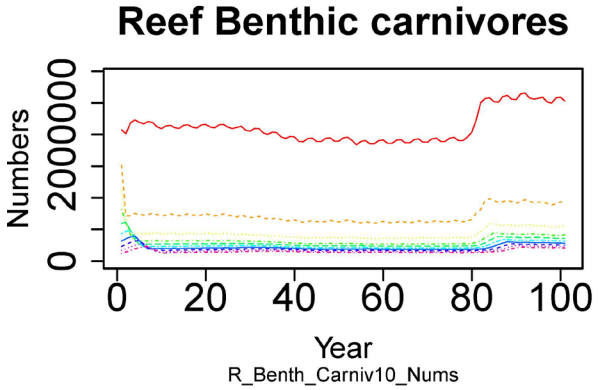
Reef Benthic carnivores
Numbers
0
2000000
0
20
40
60
80
100
Year
R_Benth_Carniv10_Nums

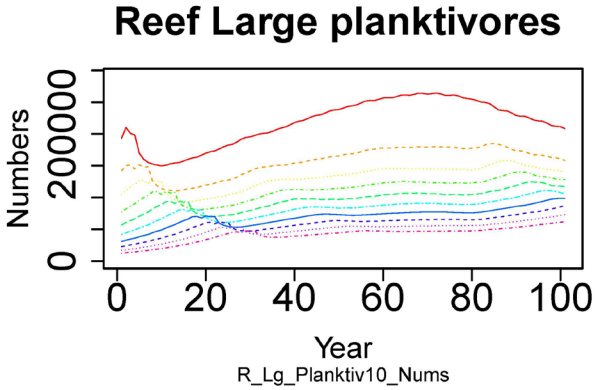
Reef Large planktivores
Numbers
0
200000
0
20
40
60
80
100
Year
R_Lg_Planktiv10_Nums

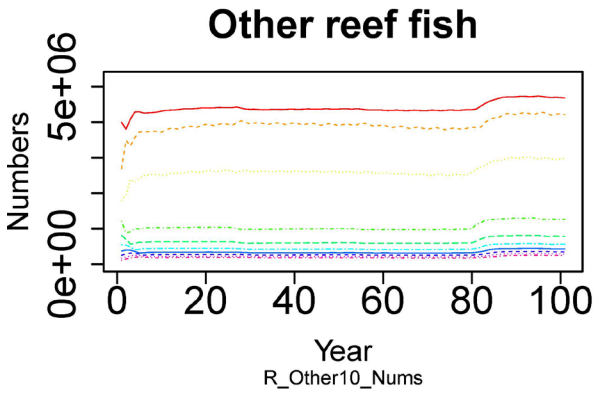
Other reef fish
Numbers
0e+00
5e+06
0
20
40
60
80
100
Year
R_Other10_Nums

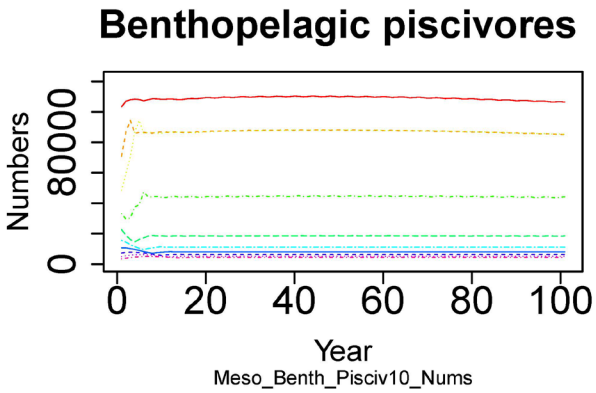
Benthopelagic piscivores
Numbers
0
80000
0
20
40
60
80
100
Year
Meso_Benth_Pisciv10_Nums

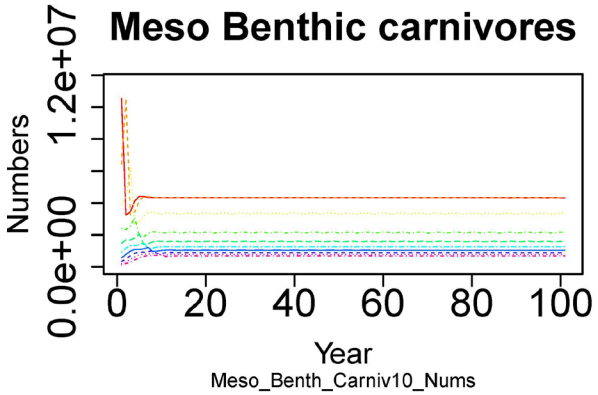
Meso Benthic carnivores
Numbers
0.0e+00
1.2e+07
0
20
40
60
80
100
Year
Meso_Benth_Carniv10_Nums

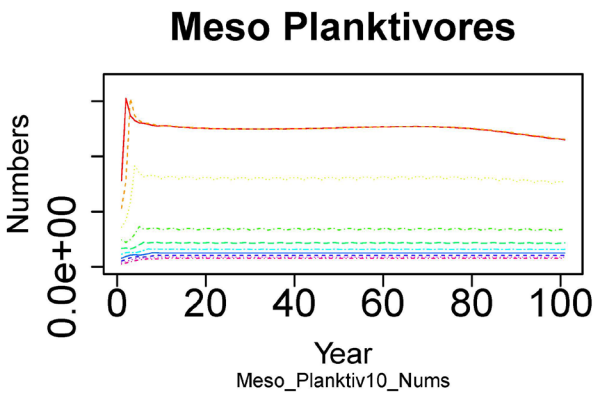
Meso Planktivores
Numbers
0.0e+00
0
20
40
60
80
100
Year
Meso_Planktiv10_Nums

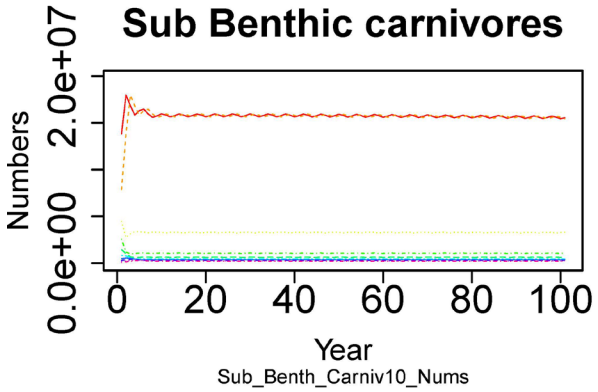
Sub Benthic carnivores
Numbers
0.0e+00
2.0e+07
0
20
40
60
80
100
Year
Sub_Benth_Carniv10_Nums

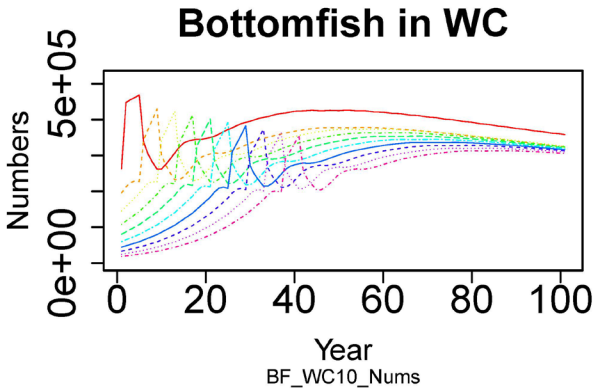
Bottomfish in WC
Numbers
0e+00
5e+05
0
20
40
60
80
100
Year
BF_WC10_Nums

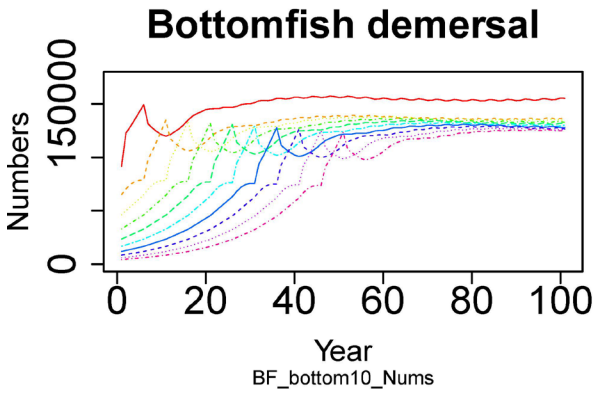
Bottomfish demersal
Numbers
0
150000
0
20
40
60
80
100
Year
BF_bottom10_Nums

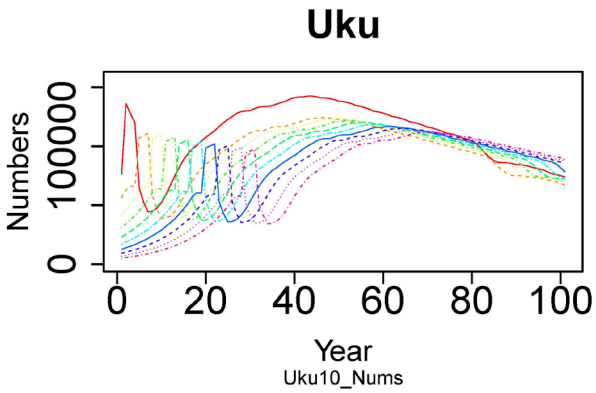
Uku
Numbers
0
100000
0
20
40
60
80
100
Year
Uku10_Nums

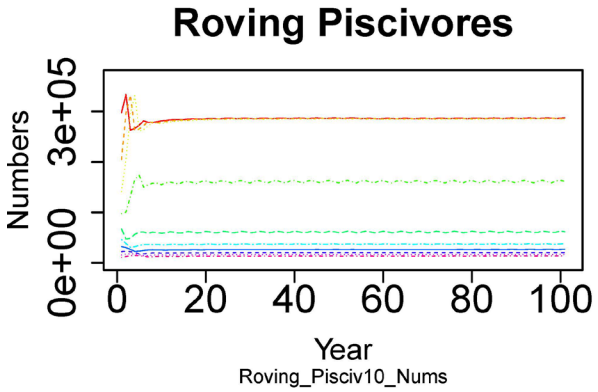
Roving Piscivores
Numbers
0e+00
3e+05
0
20
40
60
80
100
Year
Roving_Pisciv10_Nums

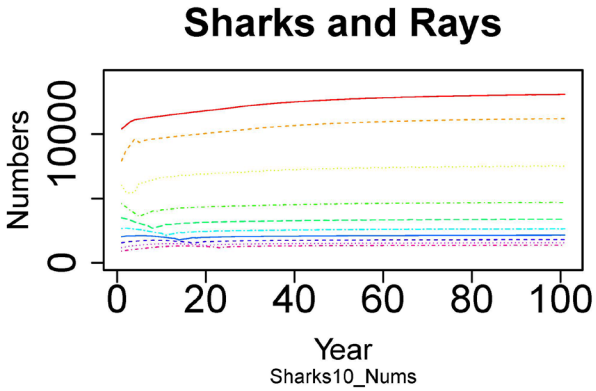
Sharks and Rays
Numbers
0
10000
0
20
40
60
80
100
Year
Sharks10_Nums

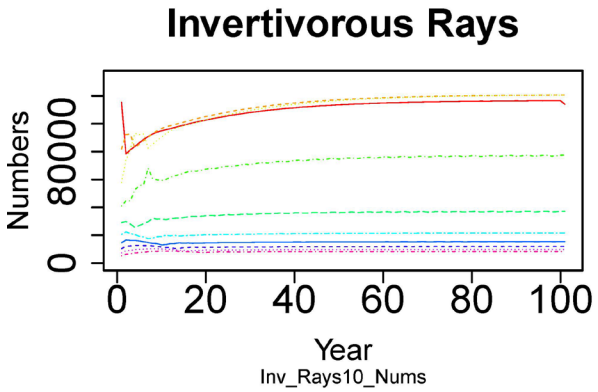
Invertivorous Rays
Numbers
0
80000
0
20
40
60
80
100
Year
Inv_Rays10_Nums

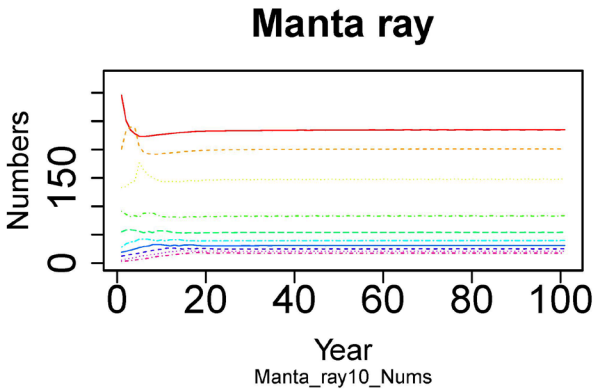
Manta ray
Numbers
0
150
0
20
40
60
80
100
Year
Manta_ray10_Nums

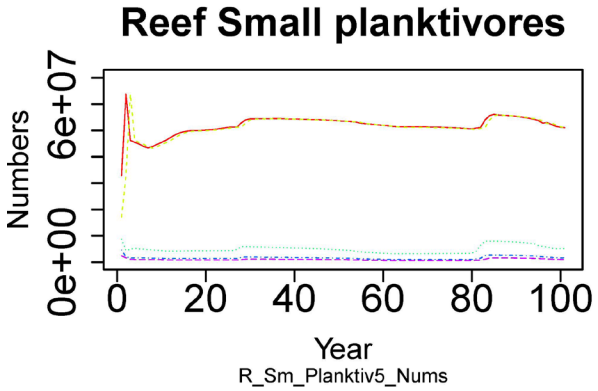
Reef Small planktivores
Numbers
0e+00
6e+07
0
20
40
60
80
100
Year
R_Sm_Planktiv5_Nums

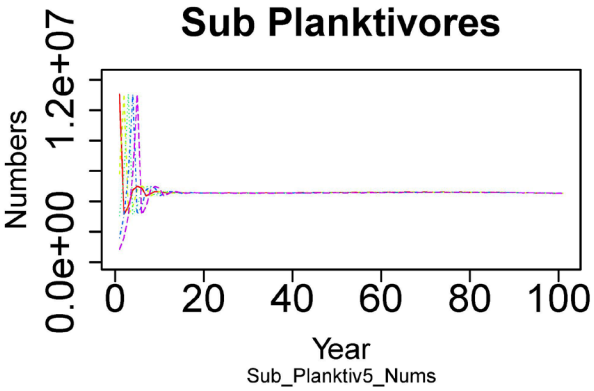
Sub Planktivores
Numbers
0.0e+00
1.2e+07
0
20
40
60
80
100
Year
Sub_Planktiv5_Nums

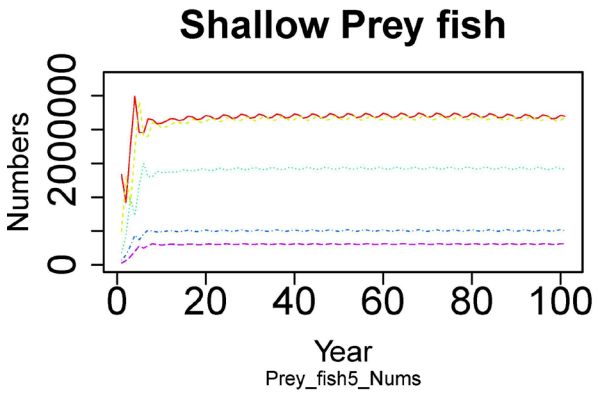
Shallow Prey fish
Numbers
0
2000000
0
20
40
60
80
100
Year
Prey_fish5_Nums

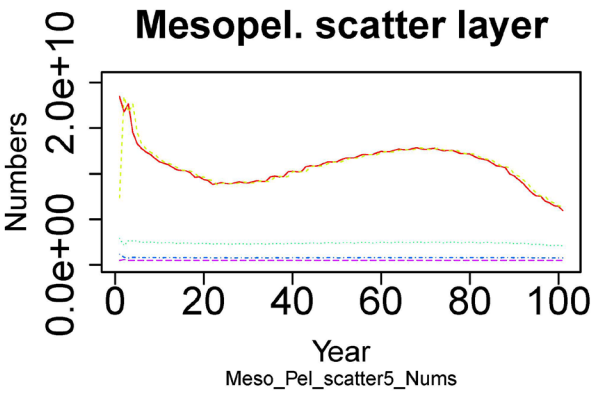
Mesopel. scatter layer
Numbers
0.0e+00
2.0e+10
0
20
40
60
80
100
Year
Meso_Pel_scatter5_Nums

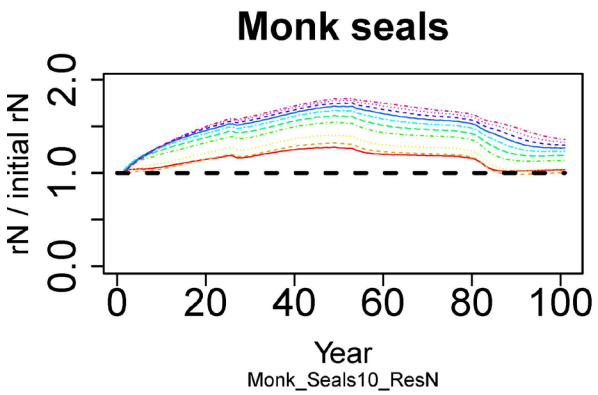
Monk seals
rN / initial rN
0.0
1.0
2.0
0
20
40
60
80
100
Year
Monk_Seals10_ResN

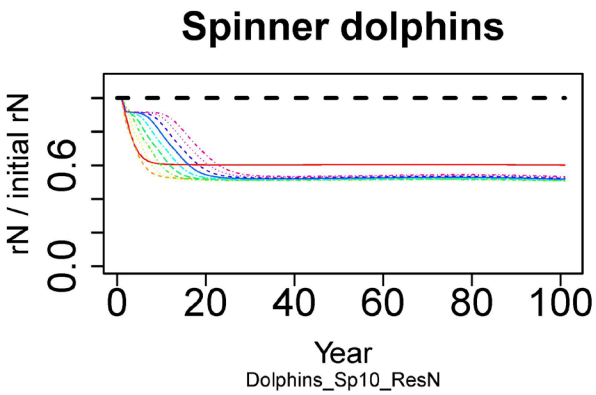
Spinner dolphins
rN / initial rN
0.0
0.6
0
20
40
60
80
100
Year
Dolphins_Sp10_ResN

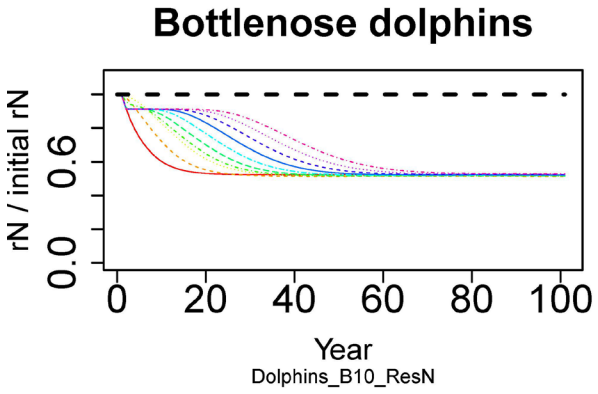
Bottlenose dolphins
rN / initial rN
0.0
0.6
0
20
40
60
80
100
Year
Dolphins_B10_ResN

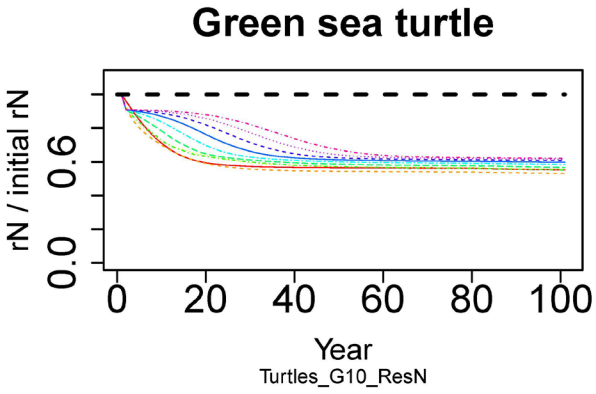
Green sea turtle
rN / initial rN
0.0
0.6
0
20
40
60
80
100
Year
Turtles_G10_ResN

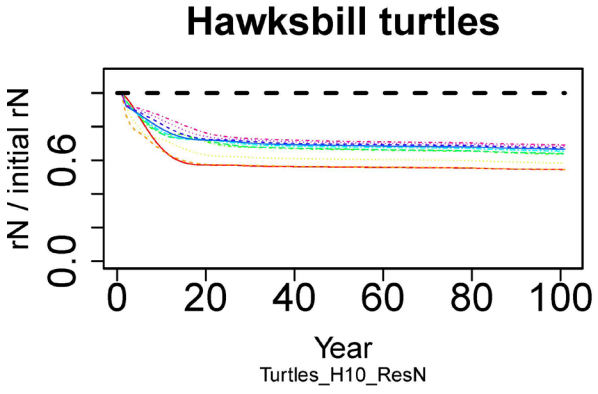
Hawksbill turtles
rN / initial rN
0.0
0.6
0
20
40
60
80
100
Year
Turtles_H10_ResN

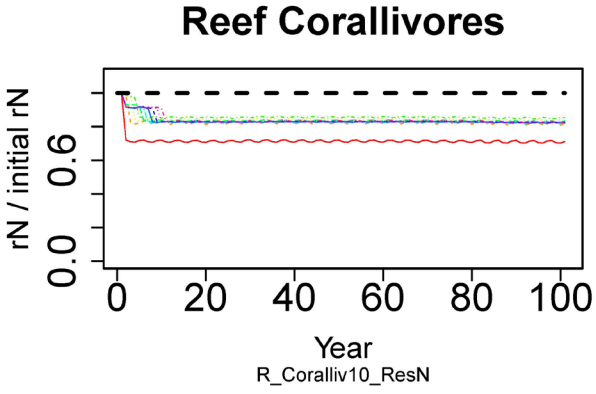
Reef Corallivores
rN / initial rN
0.0
0.6
0
20
40
60
80
100
Year
R_Coralliv10_ResN

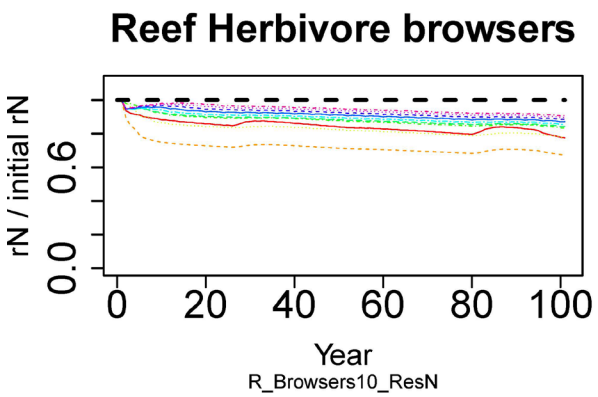
Reef Herbivore browsers
rN / initial rN
0.0
0.6
0
20
40
60
80
100
Year
R_Browsers10_ResN

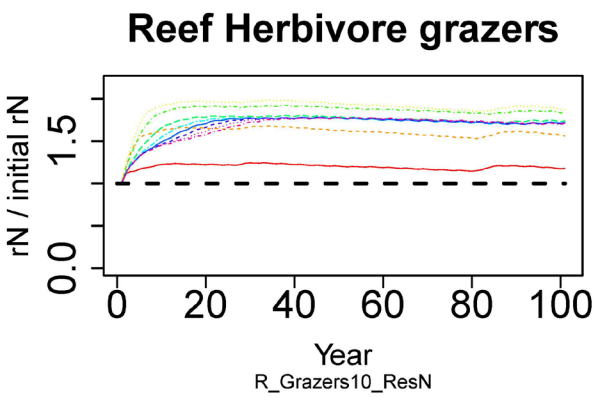
Reef Herbivore grazers
rN / initial rN
0.0
1.5
0
20
40
60
80
100
Year
R_Grazers10_ResN

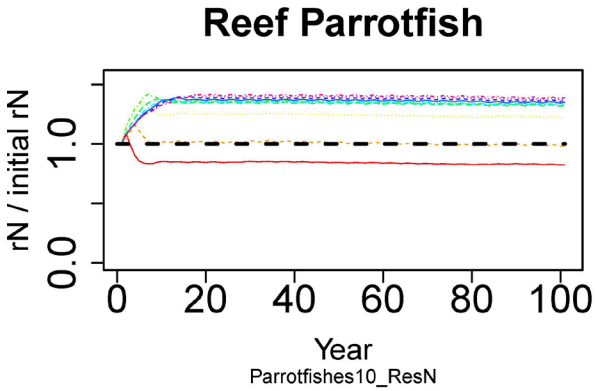
Reef Parrotfish
rN / initial rN
0.0
1.0
0
20
40
60
80
100
Year
Parrotfishes10_ResN

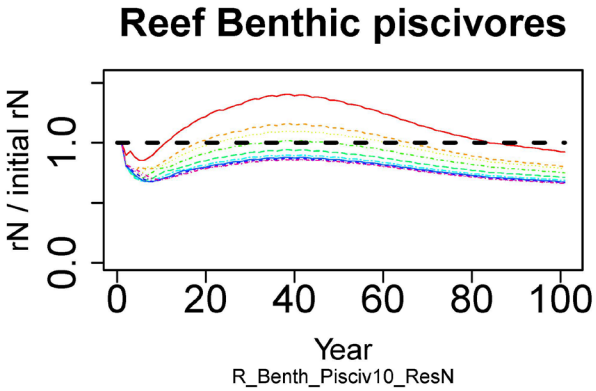
Reef Benthic piscivores
rN / initial rN
0.0
1.0
0
20
40
60
80
100
Year
R_Benth_Pisciv10_ResN

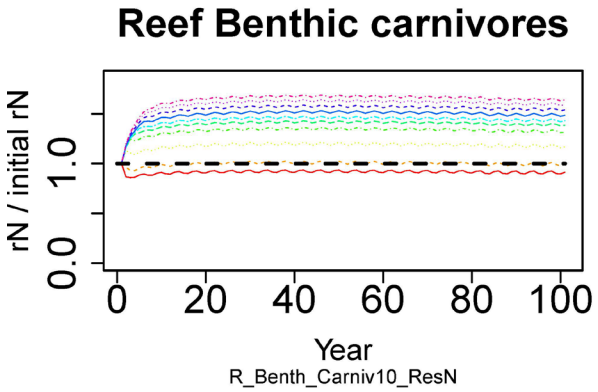
Reef Benthic carnivores
rN / initial rN
0.0
1.0
0
20
40
60
80
100
Year
R_Benth_Carniv10_ResN

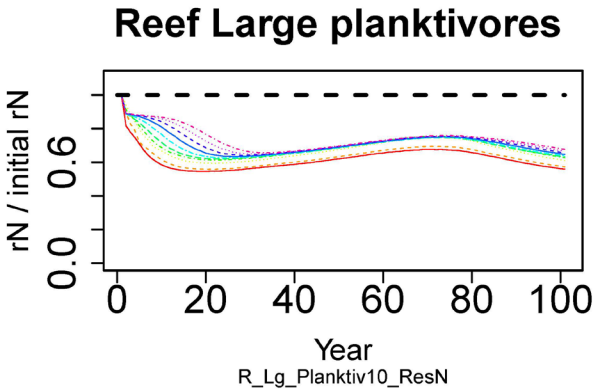
Reef Large planktivores
rN / initial rN
0.0
0.6
0
20
40
60
80
100
Year
R_Lg_Planktiv10_ResN

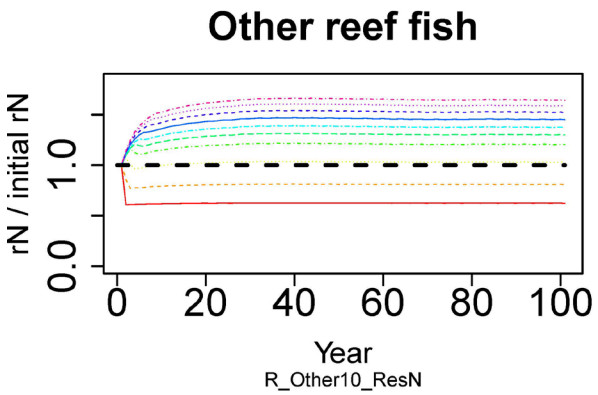
Other reef fish
rN / initial rN
0.0
1.0
0
20
40
60
80
100
Year
R_Other10_ResN

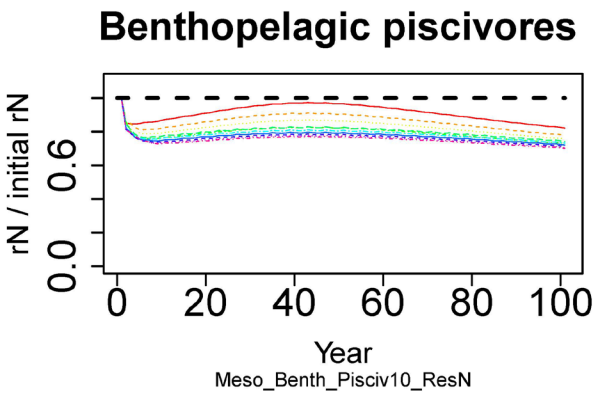
Benthopelagic piscivores
rN / initial rN
0.0
0.6
0
20
40
60
80
100
Year
Meso_Benth_Pisciv10_ResN

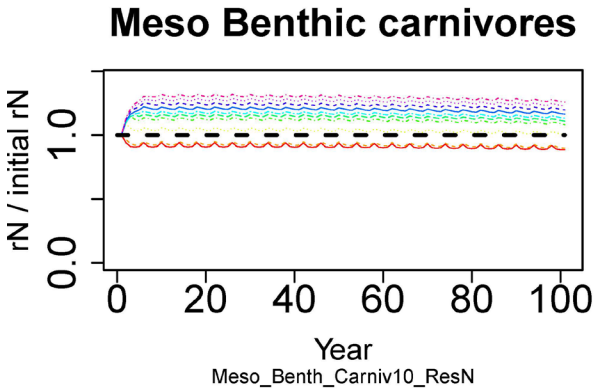
Meso Benthic carnivores
rN / initial rN
0.0
1.0
0
20
40
60
80
100
Year
Meso_Benth_Carniv10_ResN

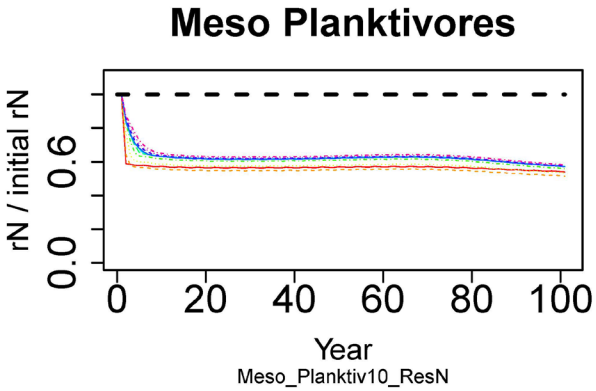
Meso Planktivores
rN / initial rN
0.0
0.6
0
20
40
60
80
100
Year
Meso_Planktiv10_ResN

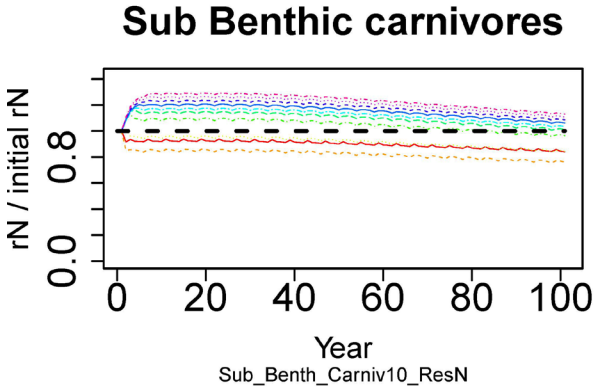
Sub Benthic carnivores
rN / initial rN
0.0
0.8
0
20
40
60
80
100
Year
Sub_Benth_Carniv10_ResN

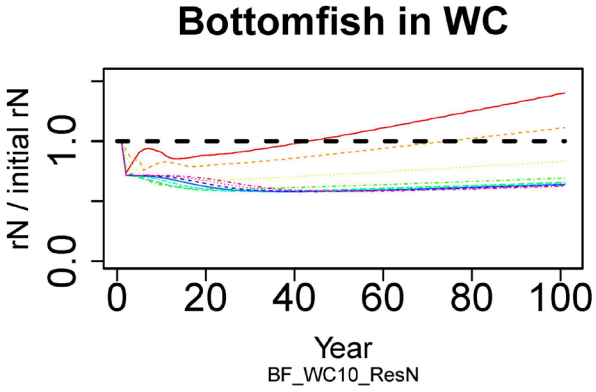
Bottomfish in WC
rN / initial rN
0.0
1.0
0
20
40
60
80
100
Year
BF_WC10_ResN

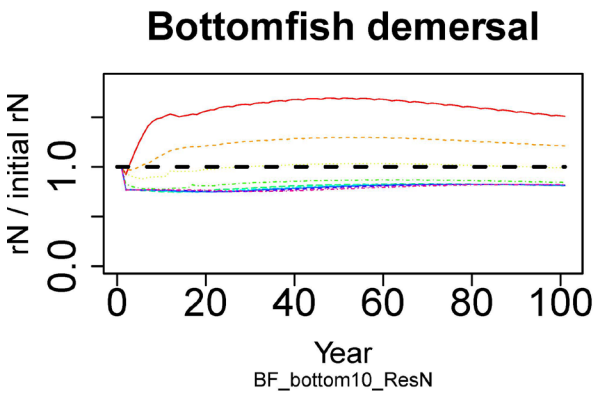
Bottomfish demersal
rN / initial rN
0.0
1.0
0
20
40
60
80
100
Year
BF_bottom10_ResN

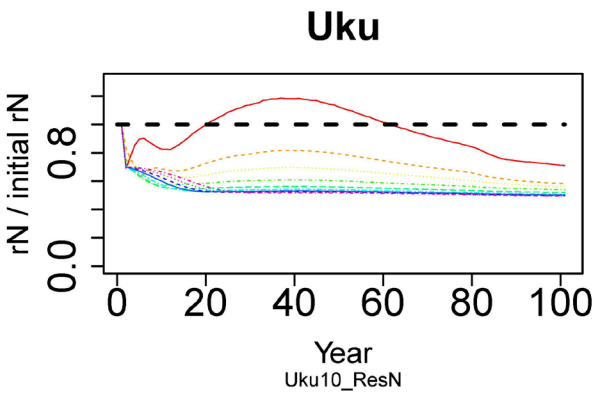
Uku
rN / initial rN
0.0
0.8
0
20
40
60
80
100
Year
Uku10_ResN

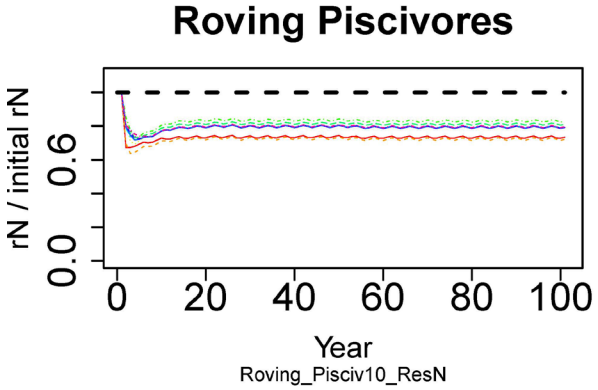
Roving Piscivores
rN / initial rN
0.0
0.6
0
20
40
60
80
100
Year
Roving_Pisciv10_ResN

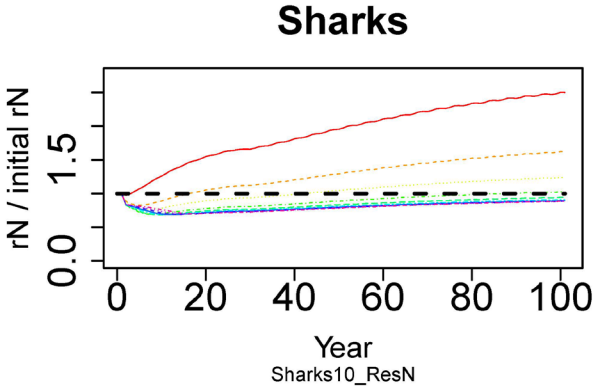
Sharks
rN / initial rN
0.0
1.5
0
20
40
60
80
100
Year
Sharks10_ResN

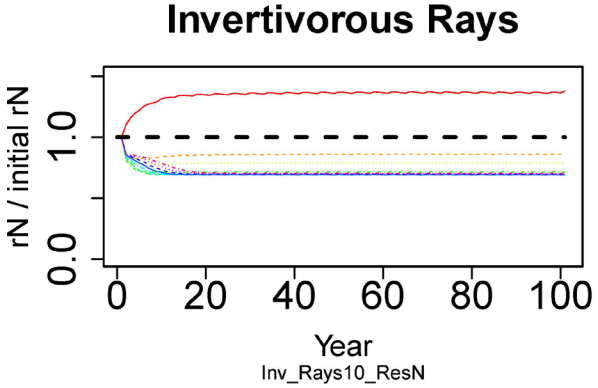
Invertivorous Rays
rN / initial rN
0.0
1.0
0
20
40
60
80
100
Year
Inv_Rays10_ResN

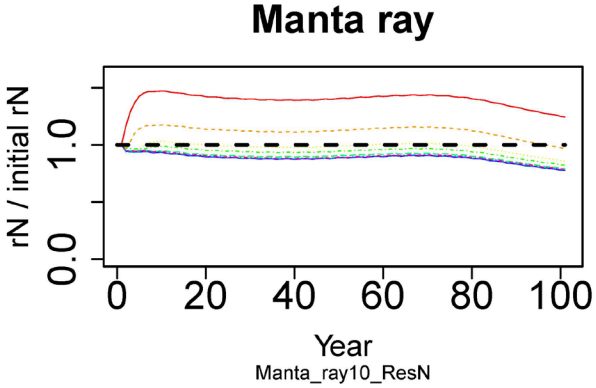
Manta ray
rN / initial rN
0.0
1.0
0
20
40
60
80
100
Year
Manta_ray10_ResN

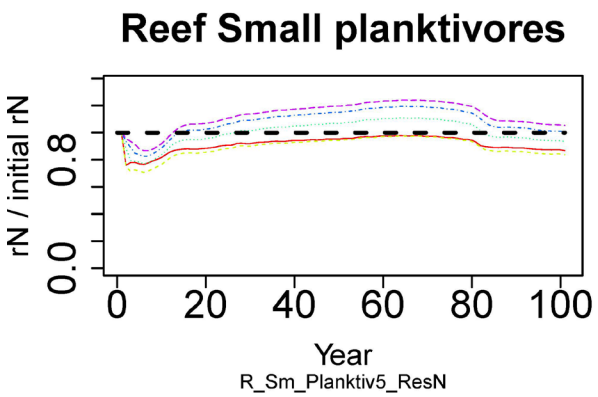
Reef Small planktivores
rN / initial rN
0.0
0.8
0
20
40
60
80
100
Year
R_Sm_Planktiv5_ResN

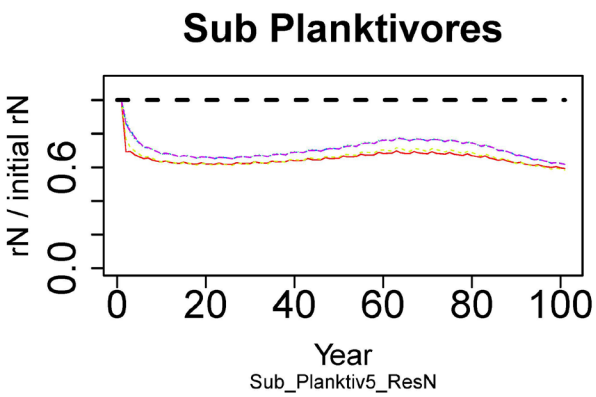
Sub Planktivores
rN / initial rN
0.0
0.6
0
20
40
60
80
100
Year
Sub_Planktiv5_ResN

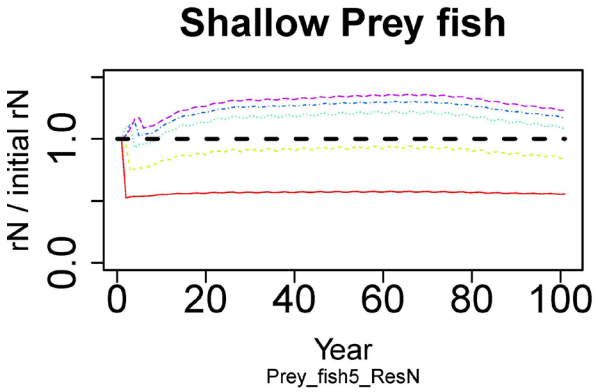
Shallow Prey fish
rN / initial rN
0.0
1.0
0
20
40
60
80
100
Year
Prey_fish5_ResN

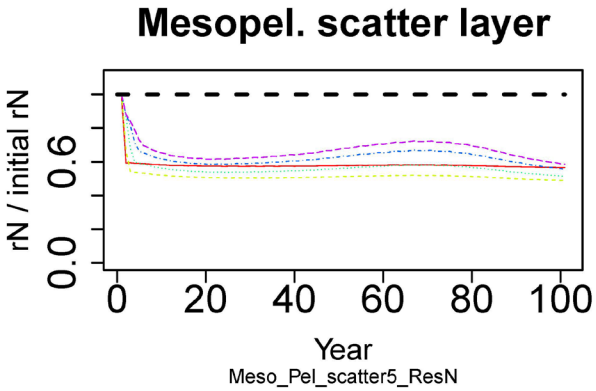
Mesopel. scatter layer
rN / initial rN
0.0
0.6
0
20
40
60
80
100
Year
Meso_Pel_scatter5_ResN

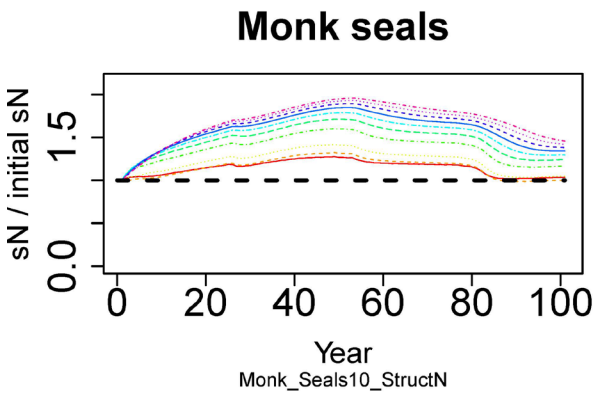
Monk seals
sN / initial sN
0.0
1.5
0
20
40
60
80
100
Year
Monk_Seals10_StructN

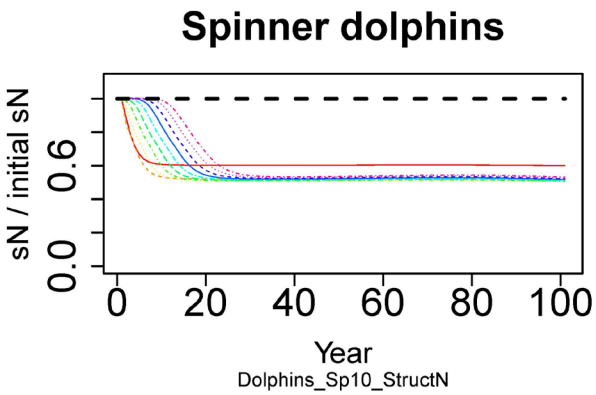
Spinner dolphins
sN / initial sN
0.0
0.6
0
20
40
60
80
100
Year
Dolphins_Sp10_StructN

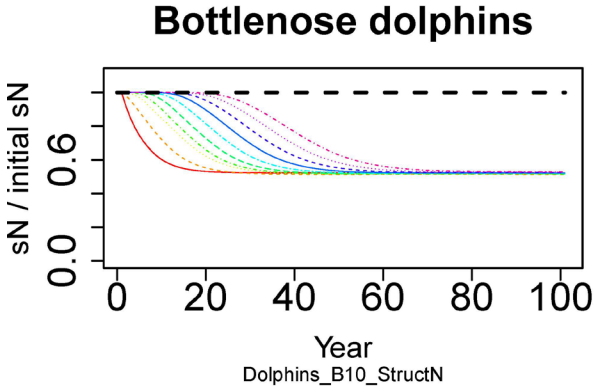
Bottlenose dolphins
sN / initial sN
0.0
0.6
0
20
40
60
80
100
Year
Dolphins_B10_StructN

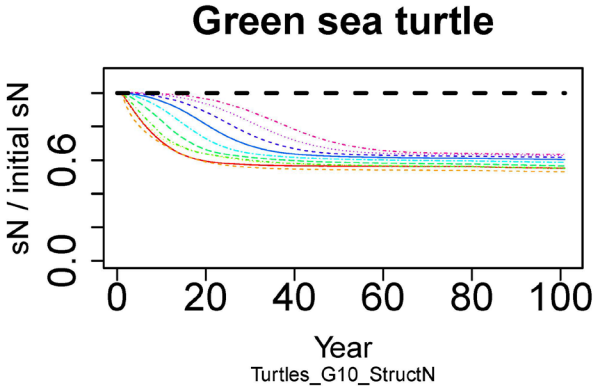
Green sea turtle
sN / initial sN
0.0
0.6
0
20
40
60
80
100
Year
Turtles_G10_StructN

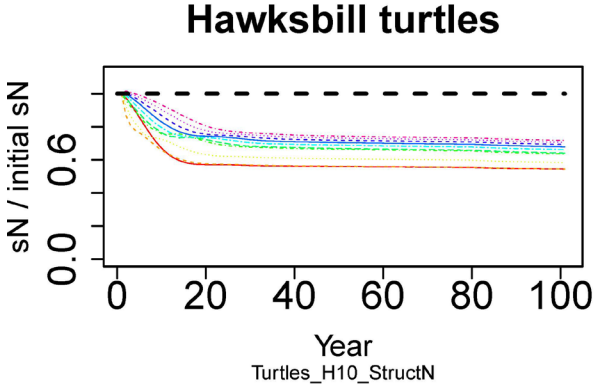
Hawksbill turtles
sN / initial sN
0.0
0.6
0
20
40
60
80
100
Year
Turtles_H10_StructN

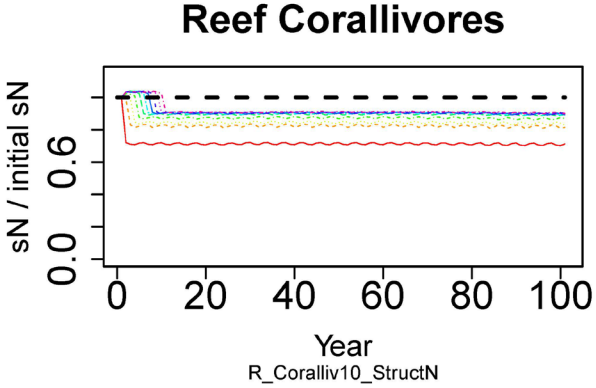
Reef Corallivores
sN / initial sN
0.0
0.6
0
20
40
60
80
100
Year
R_Coralliv10_StructN

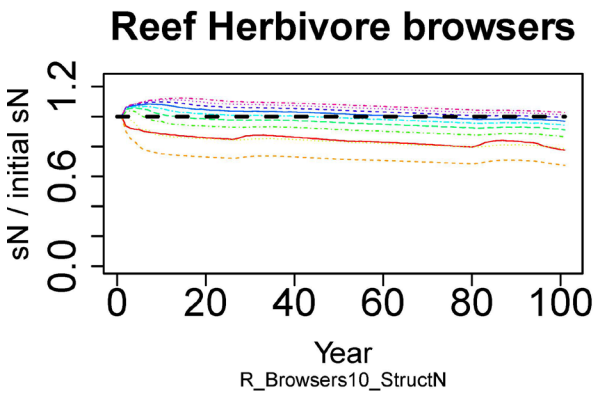
Reef Herbivore browsers
sN / initial sN
0.0
0.6
1.2
0
20
40
60
80
100
Year
R_Browsers10_StructN

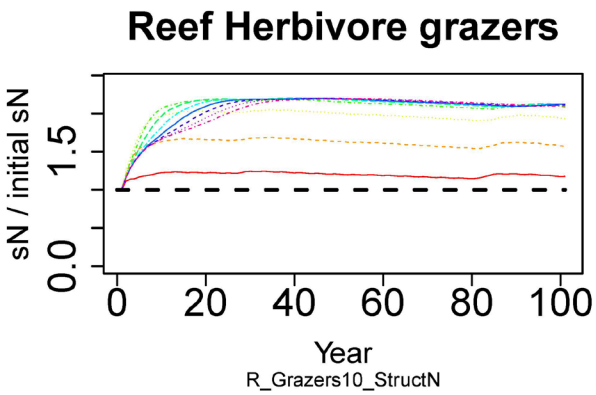
Reef Herbivore grazers
sN / initial sN
0.0
1.5
0
20
40
60
80
100
Year
R_Grazers10_StructN

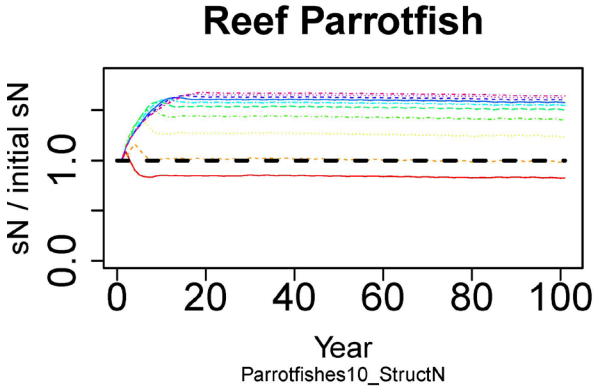
Reef Parrotfish
sN / initial sN
0.0
1.0
0
20
40
60
80
100
Year
Parrotfishes10_StructN

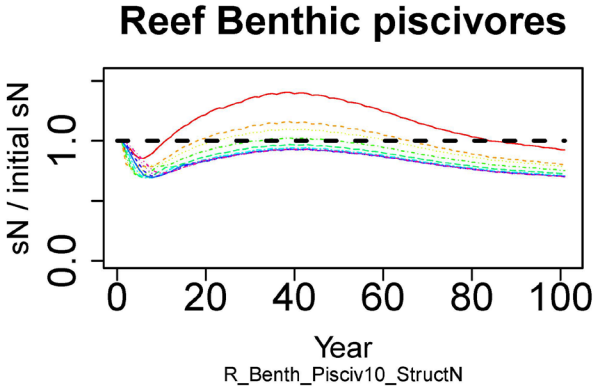
Reef Benthic piscivores
sN / initial sN
0.0
1.0
0
20
40
60
80
100
Year
R_Benth_Pisciv10_StructN

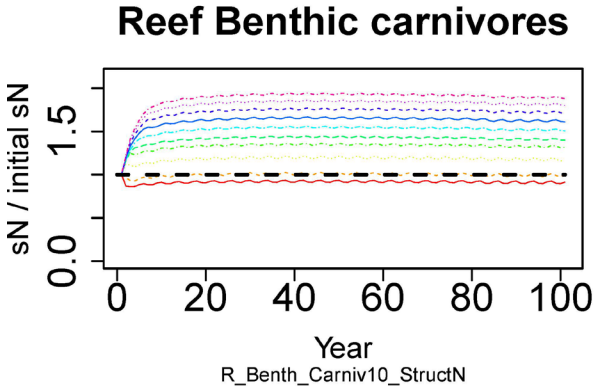
Reef Benthic carnivores
sN / initial sN
0.0
1.5
0
20
40
60
80
100
Year
R_Benth_Carniv10_StructN

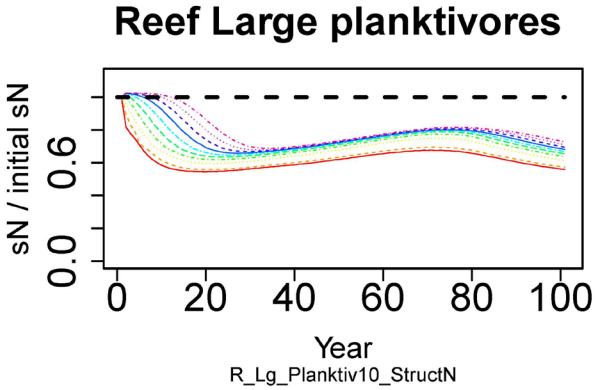
Reef Large planktivores
sN / initial sN
0.0
0.6
0
20
40
60
80
100
Year
R_Lg_Planktiv10_StructN

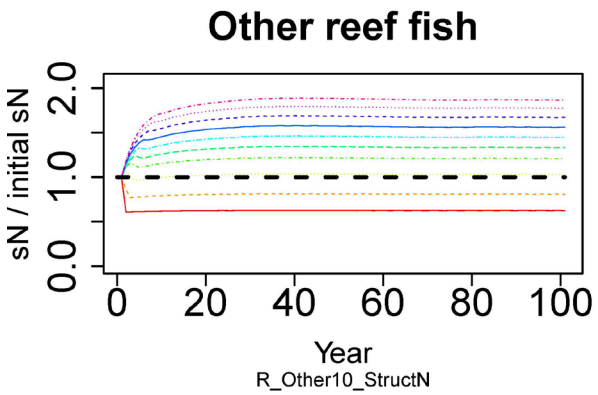
Other reef fish
sN / initial sN
0.0
1.0
2.0
0
20
40
60
80
100
Year
R_Other10_StructN

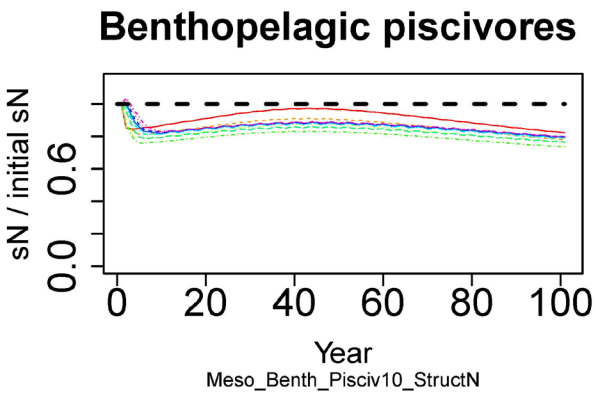
Benthopelagic piscivores
sN / initial sN
0.0
0.6
0
20
40
60
80
100
Year
Meso_Benth_Pisciv10_StructN

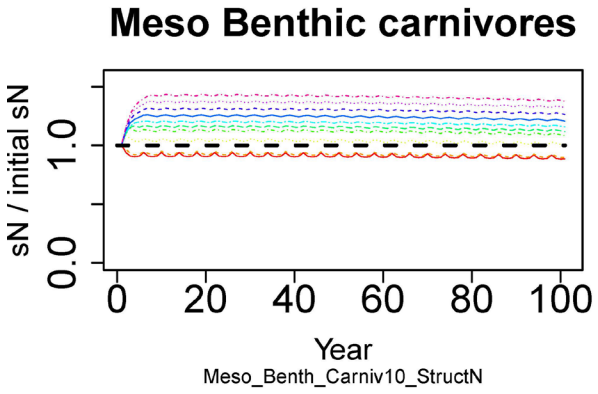
Meso Benthic carnivores
sN / initial sN
0.0
1.0
0
20
40
60
80
100
Year
Meso_Benth_Carniv10_StructN

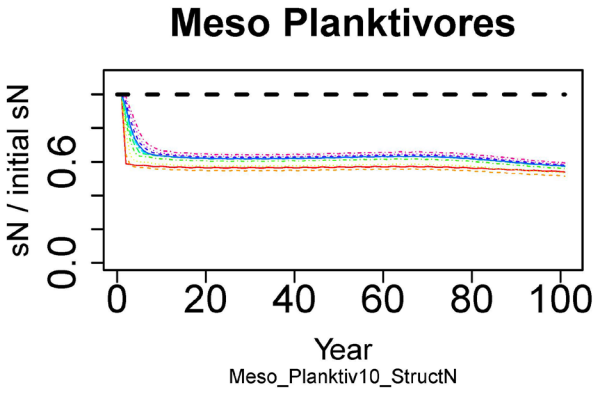
Meso Planktivores
sN / initial sN
0.0
0.6
0
20
40
60
80
100
Year
Meso_Planktiv10_StructN

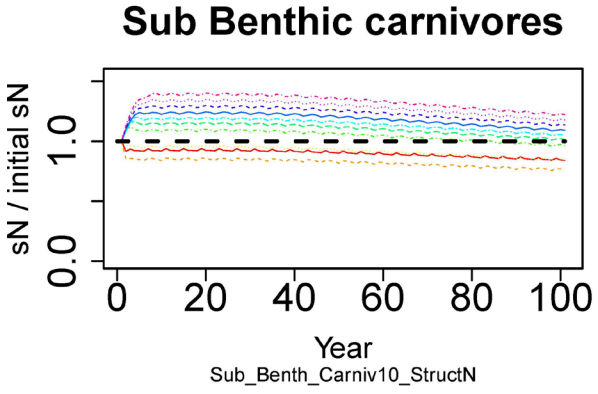
Sub Benthic carnivores
sN / initial sN
0.0
1.0
0
20
40
60
80
100
Year
Sub_Benth_Carniv10_StructN

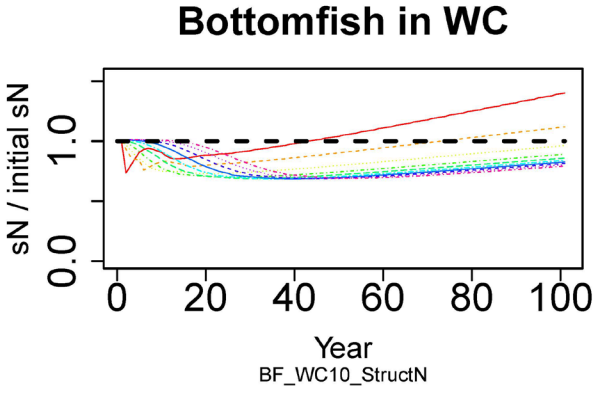
Bottomfish in WC
sN / initial sN
0.0
1.0
0
20
40
60
80
100
Year
BF_WC10_StructN

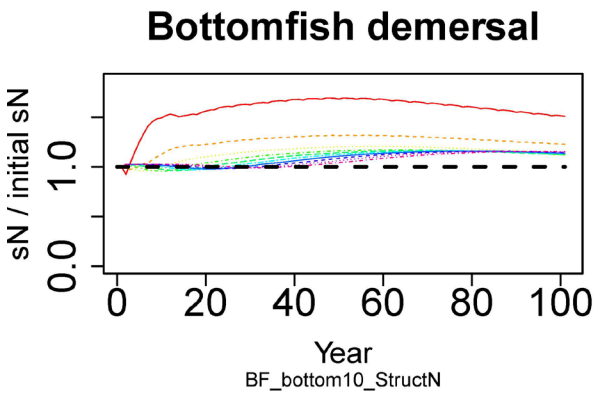
Bottomfish demersal
sN / initial sN
0.0
1.0
0
20
40
60
80
100
Year
BF_bottom10_StructN

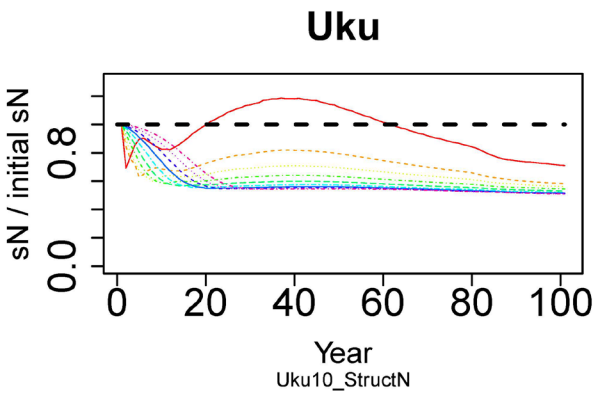
Uku
sN / initial sN
0.0
0.8
0
20
40
60
80
100
Year
Uku10_StructN

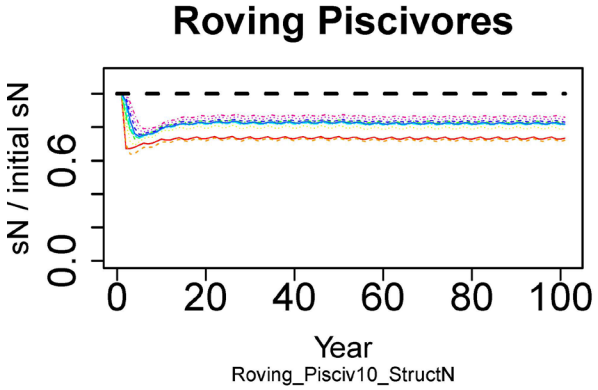
Roving Piscivores
sN / initial sN
0.0
0.6
0
20
40
60
80
100
Year
Roving_Pisciv10_StructN

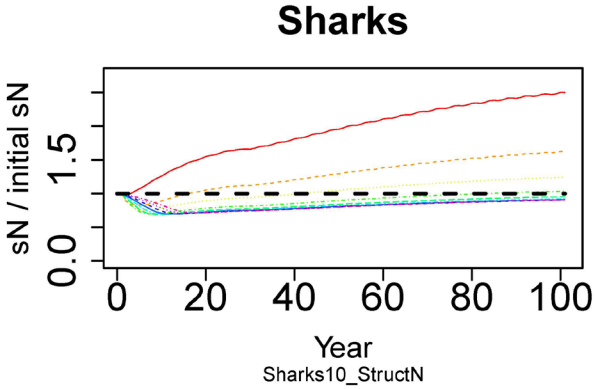
Sharks
sN / initial sN
0.0
1.5
0
20
40
60
80
100
Year
Sharks10_StructN

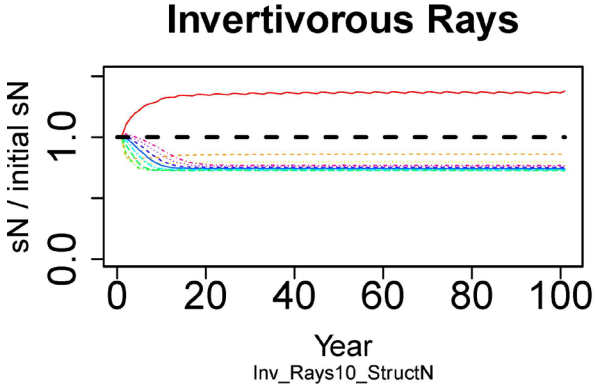
Invertivorous Rays
sN / initial sN
0.0
1.0
0
20
40
60
80
100
Year
Inv_Rays10_StructN

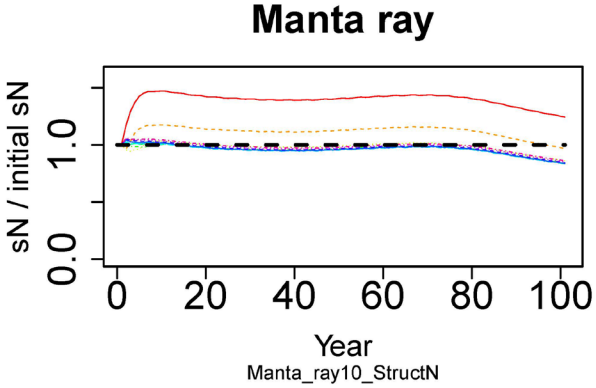
Manta ray
sN / initial sN
0.0
1.0
0
20
40
60
80
100
Year
Manta_ray10_StructN

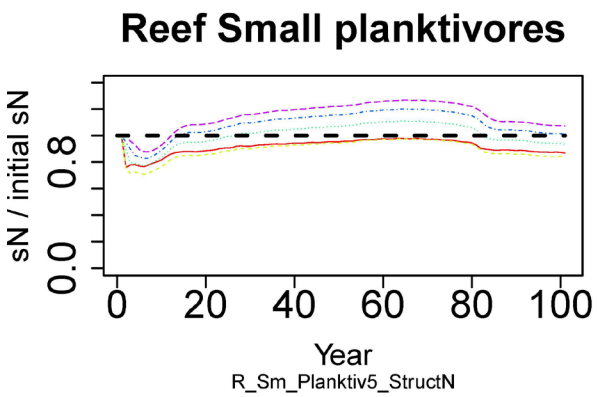
Reef Small planktivores
sN / initial sN
0.0
0.8
0
20
40
60
80
100
Year
R_Sm_Planktiv5_StructN

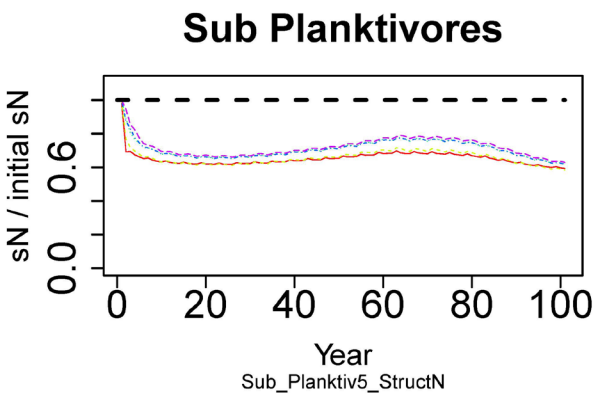
Sub Planktivores
sN / initial sN
0.0
0.6
0
20
40
60
80
100
Year
Sub_Planktiv5_StructN

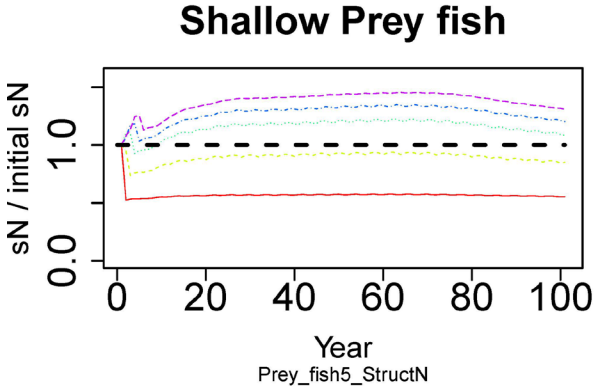
Shallow Prey fish
sN / initial sN
0.0
1.0
0
20
40
60
80
100
Year
Prey_fish5_StructN

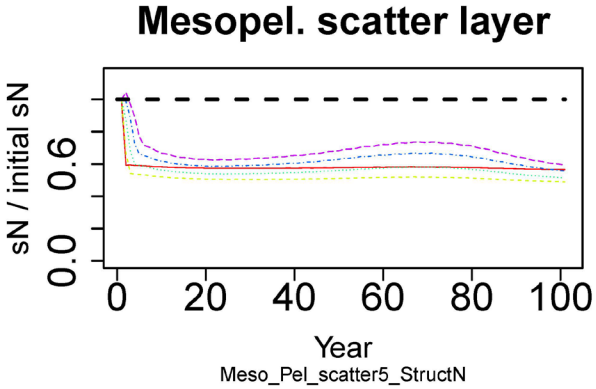
Mesopel. scatter layer
sN / initial sN
0.0
0.6
0
20
40
60
80
100
Year
Meso_Pel_scatter5_StructN

Appendix J: Validation with fixed mortality per gear type

Tables A5–7 provide the results of the skill assessments of the model to reproduce similar catches by gear type or fishery forcing the model with a fixed fishing mortality as observed catches. These tables are followed by the figures to visually compare the results.

Table A5. Results of 6 complimentary skill assessments of modeled vs. observed catches of targeted functional groups by gear type or fishery. Numbers in bold indicate a significance at $p<0.05$.

Gear/Fishery	Group	Spearman Correlation	Average Error	Average Absolute Error	Mean Squared Error	Reliability index	Model Efficiency
BFcomm/rec	BFB	-0.005	15.125	15.125	15.478	1.694	-20.9
BFcomm/rec	BFW	0.109	-33.031	41.329	45.479	1.561	-0.9
BFcomm/rec	PIS	-0.176	-1.201	1.607	2.285	1.636	-2628.1
BFcomm/rec	UKU	**-0.669**	-2.584	2.584	2.804	8.988	-711.6
Line	PIS	0.205	-82.719	107.922	147.445	1.462	-1450.2
Line	RBC	0.297	-62.752	63.649	81.132	2.180	-1305.4
Line	RBR	**0.486**	-25.386	25.386	41.993	4.815	-21112.7
Line	RGR	-0.127	13.343	13.343	13.658	2.792	-3913.2
Line	RLP	0.000	-3.590	4.458	6.959	1.970	-23.5
Line	RPA	-0.059	0.205	0.402	0.475	1.712	-377.4
Line	SHP	0.371	-64.251	64.251	73.684	2.431	-1342.0
Line	UKU	0.023	-42.422	42.422	48.274	2.853	-37.9
Net	PIS	-0.013	-3.314	3.805	5.066	1.542	-1935.0
Net	RBC	**0.739**	-1.993	9.291	12.155	1.604	-152.7
Net	RBR	0.371	-33.328	33.791	62.552	2.376	-2542.4
Net	RGR	0.153	37.109	37.109	39.690	1.896	-2027.0
Net	RLP	**-0.600**	-3.400	3.473	4.045	2.140	-23.7
Net	RPA	-0.159	3.385	3.385	3.595	2.003	-542.8
Net	SHP	**-0.615**	-167.874	168.247	203.505	1.826	-414.3
Net	UKU	-0.143	-0.008	0.010	0.022	4.522	-652.6
other	SHP	**-0.489**	15.356	37.126	44.750	1.534	-56.1
other	RBC	0.083	-0.340	0.456	0.558	1.589	-211.2
other	RBR	0.074	0.172	0.661	0.891	7.658	-770.1
other	RGR	**0.522**	14.661	14.661	14.777	4.695	-6112.1
other	RLP	0.325	-0.960	1.126	1.670	2.632	-79.1
other	RPA	**-0.710**	-1.031	1.140	1.493	2.298	-5710.6
Spear	PIS	0.222	-4.012	5.358	7.258	1.455	-1366.9
Spear	RBC	0.383	-1.142	8.386	10.347	1.440	-107.8
Spear	RBR	0.356	-13.012	13.012	21.749	3.202	-6191.6
Spear	RGR	-0.377	89.990	89.990	91.385	2.976	-4333.1
Spear	RLP	**-0.550**	-6.069	6.963	9.926	2.068	-30.0

Gear/Fishery	Group	Spearman Correlation	Average Error	Average Absolute Error	Mean Squared Error	Reliability index	Model Efficiency
Spear	RPA	-0.333	20.460	21.739	24.652	1.696	-345.7
Spear	SHP	0.346	-12.950	12.950	13.714	15.697	-135537.8
Spear	UKU	0.133	-6.153	6.379	8.066	2.191	-16.7

Table A6. Results of 6 complimentary skill assessments of modeled vs. observed catches of non-targeted functional groups by gear type or fishery. Numbers in bold indicate a significance at $p<0.05$.

Gear/Fishery	Group	Spearman Correlation	Average Error	Average Absolute Error	Mean Squared Error	Reliability index	Model Efficiency
BFcomm/rec	SBC	**-0.778**	1.482	6.921	7.275	2.635	-1786.3
BFcomm/rec	SPL	0.275	0.137	0.166	0.187	2.375	-388.4
Line	RBP	0.265	0.785	2.409	2.867	2.627	-4.8
Line	ROF	0.093	-1.181	18.217	22.001	1.854	-624.9
Line	RSP	-0.164	-2.658	2.663	4.177	7.821	-7450.3
Line	MBC	-0.027	50.449	50.449	50.499	8.302	-6684.1
Line	MBP	**-0.819**	-0.132	0.404	0.512	1.465	-138.2
Line	MPL	**-0.875**	4.463	6.208	7.159	4.200	-305.3
Line	SHR	-0.152	-21.478	27.599	67.174	5.110	-21333.4
Net	RBP	-0.178	0.029	0.039	0.044	5.092	-9.7
Net	ROF	-0.121	0.080	0.312	0.362	1.870	-398.6
Net	RSP	**-0.408**	-0.314	0.314	0.382	5.924	-1583.0
Net	SHR	**-0.615**	0.001	0.065	0.148	7.450	-3090.5
Net	MBC	**0.711**	40.999	40.999	43.641	2.658	-2967.4
Net	MBP	-0.153	0.135	0.135	0.139	14.897	-532.5
Net	MPL	**0.590**	-3.575	3.575	4.734	5.152	-32463.9
other	RBP	0.027	0.085	0.088	0.094	3.915	-6.6
other	RSP	**-0.676**	-0.034	0.036	0.055	5.551	-1986.2
other	ROF	**-0.700**	-2.059	2.059	3.198	7.194	-221566.9
other	SHR	-0.238	-0.172	0.175	0.261	6.451	-19501.0
other	MBC	**0.495**	-12.731	13.575	21.339	2.216	-26689.2
other	MBP	0.328	-0.362	0.405	0.611	5.031	-15152.4
other	MPL	**0.510**	-3.135	6.467	7.977	1.492	-145.6
Spear	RBP	**0.450**	9.342	9.342	9.903	5.012	-7.2
Spear	RSP	**0.597**	-0.213	0.218	0.305	4.377	-1133.8
Spear	ROF	-0.067	-0.797	1.013	1.378	1.821	-1440.1
Spear	MBC	-0.044	53.598	53.598	53.764	11.846	-7050.5
Spear	MBP	**0.506**	0.420	0.502	0.537	7.009	-368.8
Spear	MPL	-0.247	6.791	7.222	8.091	2.649	-260.9

Table A7. Results of 6 complimentary skill assessments of modeled vs. observed catches of invertebrate functional groups by gear type. Numbers in bold indicate a significance at $p<0.05$.

Gear/Fishery	Group	Spearman Correlation	Average Error	Average Absolute Error	Mean Squared Error	Reliability index	Model Efficiency
Line	CEP	-0.054	0.820	1.513	1.812	3.280	-3619.3
Line	LOB	0.239	-0.002	0.002	0.004	28.487	-499989.0
Line	OCT	0.278	-0.271	0.273	0.490	34.588	-42231.0
Net	BC	0.016	0.005	0.005	0.005	4.143	-23.8
Net	LOB	-0.027	-0.257	0.259	0.366	28.141	-4966813.3
Net	OCT	0.317	-0.090	0.090	0.133	23.225	-12544.6
other	BC	**0.474**	-8.553	9.692	12.144	2.042	-39.8
other	BFF	**-0.831**	-1.245	6.656	8.129	2.107	-341.3
other	BG	0.231	-0.003	0.014	0.021	6.292	-155655.7
other	BIV	**0.623**	0.425	0.501	0.528	6.118	-10923.4
other	CEP	-0.240	0.364	0.508	0.609	2.575	-2310.4
other	LOB	-0.314	-21.602	22.698	43.707	3.157	-37459.7
other	MAF	0.066	2.549	4.134	4.769	1.828	-2278.0
other	OCT	**-0.535**	-4.797	4.797	5.038	9.180	-318.9
Spear	LOB	0.233	3.364	3.524	4.035	1.655	-241.7
Spear	BC	**0.695**	0.335	0.335	0.348	2.716	-13.4
Spear	BIV	**0.705**	0.033	0.040	0.043	4.834	-10735.8
Spear	CEP	0.243	-0.001	0.008	0.013	3.762	-40218.3
Spear	OCT	**0.609**	25.098	25.098	29.673	2.587	-1.7

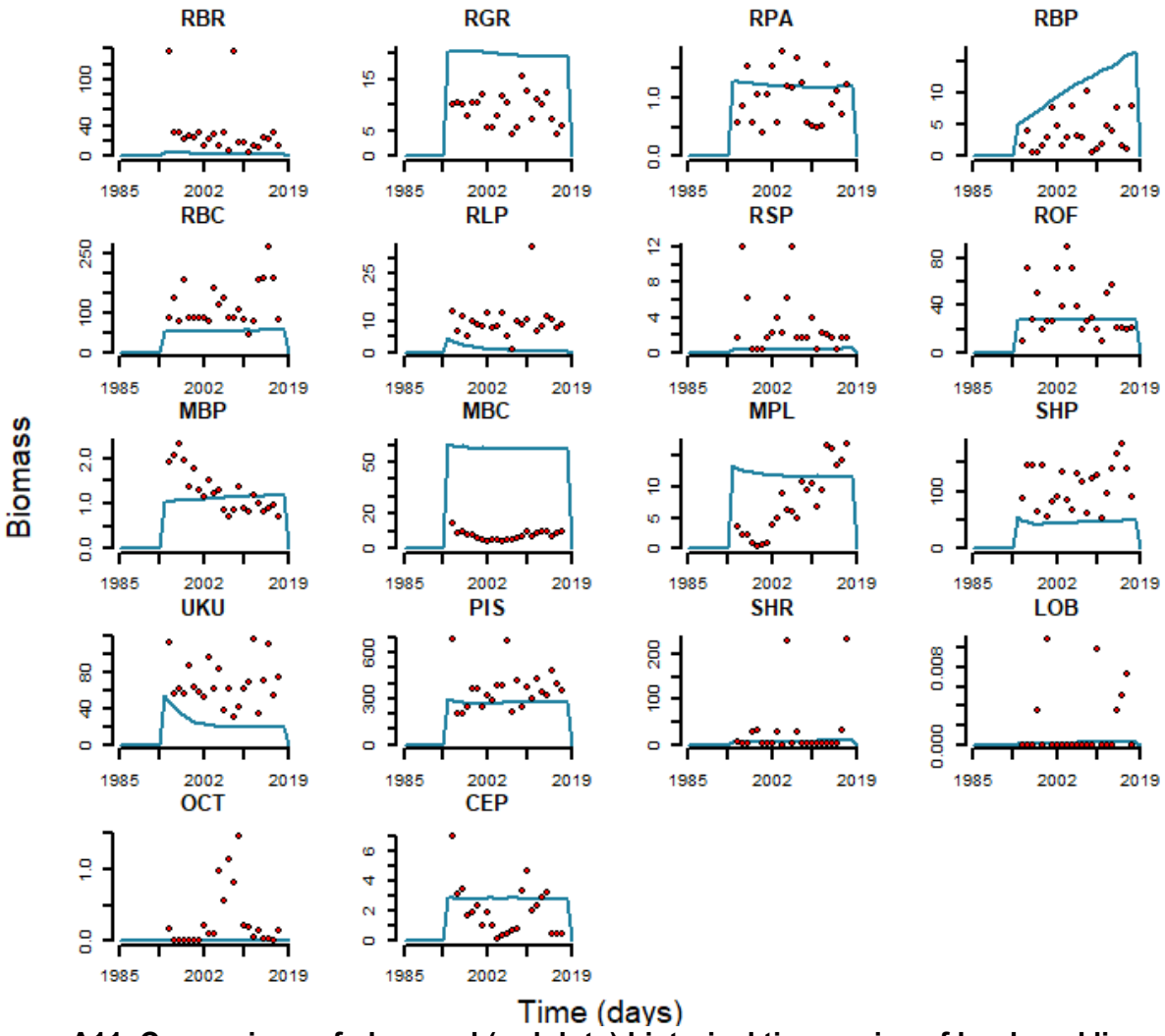

Figure A11. Comparison of observed (red dots) historical time series of hook and line catches per functional groups and modeled (blue line) catches with a fixed fishing mortality.

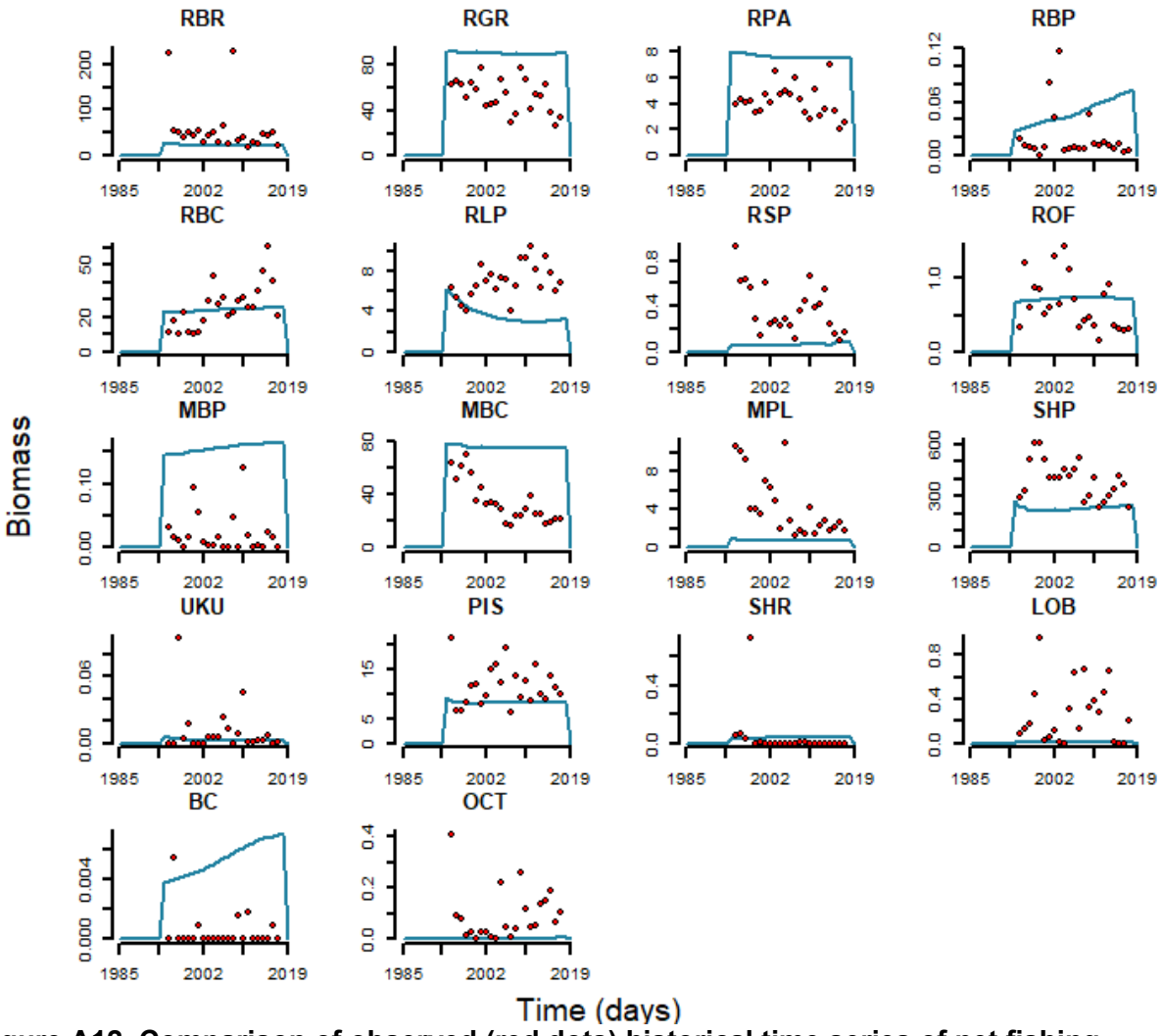

Figure A12. Comparison of observed (red dots) historical time series of net fishing catches per functional groups and modeled (blue line) catches with a fixed fishing mortality.

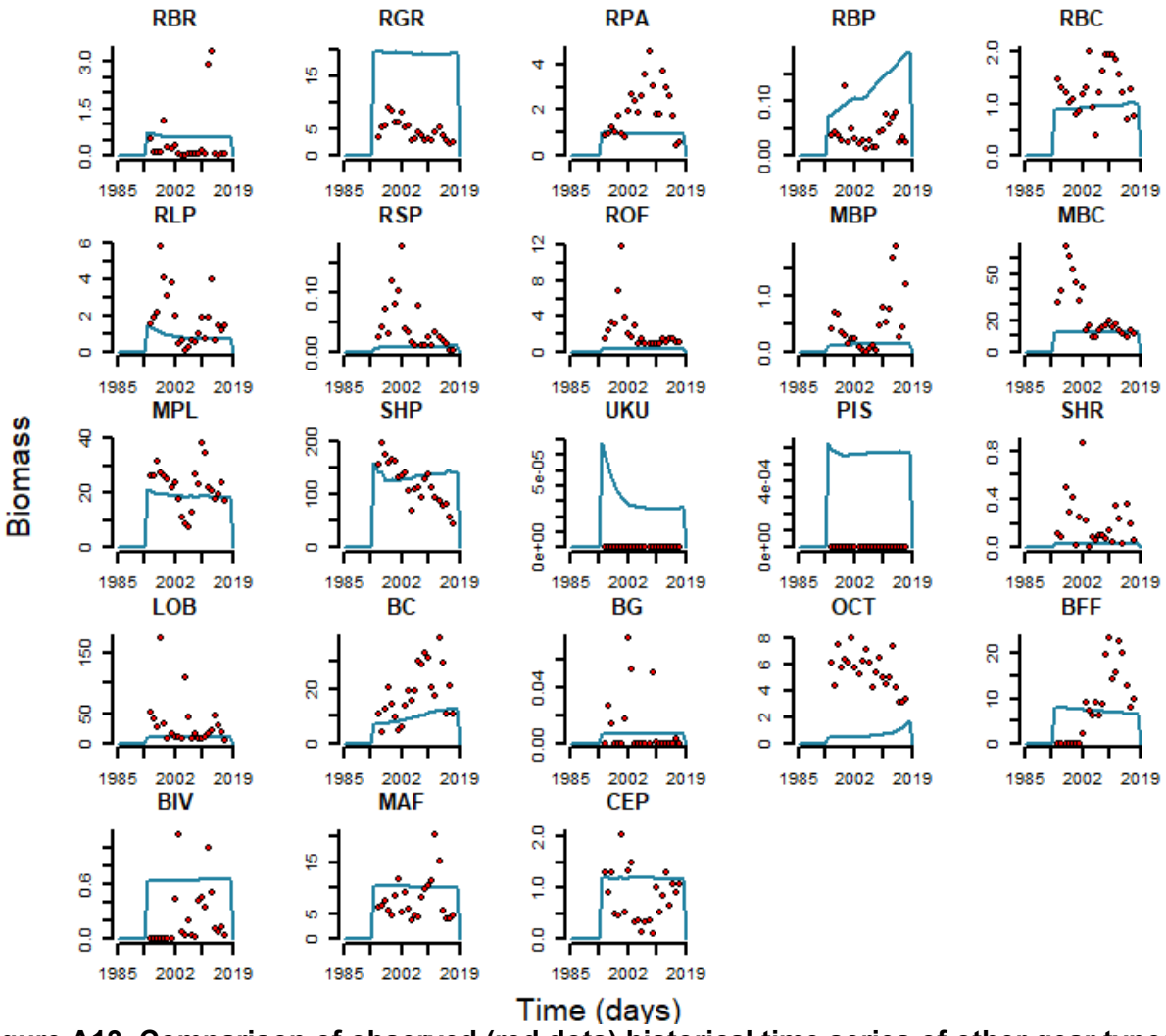

Figure A13. Comparison of observed (red dots) historical time series of other gear types catches per functional groups and modeled (blue line) catches with a fixed fishing mortality.

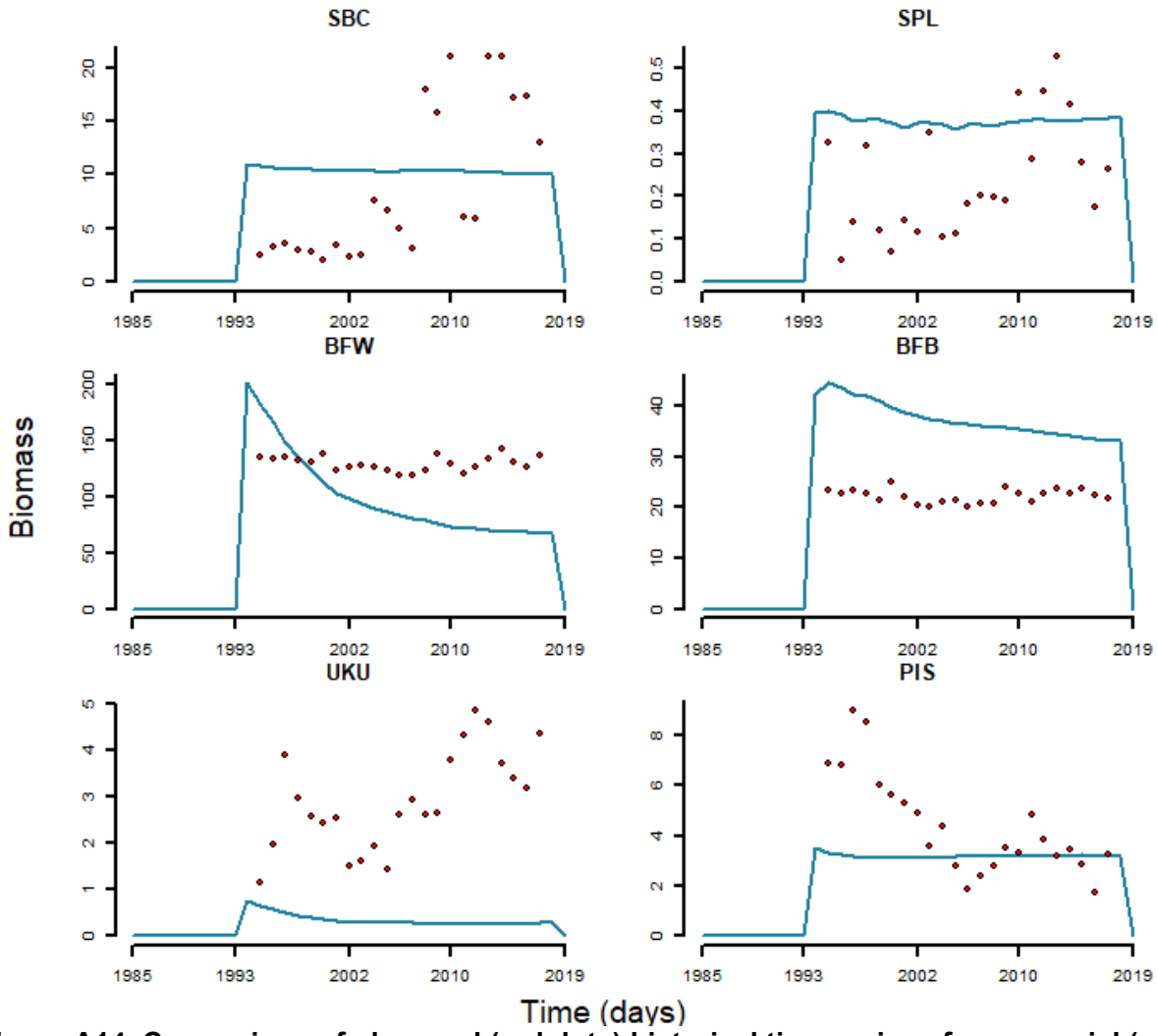

Figure A14. Comparison of observed (red dots) historical time series of commercial (or recreational) deep-water catches per functional groups and modeled (blue line) catches with a fixed fishing mortality.